QUANTITATIVE ANALYSIS OF FEEDBACKS IN CLIMATE MODEL SIMULATIONS OF CO_2-INDUCED WARMING

Michael E. Schlesinger
Department of Atmospheric Sciences and
Climatic Research Institute
Oregon State University
Corvallis, Oregon 97331
U.S.A.

ABSTRACT. The CO_2-induced warming of the Earth's surface air temperature simulated by energy balance models (EBMs), radiative-convective models (RCMs) and general circulation models (GCMs) is analyzed in terms of the direct radiative forcing of the increased CO_2 concentration, the resultant warming that would occur if the climate system had no feedback mechanisms, and the feedbacks that either enhance or diminish the zero-feedback warming. The total feedback in EBMs ranges from 0 to 0.94 on a scale of $-\infty$ to 1; this wide range is due to the inability of EBMs to determine the behavior of the climate system away from the energy balance level. The total feedback in RCMs ranges from -1.5 to 0.7; this wide range is due to differences in the treatment of the individual feedback mechanisms in RCMs. The total feedback of a single GCM simulation is 0.71, of which water vapor feedback is the single most important contributor, followed by cloud feedback and surface albedo feedback, with the lapse rate feedback making a negative contribution. It is concluded that the analysis of feedbacks in climate model simulations is a useful method of model intercomparison that provides insight on the causes of the differences in the models' simulated CO_2-induced warming.

1. INTRODUCTION

If the Earth's atmosphere were composed of only its two major constituents, nitrogen (N_2, 78% by volume) and oxygen (O_2, 21%), the Earth's surface temperature would be close to the -18°C radiative-equilibrium value necessary to balance the approximately 240 Wm^{-2} of solar radiation absorbed by the surface-atmosphere system. The fact that the Earth's surface temperature is a life-supporting 15°C is a consequence of the "greenhouse effect" of the atmosphere's minor constituents, mainly water vapor (H_2O, 0.2%) and carbon dioxide (CO_2, 0.03%). Measurements taken at Mauna Loa, Hawaii show that the CO_2 concentration has increased from 316 parts per million by volume (ppmv) in 1959 to 342 ppmv in 1983 (Elliott et al., 1985), an 8% increase in 24 years. A variety of direct CO_2 measurements and indirect reconstructions indicate

M. E. Schlesinger (ed.), Physically-Based Modelling and Simulation of Climate and Climatic Change – Part II, 653–735.

that the preindustrial CO_2 concentration during the period 1800 to 1850 was 270±10 ppmv (World Meteorological Organization [WMO] 1983). A study by Rotty (1983) reports that the CO_2 emission from the consumption of fossil fuels (gas, oil, coal) increased at a nearly constant rate of 4.6% per year from 1860 to 1973, and has continued to increase since 1973 at the diminished growth rate of 2.3% per year. Projections of the future usage of fossil fuels, such as the probablistic scenario analysis of Nordhaus and Yohe (1983), indicate that the CO_2 concentration could reach twice the preindustrial value sometime during the 21st century. In view of the role of CO_2 in helping to maintain the present surface temperature 33°C above the radiative-equilibrium value, would such a doubling of the CO_2 concentration substantially alter the Earth's climate?

To address this question three different types of climate model have been used to simulate the change in the equilibrium climate resulting from an increase in the CO_2 concentration: energy balance models (EBMs), radiative-convective models (RCMs), and general circulation models (GCMs). In this paper we analyze the CO_2-induced warming simulated by each of these types of models in terms of the direct radiative forcing of the increased CO_2 concentration, the resultant warming that would occur if the climate system had no feedback mechanisms, and the feedbacks that either enhance or diminish the zero-feedback warming. This analysis enables these feedback mechanisms to be intercompared among the models. Such an intercomparison provides insight on the causes of the differences in the CO_2-induced warming simulated by the models.

2. ENERGY BALANCE MODELS

Energy balance models predict the change in temperature at the Earth's surface that results from a change in heating based on the requirement that the net flux of energy does not change. The earliest estimates of the CO_2-induced temperature change were obtained from surface energy balance models (SEBMs) wherein the energy balance condition was applied at the Earth's surface. Later, planetary energy balance models (PEBMs) were used to determine the CO_2-induced temperature change from the balance condition applied at the top of the atmosphere. In this section we review these EBM studies of CO_2-induced temperature change, beginning with the historically-first SEBMs, and concluding with PEBMs. First, however, we introduce a formulation for EBMs which is generalized to encompass both SEBMs and PEBMs. This formulation also facilitates the quantitative evaluation of feedback, thus enabling comparison of EBMs among themselves and with the RCMs and GCMs.

2.1. Generalized Formulation

Energy balance models predict the change in temperature at the Earth's surface, ΔT_*, from the requirement that $\Delta N = 0$, where N is the net energy flux expressed by

; the period 1800 to 1850
:ion [WMO] 1983). A study
:rom the consumption of
:arly constant rate of
ued to increase since
year. Projections of the
iblistic scenario analysis
CO_2 concentration could
iring the 21st century.
in the present surface
im value, would such a
' alter the Earth's

ypes of climate model
uilibrium climate result-
energy balance models
l general circulation
$_2$-induced warming simu-
of the direct radiative
resultant warming that
ick mechanisms, and the
ero-feedback warming.
to be intercompared
'ides insight on the
irming simulated by the

iperature at the Earth's
ased on the requirement
'he earliest estimates of
d from surface energy
ice condition was applied
y balance models (PEBMs)
ure change from the bal-
here. In this section we
ture change, beginning
ng with PEBMs. First,
iich is generalized to en-
also facilitates the
ing comparison of EBMs

iperature at the Earth's
where N is the net

$$N = N(\underline{E},\ T_*,\ \underline{I}). \tag{1}$$

Here $\underline{E}$ is a vector of quantities that can be regarded as external to the climate system, that is, quantities whose change can lead to a change in climate, but which are independent of climate. $\underline{I}$ is a vector of quantities that are internal to the climate system, that is, quantities that can change as the climate changes and, in so doing, feed back to modify the climate change. The external quantities include, for example, the solar constant, the optically-active ejecta from volcanic eruptions and the CO_2 concentration (although eventually it may change as a result of climate change). The internal quantities include all the variables of the climate system other than T_*. Because T_* is the only dependent variable in an EBM, the internal quantities must be represented therein by

$$\underline{I} = \underline{I}(T_*). \tag{2}$$

A small change in the energy flux, ΔN, can be expressed by Eqs. (1) and (2) as

$$\Delta N = \sum_i \frac{\partial N}{\partial E_i}\,\Delta E_i + \left(\frac{\partial N}{\partial T_*} + \sum_j \frac{\partial N}{\partial I_j}\frac{dI_j}{dT_*}\right)\Delta T_* \,. \tag{3}$$

This can be written in a more convenient and instructive way as

$$\Delta N = \Delta Q - G_f^{-1}\,\Delta T_* \,, \tag{4}$$

where

$$\Delta Q = \sum_i \frac{\partial N}{\partial E_i}\,\Delta E_i \tag{5}$$

is the change in N due to a change in one or more external quantity, ΔE_i, and

$$G_f^{-1} = -\frac{dN}{dT_*} = -\frac{\partial N}{\partial T_*} - \sum_j \frac{\partial N}{\partial I_j}\frac{dI_j}{dT_*} \tag{6}$$

is the change in N resulting from a temperature change, ΔT_*. From Eq. (4) the energy balance requirement, $\Delta N = 0$, gives

$$\Delta T_* = G_f\,\Delta Q \ , \tag{7}$$

from which it is seen that G_f is the gain (output/input) of the system.

It is useful to express G_f as

$$G_f^{-1} = G_o^{-1} - F \ , \tag{8}$$

where

$$G_o = -\left(\frac{\partial N}{\partial T_*}\right)^{-1} \tag{9}$$

is the climate system gain in the absence of feedback and

$$F = \sum_j \frac{\partial N}{\partial I_j} \frac{dI_j}{dT_*} \tag{10}$$

represents the feedbacks. Then, by Eq. (7),

$$\Delta T_* = \frac{G_o}{1 - G_o F} \Delta Q \quad . \tag{11}$$

This relation can be represented by a system block diagram as shown in Fig. 1. If N is independent of the internal quantities $\underline{I}$, or if $\underline{I}$ is independent of T_*, then $F = 0$ and the input ΔQ to the system is directly transferred to the output

$$\Delta T_* = (\Delta T_*)_o \equiv G_o \, \Delta Q \tag{12}$$

by means of only those processes for which N explicitly depends on T_*. However, if N also depends implicitly on T_*, through its dependence on the internal quantities and their dependence on T_*, part of the output

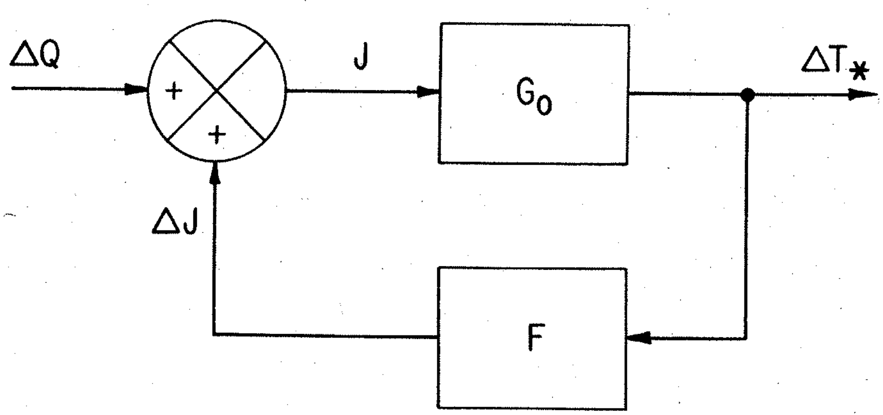

Figure 1. Block diagram of the climatic system with a feedback loop. Here ΔQ is the forcing of the climate system, for example, due to a change in the CO_2 concentration; ΔT_* is the response of the surface temperature as a result of the zero-feedback gain, G_o, and the feedback, $f = G_oF$, of the climate system. The quantity $J = \Delta Q + \Delta J$, where $\Delta J = F\Delta T_*$ and $\Delta T_* = G_oJ$.

is transferred through
be seen from Fig. 1, th

$J = \Delta Q + \Delta J$,

where ΔQ is the externa

$\Delta J = F\Delta T_*$

is the contribution of
system is

$\Delta T_* = G_oJ = G$

Solving for ΔT_* then gi
surface temperature ΔT_*
tem with feedback.
The effect of the
ratio of the ΔT_* with f
Eqs. (11) and (12), we

$R_f \equiv \frac{\Delta T_*}{(\Delta T_*)_o} =$

where

$f = G_oF$

is the feedback factor
feedback.[1] For $f = 0$,
temperature change. Si
negative feedback (see
indefinitely, $R_f \to 0$ an
ΔT_* does not change sig
latter represents posit
unity, $R_f \to \infty$ and $\Delta T_* \to$
beyond unity, R_f would
values as $f \to \infty$. Clear
However, as we shall se
positive feedbacks that
obtained for heating ΔC

1 Hansen et al. (1984)
f) the net feedback

2 If $f > 1$, an increas
in the solar constar
decrease in energy Δ

(9)

edback and

(10)

(11)

ock diagram as shown in
antities I, or if I is
to the system is directly

(12)

plicitly depends on T_*.
rough its dependence on
T_*, part of the output

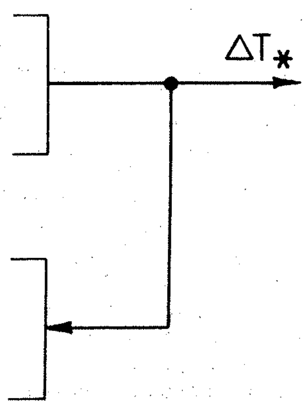

with a feedback loop.
or example, due to a
ponse of the surface tem-
G_o, and the feedback,
$= \Delta Q + \Delta J$, where

is transferred through a feedback loop back to the input. Then, as can be seen from Fig. 1, the input to the climate system, J, is

$$J = \Delta Q + \Delta J \ , \tag{13}$$

where ΔQ is the external forcing and

$$\Delta J = F\Delta T_* \tag{14}$$

is the contribution of the feedbacks, and the output of the climate system is

$$\Delta T_* = G_o J = G_o(\Delta Q + F\Delta T_*) \quad . \tag{15}$$

Solving for ΔT_* then gives Eq. (11). Consequently, the response of the surface temperature ΔT_* to the forcing ΔQ is analogous to that of a system with feedback.

The effect of the feedback can be characterized on the basis of the ratio of the ΔT_* with feedback to that without feedback. Thus, by Eqs. (11) and (12), we define the feedback gain ratio

$$R_f \equiv \frac{\Delta T_*}{(\Delta T_*)_o} = \frac{G_f}{G_o} = \frac{1}{1 - f} \quad , \tag{16}$$

where

$$f = G_o F \tag{17}$$

is the feedback factor (Bode, 1975, p. 32) or, here, simply the feedback.[1] For $f = 0$, $R_f = 1$; hence $(\Delta T_*)_o$ represents the zero-feedback temperature change. Since $0 < R_f < 1$ for $f < 0$, the latter represents negative feedback (see Fig. 2). As negative feedback increases indefinitely, $R_f \to 0$ and $\Delta T_* \to 0$; however, it is important to note that ΔT_* does not change sign as $f \to -\infty$. Since $R_f > 1$ for $0 < f < 1$, the latter represents positive feedback. As positive feedback approaches unity, $R_f \to \infty$ and $\Delta T_* \to \infty$. If the positive feedback could be extended beyond unity, R_f would change sign and approach zero from negative values as $f \to \infty$. Clearly, the region $f > 1$ is physically meaningless.[2] However, as we shall see, one SEBM has estimated de facto such strong positive feedbacks that $f > 1$ and a temperature decrease $\Delta T_* < 0$ was obtained for heating $\Delta Q > 0$!

---

[1] Hansen et al. (1984) call f (their g) the system gain and R_f (their f) the net feedback factor.

[2] If $f > 1$, an increase in energy $\Delta Q > 0$, for example from an increase in the solar constant, would result in a cooling $\Delta T_* < 0$, and a decrease in energy $\Delta Q < 0$ in a warming $\Delta T_* > 0$.

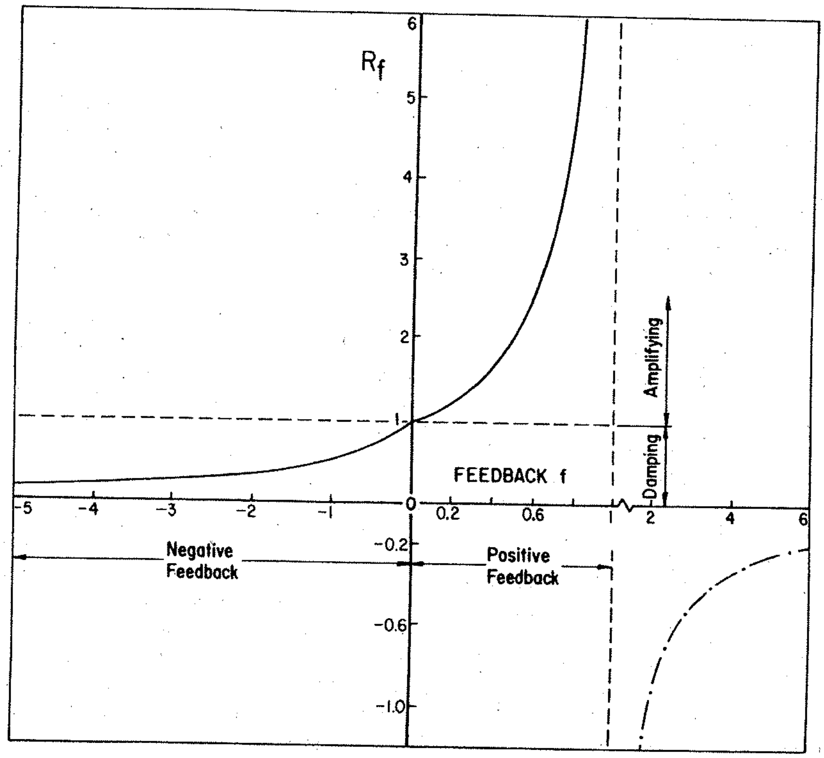

Figure 2. The feedback gain ratio $R_f = \Delta T_s/(\Delta T_s)_o$ of the surface temperature change with feedback (ΔT_s) to the surface temperature change without feedback $(\Delta T_s)_o$ versus the feedback f.

From Eqs. (5), (9), (10), (16) and (17) we can write

$$\Delta T_* = \frac{G_o}{1 - f} \Delta Q \ , \tag{18}$$

where

$$f = G_o \sum_j \frac{\partial N}{\partial I_j} \frac{dI_j}{dT_*} \ , \tag{19}$$

$$G_o = -\left(\frac{\partial N}{\partial T_*}\right)^{-1} \tag{20}$$

and

$$\Delta Q = \sum_i \frac{\partial N}{\partial E_i} \Delta E_i$$

Thus, the determination
tion requires knowledge
feedback gain of the sys
quire knowledge of the p
concentration, the tempe
the total derivative of
temperature. In the nex
models from this vantage

2.2. Surface Energy Bal

The net downward energy
expressed by

$$N_s = S_s - R_s -$$

where S_s is the net down
terrestrial (longwave) r
tent heat due to evapora
and H_s is the net upward
T_* is the temperature of
The results from th
the thermal forcing ΔQ f
$\Delta C/C$, the system gain, G
The table shows that the
most two orders of magni
wide range is due to dif
with ΔQ varying by a fac
Because the differences
ated by the use of conte
of radiative transfer (s
an examination of the re

2.2.1. Callendar (1938
CO_2-induced warming was
his study S_s, E_s and H_s

$$N_s = R_s^{\downarrow}(C) - ($$

where $R_s^{\downarrow}$ and σT_s^4 are the
tively, C represents the
Boltzmann constant (5.6
a function of T_s, the z

$$G_o = (4\sigma T_s^3)^{-1}$$

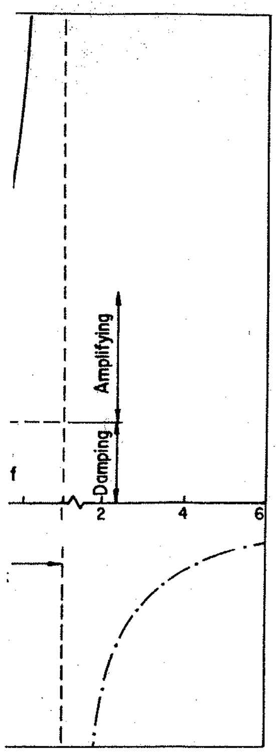

$_s)_o$ of the surface tem-
ace temperature change

can write

(18)

(19)

(20)

$$\Delta Q = \sum_i \frac{\partial N}{\partial E_i} \Delta E_i \ . \tag{21}$$

Thus, the determination of ΔT_* induced by an increase in CO_2 concentration requires knowledge of the associated thermal forcing ΔQ, the zero-feedback gain of the system G_o, and the feedback f. These in turn require knowledge of the partial derivatives of N with respect to the CO_2 concentration, the temperature, and the internal quantities, as well as the total derivative of the internal quantities with respect to the temperature. In the next section we examine the surface energy balance models from this vantage point.

2.2. Surface Energy Balance Models

The net downward energy flux at the Earth's surface, N_s, can be expressed by

$$N_s = S_s - R_s - E_s - H_s \ , \tag{22}$$

where S_s is the net downward solar radiation flux, R_s is the net upward terrestrial (longwave) radiation flux, E_s is the net upward flux of latent heat due to evaporation of water and sublimation of snow and ice, and H_s is the net upward sensible heat flux. In SEBMs the temperature T_* is the temperature of the Earth's surface, T_s.

The results from three SEBMs are presented in Table 1 in terms of the thermal forcing ΔQ for a fractional increase in CO_2 concentration, $\Delta C/C$, the system gain, G_f, and the surface temperature response, ΔT_s. The table shows that the values of ΔT_s for a CO_2 doubling range over almost two orders of magnitude, from about 0.2°C to almost 10°C. This wide range is due to differences in both ΔQ and G_f among the models, with ΔQ varying by a factor of about 7, and G_f by a factor of about 30. Because the differences shown in Table 1 for ΔQ can be virtually eliminated by the use of contemporary line-by-line or calibrated band models of radiative transfer (see Luther, 1984), we restrict attention here to an examination of the reasons for the large variation in G_f.

2.2.1. Callendar (1938). One of the earliest calculations of CO_2-induced warming was performed by Callendar (1938) with an SEBM. In his study S_s, E_s and H_s were ignored so that Eq. (22) becomes

$$N_s = R_s^{\downarrow}(C) - \sigma T_s^4 \ , \tag{23}$$

where $R_s^{\downarrow}$ and σT_s^4 are the downward and upward longwave fluxes, respectively, C represents the CO_2 concentration, and σ is the Stefan-Boltzmann constant (5.6687×10^{-8} Wm^{-2} K^{-4}). Since $R_s^{\downarrow}$ is not explicitly a function of T_s, the zero-feedback gain is, by Eqs. (20) and (23),

$$G_o = (4\sigma T_s^3)^{-1} \ . \tag{24}$$

Table 1. Forcing, gain and response of selected surface energy balance models

Model	$\Delta C/C$	ΔQ (Wm^{-2})	G_f $(°C/Wm^{-2})$	ΔT_s $(°C)$
Callendar (1938)	1	6.72	0.195	1.3
Möller (1963)	1	3.08	3.113	9.6
Newell and Dopplick (1979)	0.8	1	0.237	0.24

Thus, G_o rapidly decreases with increasing T_s. For T_s = 283 K assumed by Callendar, $G_o = 0.195°C/(Wm^{-2})$. Callendar did not consider any feedback, hence as shown in Table 2, f = 0 and $G_f = G_o = 0.195°C/(Wm^{-2})$.

2.2.2. Möller (1963). Möller (1963) considered three SEBMs. First, Möller assumed that the surface energy flux was

$$N_s = R_s^{\downarrow}(C,T_a) - \sigma T_s^4 \quad , \tag{25}$$

where T_a represents the vertical profile of atmospheric temperature. Again, because $R_s^{\downarrow}$ is not explicitly a function of T_s, the zero-feedback gain is given by Eq. (24) as $G_o = 0.185°C/(Wm^{-2})$ for the assumed T_s = 288 K. The internal variables in this model are the atmospheric temperatures, so by Eqs. (19) and (25)

$$f = G_o \sum \frac{\partial R_s^{\downarrow}}{\partial T_a} \frac{dT_a}{dT_s} = G_o \frac{dR_s^{\downarrow}}{dT_s} \quad . \tag{26}$$

Möller prescribed $T_a = -55°C$ in the stratosphere and $T_a = T_s - \Gamma z$ in the troposphere, where z is altitude, and the lapse rate $\Gamma = 6.5°C\ km^{-1}$. Instead of determining f by Eq. (26), Möller determined $dN_s/dT_s = (dR_s^{\downarrow}/dT_s) - 4\sigma T_s^3$ by computing N_s from a radiation diagram for several values of T_s, each with the attendant change in T_a, and then by expressing the result as $N_s(T_s)$ by an approximate interpolation formula. The result can be written by Eq. (6) as

$$G_f \equiv - \left(\frac{dN_s}{dT_s}\right)^{-1} = 0.477°C\ (Wm^{-2})^{-1} \quad , \tag{27}$$

which is in agreement with the value found similarly by Plass (1956). Then by Eq. (16) we find of selected surface

G_f (°C/Wm 2)	ΔT_s (°C)
0.195	1.3
3.113	9.6
0.237	0.24

For T_s = 283 K assumed
lid not consider any feed-
: G_o = 0.195°C/(Wm^{-2}).

:d three SEBMs. First,
;

(25)

ıospheric temperature.
of T_s, the zero-feedback
') for the assumed
iel are the atmospheric

(26)

re and $T_a = T_s - \Gamma z$ in the
e rate Γ = 6.5°C km^{-1}.
etermined dN_s/dT_s =
ion diagram for several
1 T_a, and then by express-
erpolation formula. The

(27)

ilarly by Plass (1956).

Table 2. Gain and feedback characteristics of selected surface energy balance models

Model	Fluxes Included	V_s (ms^{-1})	G_o (°C/Wm^{-2})	Feedbacks					G_f (°C/Wm^{-2})
				f_{TR}	f_{WR}	f_{WE}	f_{TH}	f	
Callendar (1938)	$R_s^{\downarrow}$, σT_s^4	--	0.1950	0	0	0	0	0	0.195
Möller (1963)	$R_s^{\downarrow}$, σT_s^4, S_s	--	0.1850	0.6122	0.3284	0	0	0.9406	3.113
Newell and Dopplick (1979)	$R_s^{\downarrow}$, σT_s^4, S_s, E_s, H_s	0	0.1633	0.8411	0	0	0	0.8411	1.028
		3	0.0260	0.1342	0	0	0	0.1342	0.030
		6	0.0142	0.0733	0	0	0	0.0733	0.015
Illustration based on Newell and Dopplick (1979)	$R_s^{\downarrow}$, σT_s^4, S_s, E_s, H_s	0	0.1633	0.8411	0	0	0	0.8411	1.028
		3	0.0260	0.1342	0	0.6431	0.1958	0.9731	0.967
		6	0.0142	0.0733	0	0.7024	0.2139	0.9896	1.365

$$f = f_{TR} = 1 - \frac{G_o}{G_f} = 0.6122 \quad . \tag{28}$$

Since this positive feedback is due to the increase in $R_s^{\downarrow}$ that occurs when T_a increases, the latter as a result of the increase in T_s, we shall call it a temperature/radiation feedback, f_{TR} (Table 2).

As a second SEBM, Möller assumed that

$$N_s = R_s^{\downarrow}(C,T_a,W) - \sigma T_s^4 \quad , \tag{29}$$

where

$$W = \int_0^{\infty} \rho_a \, q_a \, dz \tag{30}$$

represents the total amount of water vapor in the atmospheric column, with ρ_a the air density and q_a the specific humidity. The internal variables are now T_a and W, and

$$f = f_{TR} + G_o \frac{\partial R_s^{\downarrow}}{\partial W} \frac{dW}{dT_s} \quad . \tag{31}$$

Again Möller did not determine f from Eq. (31), but instead he determined dN_s/dT_s by computing N_s from a radiation diagram for several values of T_s with the relative humidity RH assumed constant at 75%. In this case, T_a and W increase as T_s increases, the latter by Eq. (30) because $q_a = RH\, q^*(T_s,p)$, where q^* is the saturation specific humidity, and q^* increases rapidly with T_s. From an approximate interpolation formula for $N_s(T_s,W)$ Möller obtained $G_f = -2.864°C/(Wm^{-2})$. Then by Eqs. (28) and (31) we find $f = 1.0646$ and

$$f_{WLR} \equiv G_o \frac{\partial R_s^{\downarrow}}{\partial W} \frac{dW}{dT_s} = 0.4524 \quad , \tag{32}$$

where f_{WLR} is a water vapor/longwave radiation feedback due to the increase in $R_s^{\downarrow}$ as W increases, that is, the greenhouse effect for water vapor, and the increase in W with T_s as a result of the constant RH.

The combination of f_{TR} and f_{WLR} is larger than unity, hence these positive feedbacks combine to yield the physically unrealistic result that $\Delta T_s < 0$ for $\Delta Q > 0$. Möller realized this inconsistency and therefore proposed a third SEBM, namely,

$$N_s = S_s(W) + R_s^{\downarrow}(C,T_a,W) - \sigma T_s^4 \quad . \tag{33}$$

Then,

$f = f_{TR} + f_{WLR}$

where

$f_{WSR} \equiv G_o \frac{\partial S_s}{\partial W}$

is a water vapor/solar r
from his radiation diagr
$G_f = 3.113°C/(Wm^{-2})$. Th
$f_{WSR} = -0.1240$. The wat
since S_s decreases as W
RH. The two effects of
single water vapor/radia

$f_{WR} = f_{WLR} + f$

The combined effect of t
radiation feedbacks is s

2.2.3. Newell and Doppl
concerned about the 2-3°
radiative-convective and
investigated the effects
CO_2-induced temperature

$N_s = S_s(C,q_a)$

$- E_s(T_s,q$

where

$E_s = 6080\ V_s(q$

and

$H_s = 2.51\ V_s(T$

Here T_a and q_a represent
the surface air, V_s the
tion specific humidity a
Eq. (20) we find

$G_o = -(\frac{\partial N_s}{\partial T_s})^{-1}$

(28)

ease in $R_s^\downarrow$ that occurs
e increase in T_s, we
f_{TR} (Table 2).

(29)

(30)

he atmospheric column,
midity. The internal

(31)

, but instead he deter-
diagram for several
umed constant at 75%. In
the latter by Eq. (30)
ration specific humidity,
roximate interpolation
64°C/(Wm^{-2}). Then by

(32)

feedback due to the in-
nhouse effect for water
lt of the constant RH.
than unity, hence these
ally unrealistic result
inconsistency and there-

(33)

Then,

$$f = f_{TR} + f_{WLR} + f_{WSR} \quad , \tag{34}$$

where

$$f_{WSR} \equiv G_o \frac{\partial S_s}{\partial W} \frac{dW}{dT_s} \tag{35}$$

is a water vapor/solar radiation feedback. Möller determined dN_s/dT_s from his radiation diagram and a model for the solar radiation and found $G_f = 3.113°C/(Wm^{-2})$. Then by Eqs. (28), (32) and (34), $f = 0.9406$ and $f_{WSR} = -0.1240$. The water vapor/solar radiation feedback is negative since S_s decreases as W increases, and W increases with T_s for fixed RH. The two effects of water vapor on radiation can be combined into a single water vapor/radiation feedback, f_{WR}, as

$$f_{WR} = f_{WLR} + f_{WSR} = 0.3284 \quad . \tag{36}$$

The combined effect of the temperature/radiation and water vapor/radiation feedbacks is strongly positive (Table 2).

2.2.3. Newell and Dopplick (1979). Newell and Dopplick (1979), concerned about the 2-3°C warming of the tropical oceans simulated by radiative-convective and general circulation models for a CO_2 doubling, investigated the effects of the latent and sensible heat fluxes on the CO_2-induced temperature change. Their SEBM is described by

$$\begin{aligned} N_s = {} & S_s(C,q_a) + R_s^\downarrow(C,T_a,q_a) - \sigma T_s^4 \\ & - E_s(T_s,q_a) - H_s(T_s,T_a) \quad , \end{aligned} \tag{37}$$

where

$$E_s = 6080\, V_s(q_s^* - q_a) \quad , \tag{38}$$

and

$$H_s = 2.51\, V_s(T_s - T_a) \quad . \tag{39}$$

Here T_a and q_a represent the temperature and specific humidity (g/kg) of the surface air, V_s the surface wind speed (m s^{-1}), and q_s^* the saturation specific humidity at T_s and surface pressure p_s (mb). From Eq. (20) we find

$$G_o = -\left(\frac{\partial N_s}{\partial T_s}\right)^{-1} = \left[4\sigma T_s^3 + V_s\left(6080 \frac{\partial q_s^*}{\partial T_s} + 2.51\right)\right]^{-1} \quad . \tag{40}$$

Comparing this with Eq. (24) shows that G_o depends upon which fluxes are included in the surface energy budget; here, G_o depends on V_s as well as T_s. (This definition of G_o is not unique. Alternatively, G_o can be defined as in Eq. (27) with E_s and H_s then contributing only to f.) From Eq. (19)

$$f = f_{TR} + f_{WR} + f_{WE} + f_{TH} \quad , \tag{41}$$

where

$$f_{TR} = G_o \frac{\partial R_s^{\downarrow}}{\partial T_a} \frac{dT_a}{dT_s} \quad , \tag{42}$$

$$f_{WR} = G_o\left(\frac{\partial R_s^{\downarrow}}{\partial q_a} + \frac{\partial S_s}{\partial q_a}\right) \frac{dq_a}{dT_s} \quad , \tag{43}$$

$$f_{WE} = - G_o \frac{\partial E_s}{\partial q_a} \frac{dq_a}{dT_s} = G_o(6080\ V_s) \frac{dq_a}{dT_s} \quad , \tag{44}$$

and

$$f_{TH} = - G_o \frac{\partial H_s}{\partial T_a} \frac{dT_a}{dT_s} = G_o(2.51\ V_s) \frac{dT_a}{dT_s} \quad . \tag{45}$$

f_{WE} represents a water vapor/evaporation feedback and f_{TH} a temperature/sensible heat feedback.

Following the approach taken by Plass (1956) and Möller (1963), Newell and Dopplick determined the equivalent of f_{TR}/G_o from an expression for $\sigma T_s^4 - R_s^{\downarrow}(T_s,q_a)$ given by Privett (1960). The result can be written as

$$f_{TR} = G_o\left(0.474 + 0.075\sqrt{q_a p_s/0.622}\right) 4\sigma T_s^3 \quad . \tag{46}$$

In so doing, because $R_s^{\downarrow}$ is not explicitly a function of T_s, it was implicitly assumed that T_a is not constant, but rather changes as T_s changes. However, Newell and Dopplick otherwise explicitly assumed that both T_a and q_a do not change as T_s changes; hence by Eqs. (43)-(45), it was assumed that $f_{WR} = f_{WE} = f_{TH} = 0$ and, therefore, $f = f_{TR}$. It is evident that $f_{TR} \neq 0$ and $f_{TH} = 0$ are consistent for this model only for $V_s = 0$.

For $T_s = 300$ K and $q_a = 15 \times 10^{-3}$, as selected by Newell and Dopplick, with $p_s = 1000$ mb,

$$G_o = (6.122 + 10.757\ V_s)^{-1} \tag{47}$$

and

$$f = f_{TR} = 5.16\ G_o, \tag{48}$$

with the values shown in Table 2 for $V_s = 0$, 3 and 6 m s^{-1}. For $V_s = 0$, G_o is smaller than the values given by Callendar (1938) and Möller (1963) as a result of the large (tropical) value for T_s. Also, f_{TR} is larger than the values given by Callendar (1938) and Möller (1963) due to the large (tropical) values for q_a. Consequently, for the case of no latent and sensible heat transfer, that is, $V_s = 0$, G_f obtained by Newell and Dopplick is comparable to that obtained by Möller (1963) with only the temperature/radiation feedback. However, as evident from Eqs. (46), (47) and Table 2, G_o and f_{TR} both rapidly decrease as V_s increases, with the result that G_f decreases from 1.028 to 0.030°C/(Wm^{-2}) as the wind increases from 0 to only 3 m s^{-1}. This decrease in G_f with increasing V_s when the latent and sensible heat fluxes are included in the SEBM has sometimes been called negative feedback. However, as Table 2 shows, the feedback $f = f_{TR}$ is actually positive. The decrease in G_f is predominantly the result of the decrease in the zero-feedback gain G_o with increasing V_s.

The value of $G_f = 0.24$ given by Newell and Dopplick (Table 1) was obtained as a weighted average of the 3 m s^{-1} value of $G_f = 0.030$ for the 92% tropical ocean area, and the value by Möller of $G_f = 0.477$ for $f = f_{TR}$ [from Table 2 by Eq. (16)] for the 8% tropical land area and multiplication by a factor of 3.5 to account for the effect of a nonzero water vapor/radiation feedback. The climatic gain obtained by Newell and Dopplick has been cited by Idso (1980) in support of his empirical result.

The cause of the dramatic decrease in G_f with increasing V_s is the assumption that T_a and q_a do not change. This fact can be demonstrated by choosing what could be called the other limit, namely, that $T_s - T_a$ and $q_s^* - q_a$ do not change. In this limit, by Eqs. (44) and (45),

$$f_{WE} = 6080\ V_s \frac{\partial q_s^*}{\partial T_s} G_o = 8.244\ V_s\ G_o \quad , \tag{49}$$

and

$$f_{TH} = 2.510\ V_s\ G_o \quad , \tag{50}$$

with the results shown in Table 2. For $V_s = 0$, hence no latent or sensible heat, G_f is as before. However, for $V_s \neq 0$, both f_{WE} and f_{TH} are positive, with $f_{WE} = 3.3\ f_{TH}$, and increase with increasing V_s. Even ignoring f_{WR}, the sum of the feedbacks now increases with V_s. G_f still decreases from $V_s = 0$ to $V_s = 3$ m s^{-1}, but much less than for the Newell and Dopplick limit, and now increases from $V_s = 3$ to $V_s = 6$ m s^{-1}.

2.2.4. Summary. The wide range in the values of G_f obtained from SEBMs shown in Tables 1 and 2 is, in part, a consequence of the nonlinear dependence of G_f on f. From Eq. (16)

$$\frac{\partial G_f}{\partial f} = \frac{G_o}{(1-f)^2} , \tag{51}$$

hence, the change in G_f resulting from a given change in f rapidly increases as $f \to 1$ (Fig. 2). This sensitivity of G_f to f means that f must be determined with both high accuracy and precision. The difficulty of achieving this has been due to the neglect of certain fluxes in the earlier SEBMs, and to the inability of SEBMs in general to determine the behavior of the climate system away from the surface energy balance level.

The surface and the troposphere are strongly coupled, hence neither the surface nor the atmosphere can be considered in isolation. Because of the inherent difficulty of specifying the behavior of the atmosphere in terms of the surface temperature in SEBMs, i.e., $I(T_s)$, and the large sensitivity of ΔT_s in SEBMs to this specification, it is preferable to use models which calculate the atmosphere's behavior based on the fundamental laws of physics.

2.3. Planetary Energy Balance Models

The planetary radiative energy budget is

$$N_o = \frac{1-\alpha_p}{4} S_o - R_o \quad , \tag{52}$$

where N_o is the net radiation at the top of the atmosphere, S_o is the solar constant (~ 1370 Wm^{-2}), R_o is the upward longwave radiation flux at the top of the atmosphere, and α_p is the planetary albedo (~ 0.3). To balance the planetary radiative energy budget requires that $N_o = 0$; hence,

$$R_o = \frac{1-\alpha_p}{4} S_o \sim 240 \ Wm^{-2} \quad . \tag{53}$$

An effective radiating temperature of the Earth, T_e, can be defined by

$$T_e = \left(\frac{R_o}{\sigma}\right)^{1/4} \sim 255 \ K \quad . \tag{54}$$

Hence by Eqs. (52) and (54),

$$N_o = \frac{1-\alpha_p}{4} S_o - \sigma T_e^4 \quad . \tag{55}$$

N_o can be expressed in terms of the surface temperature T_s rather than T_e by introducing an effective planetary emissivity, ε_p, as

$$\varepsilon_p = \left(\frac{T_e}{T_s}\right)^4 \sim 0.6 \quad . \tag{56}$$

Then by Eq. (55)

$$N_o = \frac{1-\alpha_p}{4} S_o - \varepsilon_p \sigma T_s^4 \quad . \tag{57}$$

Letting $T_* = T_s$, the zero-feedback gain G_o is given by Eqs. (9) and (57) as

$$G_o = \left(4\varepsilon_p \sigma T_s^3\right)^{-1} \quad , \tag{58a}$$

and

$$G_o = \frac{T_s}{(1-\alpha_p)S_o} \quad , \tag{58b}$$

which can be compared with Eq. (24). It can be seen that G_o depends on T_s and ε_p (or α_p and S_o) of the unperturbed climate and, in contrast to SEBMs, does not depend on the type and treatment of the physical processes in the model. Taking T_s as being approximately equal to the observed surface air temperature, T_a = 288 K, gives $G_o \sim 0.3°C/(Wm^{-2})$.

The feedback f is given by

$$f = G_o \sum_j \frac{\partial N}{\partial I_j} \frac{dI_j}{dT_s} \quad , \tag{59}$$

where I_j are again the internal variables of the climate system. It can be seen here that the feedback depends on the specification of the behavior of the atmosphere and the Earth's surface. Thus, PEBMs also have the same problem as SEBMs, namely, the need to treat the behavior of the climate system away from the energy balance level. In PEBMs this has been done semi-empirically following the initial studies by Budyko (1969) and Sellers (1969). The equilibrium surface temperature change for a CO_2 doubling ranges in PEBMs from 0.6°C (Rasool and Schneider, 1971) to 3.3°C (Ramanathan et al., 1979).

3. RADIATIVE-CONVECTIVE MODELS

As was evident from the discussion of the preceding section, the essential difficulty in using EBMs to determine climatic change lies in their inability to determine the feedbacks accurately and precisely. This occurs because of the limited set of internal variables that can be selected in these models, and because of the limited knowledge of the relationships of the chosen internal variables to the surface temperature. Simply stated, EBMs are limited because they do not have a physically-based model of the atmosphere.

What physical processes must be included in such a model of the atmosphere if the objective is to simulate the change in the surface temperature ΔT_s induced by a change in the CO_2 concentration ΔC? If we knew ΔT_s observationally, as we will presumably in the future, then we could answer the question by sequentially inserting different processes into the model and retaining only those which significantly contribute to ΔT_s. Because we cannot do this yet, we can take the not unreasonable approach of determining which processes are required in the model to reproduce the present-day temperature profile of the atmosphere, T(z). Proceeding in this way, however, does not guarantee that some physical processes essential to the determination of ΔT_s may not be important for the reproduction of T(z), and, therefore, that some essential physical processes (and feedbacks) are not left out of the model.

3.1. Model Formulation

Certainly the transfers of solar and longwave radiation are essential physical processes in establishing the atmospheric temperature profile. Accordingly, a thermodynamic climate model based solely on the thermodynamic energy equation can be developed that includes only the heating and cooling by solar and longwave radiation, respectively, that is,

$$\rho c_p \frac{\partial T}{\partial t} = \frac{\partial S}{\partial z} - \frac{\partial R}{\partial z} \quad , \tag{60}$$

where t is time, z is altitude, ρ is density, c_p is the heat capacity at constant pressure, S is the downward solar radiation flux, and R is the net upward longwave radiation flux. The calculation of the radiative fluxes requires a radiative transfer model and knowledge of the vertical distributions of the absorbers - principally water vapor, carbon dioxide, ozone and clouds - which may be prescribed along with the solar constant, the solar zenith angle and the albedo of the Earth's surface. The atmosphere may then be subdivided vertically into layers and the radiative-equilibrium temperature for each layer determined by integrating Eq. (60) in time from an arbitrary initial temperature until $\partial T/\partial t = 0$ for all layers. Such a purely radiative thermodynamic climate model is successful in reproducing the observed vertical temperature distribution of the stratosphere, but it gives temperatures that are colder in the upper troposphere and warmer near the surface than observed (Manabe and Strickler, 1964). The resulting tropospheric temperature lapse rate, $\Gamma = -\partial T/\partial z$, is larger than the dry adiabatic lapse rate, $\Gamma_d \approx 10$ K km^{-1}, which defines the neutral stratification for the vertical displacement of unsaturated air. This superadiabatic stratification $\Gamma > \Gamma_d$ is unstable and cannot persist in the actual atmosphere due to the ameliorating processes of convection. Accordingly, Eq. (60) must be

curately and precisely.
ernal variables that can be
limited knowledge of the
s to the surface
because they do not have a

in such a model of the
e change in the surface
2 concentration ΔC? If we
ly in the future, then we
erting different processes
significantly contribute
n take the not unreasonable
equired in the model to re-
f the atmosphere, $T(z)$.
rantee that some physical
T_s may not be important for
t some essential physical
the model.

radiation are essential
heric temperature profile.
sed solely on the thermo-
includes only the heating
respectively, that is,

(60)

c_p is the heat capacity at
idiation flux, and R is the
ulation of the radiative
d knowledge of the vertical
water vapor, carbon
scribed along with the solar
edo of the Earth's surface.
ally into layers and the
ayer determined by integrat-
al temperature until
lative thermodynamic climate
ved vertical temperature
es temperatures that are
ear the surface than observ-
ing tropospheric temperature
ry adiabatic lapse rate,
ratification for the verti-
uperadiabatic stratification
actual atmosphere due to
ccordingly, Eq. (60) must be

modified to include the nonradiative transfer of energy from the surface to the atmosphere, Q_{sfc}, as well as the convective redistribution of energy within the atmosphere, Q_{conv}, that is,

$$\rho c_p \frac{\partial T}{\partial t} = \frac{\partial S}{\partial z} - \frac{\partial R}{\partial z} + Q_{sfc} + Q_{conv} \quad . \tag{61}$$

The physical processes that comprise Q_{sfc} and Q_{conv} are complex because they involve the turbulent transfer of energy in both unsaturated and saturated conditions, and would, if explicitly treated, place an impractical computational burden on the model. Consequently, simplified (parameterized) treatments of these processes have been in use since the pioneering work of Manabe and Strickler (1964) in which Q_{sfc} was determined as an equivalent radiative energy exchange and Q_{conv} determined by convective adjustment. In the latter, the temperatures of consecutive model layers are adjusted in an energetically conservative manner such that the lapse rate is restored to a prescribed value Γ_p whenever $\Gamma > \Gamma_p$. This type of model is called a radiative-convective model or RCM and, as first shown by Manabe and Strickler (1964), is capable of reproducing many of the observed features of the temperature profiles in both the stratosphere and troposphere.

Since the development of the first RCM by Manabe and Strickler (1964), a large number of RCMs have been constructed with different radiative transfer models, different parameterizations of Q_{sfc} and Q_{conv}, and additional physical processes and feedbacks of potential importance for CO_2-induced (and other) climatic changes. It will be useful in what follows to tabulate here in Table 3 the physical processes whose treatments differ among the RCMs, along with a brief descriptor and abbreviation of these different treatments.

In the following sections we first present the results for CO_2-induced temperature changes obtained by RCMs and then analyze these results in terms of the feedbacks associated with the physical processes shown in Table 3.

3.2. Results

The first study with an RCM of CO_2-induced temperature change was carried out by Manabe and Wetherald (1967). In their RCM the cosine of the zenith angle and the length of the day were taken equal to their respective annual mean values for the globe[3]. The surface energy flux was treated as an equivalent radiative exchange, convection was parameterized by convective adjustment with a fixed critical lapse rate, the atmospheric water vapor mixing ratio was calculated assuming a fixed profile of relative humidity, and three cloud layers with fixed pressure were prescribed along with a fixed surface albedo. The equilibrium

[3] The cosine of the zenith angle ζ cannot be arbitrarily chosen if an RCM is to represent the global mean; as indicated by Eq. (52), $\cos \zeta = 1/4$ is required.

Table 3. Physical processes whose treatments differ among RCMs

Physical Process	Treatment	Abbreviation
Surface energy flux	Equivalent radiative exchange	ERE
	Bulk aerodynamic exchange	BAE
Water Vapor	Fixed absolute humidity	FAH
	Fixed relative humidity	FRH
	Variable relative humidity	VRH
Convection	Fixed lapse rate	FLR
	Moist adiabatic lapse rate	MALR
	Baroclinic adjustment	BADJ
	Penetrative convection	PC
Clouds	No cloud	CLR
	Fixed cloud altitude	FCA
	Fixed cloud pressure	FCP
	Fixed cloud temperature	FCT
	Predicted clouds	PCL
	Fixed cloud cover	FCC
	Variable cloud cover	VCC
	Fixed optical depth	FOD
	Variable optical depth	VOD
Surface albedo	Fixed albedo	FAL
	Predicted albedo	PAL

vertical temperature profiles computed for prescribed CO_2 concentrations of 150, 300 and 600 ppmv are shown in Fig. 3. Each profile exhibits a troposphere between the surface and about 13 km with a lapse rate Γ equal to the prescribed critical value Γ_p, and a stratosphere from 13 to 42 km where the temperature is first isothermal and then increases with increasing altitude. The stable stratification in the stratosphere shows that it is in pure radiative equilibrium, while the critical lapse rate of the troposphere indicates that it is in radiative-convective equilibrium. Figure 3 shows that doubling the CO_2 concentration, either from 150 to 300 ppmv or from 300 to 600 ppmv, increases the temperature at the surface and in the troposphere, and decreases the temperature in the stratosphere above 20 km.

The surface temperature changes simulated by 17 RCMs for a doubled CO_2 concentration are presented in Table 4. It is seen that the values are all positive and range from a minimum of 0.48°C to a maximum of 4.20°C. In the next section we analyze the physical processes that

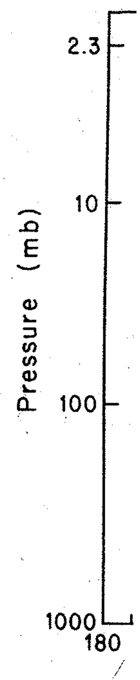

Figure 3. Vertical distr
equilibrium for fixed rel
The surface temperature c
300 ppmv and 2.36°C for 3
1967.)

result in this wide range
induced by a doubling of

3.3. Analysis and Interp

Why does the temperature
stratosphere when the CO_2
estimated surface tempera
answer these questions we
forcing due to the increa
the temperature response
examine the CO_2-induced t
the RCM studies presented

3.3.1. Direct radiative
95% of the direct radiati

differ among RCMs

	Abbreviation
exchange	ERE
ange	BAE
ty	FAH
ty	FRH
idity	VRH
	FLR
rate	MALR
	BADJ
n	PC
	CLR
	FCA
	FCP
re	FCT
	PCL
	FCC
	VCC
	FOD
h	VOD
	FAL
	PAL

escribed CO_2 concentrations
Each profile exhibits a
km with a lapse rate Γ
id a stratosphere from 13 to
ial and then increases with
ion in the stratosphere
im, while the critical lapse
in radiative-convective
ie CO_2 concentration, either
, increases the temperature
ecreases the temperature in

ed by 17 RCMs for a doubled
It is seen that the values
0.48°C to a maximum of
physical processes that

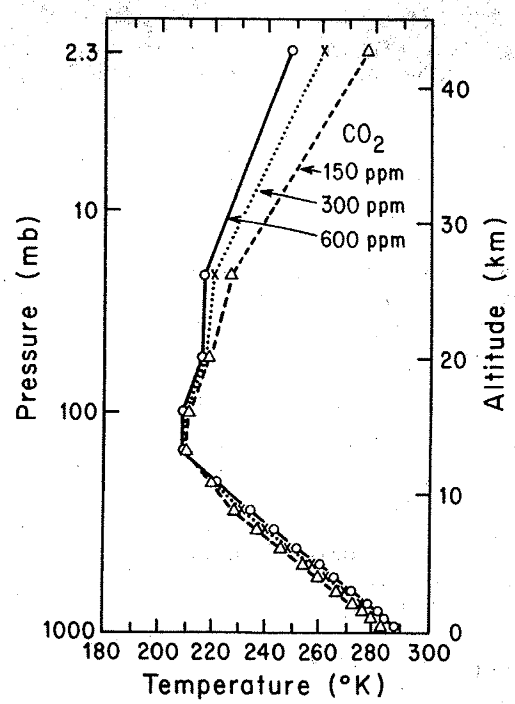

Figure 3. Vertical distributions of temperature in radiative-convective equilibrium for fixed relative humidity (FRH) and fixed clouds (FCL). The surface temperature change is 2.88°C for a CO_2 doubling from 150 to 300 ppmv and 2.36°C for 300 to 600 ppmv. (From Manabe and Wetherald, 1967.)

result in this wide range of simulated surface temperature change induced by a doubling of the CO_2 concentration.

3.3. Analysis and Interpretation of the Results

Why does the temperature increase in the troposphere and decrease in the stratosphere when the CO_2 concentration is doubled, and why do the estimated surface temperature changes vary by almost a factor of 10? To answer these questions we will first examine the direct radiative forcing due to the increased CO_2 concentration. Next, we will estimate the temperature response in the absence of feedbacks. Finally we will examine the CO_2-induced temperature change with feedbacks as revealed by the RCM studies presented in Table 4.

3.3.1. Direct radiative forcing due to increased CO_2. Because about 95% of the direct radiative forcing occurs in the longwave radiation

Table 4. The range of surface temperature change induced by a doubled CO_2 concentration as calculated by selected radiative-convective models

Study	ΔT_s (°C)
Manabe and Wetherald (1967)	1.33 - 2.92
Manabe (1971)	1.9
Augustsson and Ramanathan (1977)	1.98 - 3.2
Rowntree and Walker (1978)	0.78 - 2.76
Hunt and Wells (1979)	1.82 - 2.2
Wang and Stone (1980)	2.00 - 4.20
Charlock (1981)	1.58 - 2.25
Hansen et al. (1981)	1.22 - 3.5
Hummel and Kuhn (1981a)	0.79 - 1.94
Hummel and Kuhn (1981b)	0.8 - 1.2
Hummel and Reck (1981)	1.71 - 2.05
Hunt (1981)	0.69 - 1.82
Wang et al. (1981)	1.47 - 2.80
Hummel (1982)	1.29 - 1.83
Lindzen et al. (1982)	1.46 - 1.93
Lal and Ramanathan (1984)	1.8 - 2.4
Somerville and Remer (1984)	0.48 - 1.74

emitted by the Earth and only 5% in the shortwave solar radiation (Ramanathan et al., 1979), we consider here only the former. Figure 4 shows the change in the net upward longwave radiation flux ΔR as a function of altitude when the CO_2 concentration is doubled from 300 to 600 ppmv and the temperatures are held fixed. These changes represent the direct radiative forcing due to the CO_2 doubling and were obtained from the 33-layer Oregon State University (OSU) radiative transfer model in which the vertical profiles of temperature, water vapor and ozone were prescribed from the midlatitude summer atmosphere of McClatchey et al.

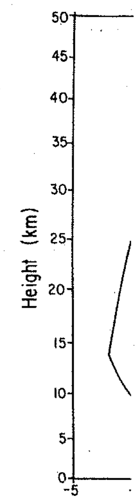

Figure 4. The change in t
an abrupt doubling of the

(1971), and in which there
everywhere, with values de
-4.5 Wm^{-2} at the tropopau
creasing at varying rates
and z = 50 km) and above.
ΔT when ΔS is neglected gi

$$\rho c_p \frac{\partial \Delta T}{\partial t} = - \frac{\partial \Delta R}{\partial z}$$

This shows that the direc
to cool the stratosphere,
troposphere, because there
upward longwave radiation

Why is $\Delta R < 0$ at the
negative in the tropospher
questions can be answered
shown in Fig. 5. In this
atmosphere and the top of
ly, level 1 is the upper
longwave transmissivity τ

rature change induced
as calculated by
odels

ΔT_s (°C)
1.33 - 2.92
1.9
1.98 - 3.2
0.78 - 2.76
1.82 - 2.2
2.00 - 4.20
1.58 - 2.25
1.22 - 3.5
0.79 - 1.94
0.8 - 1.2
1.71 - 2.05
0.69 - 1.82
1.47 - 2.80
1.29 - 1.83
1.46 - 1.93
1.8 - 2.4
0.48 - 1.74

wave solar radiation
nly the former. Figure 4
radiation flux ΔR as a func-
is doubled from 300 to 600
hese changes represent the
ling and were obtained from
adiative transfer model in
water vapor and ozone were
phere of McClatchey et al.

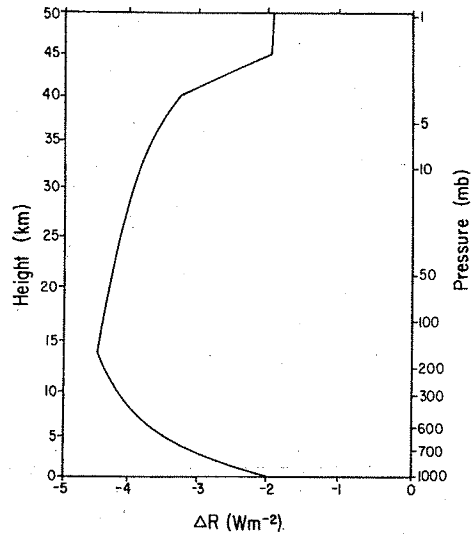

Figure 4. The change in the net upward longwave radiation flux due to an abrupt doubling of the CO_2 concentration.

(1971), and in which there were no clouds. Figure 4 shows that $\Delta R < 0$ everywhere, with values decreasing from about -2 Wm^{-2} at the surface to -4.5 Wm^{-2} at the tropopause ($p = 179$ mb and $z = 13$ km), and then increasing at varying rates to about -2 Wm^{-2} at the stratopause ($p = 1$ mb and $z = 50$ km) and above. Using Eq. (60) to give the temperature change ΔT when ΔS is neglected gives

$$\rho c_p \frac{\partial \Delta T}{\partial t} = - \frac{\partial \Delta R}{\partial z} \quad . \tag{62}$$

This shows that the direct radiative forcing of the increased CO_2 acts to cool the stratosphere, because there $\partial \Delta R/\partial z > 0$, and warm the troposphere, because there $\partial \Delta R/\partial z < 0$. At the surface the decreased net upward longwave radiation $\Delta R < 0$ acts to warm the surface.

Why is $\Delta R < 0$ at the surface (and elsewhere), and why is $\partial \Delta R/\partial z$ negative in the troposphere and positive in the stratosphere? These questions can be answered with the simple two-layer atmospheric model shown in Fig. 5. In this figure levels 0 and 2 represent the top of the atmosphere and the top of the troposphere (the tropopause), respectively, level 1 is the upper (stratospheric) layer with temperature T_1 and longwave transmissivity τ_1, level 3 is the lower (tropospheric) layer

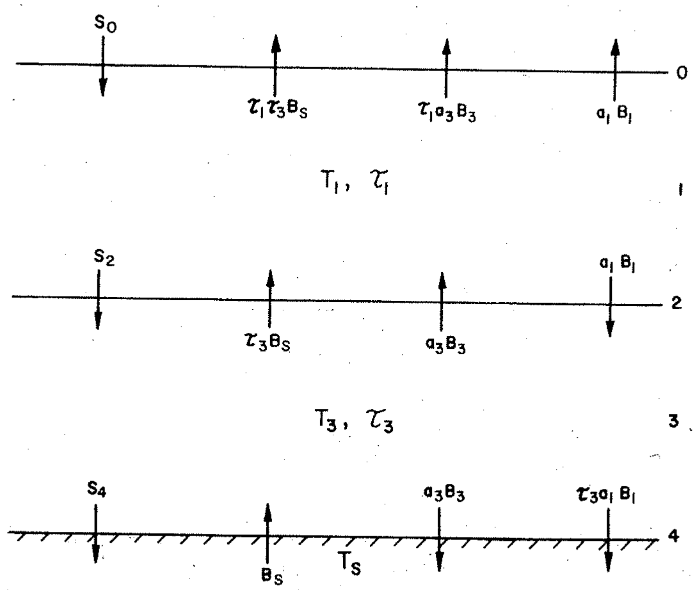

Figure 5. Two-layer model representation of the atmosphere-surface climate system. See text for nomenclature.

with temperature T_3 and longwave transmissivity τ_3, and level 4 is the Earth's surface with temperature T_s and longwave emissivity of unity. The flux of solar radiation at even level k is S_k. Longwave radiation is emitted by the surface and each atmospheric layer. The flux emitted by the surface, $B_s = \sigma T_s^4$, is attenuated by atmospheric absorption through the lower layer with absorptivity $a_3 = 1 - \tau_3$ such that the flux at level 2 is $\tau_3 B_s$. This flux is further attenuated by atmospheric absorption through the upper layer with absorptivity $a_1 = 1 - \tau_1$ such that the flux at level 0 is $\tau_1\tau_3 B_s$. Because the emissivity ε_3 is equal to the absorptivity a_3 by Kirchhoff's law, the lower layer emits radiation both upward and downward with magnitude $a_3 B_3 = a_3\sigma T_3^4$. The upward flux is attenuated by absorption through the upper layer such that the flux at level 0 is $\tau_1 a_3 B_3$. Finally, the upper layer emits radiation both upward and downward with magnitude $a_1 B_1 = a_1\sigma T_1^4$. The downward flux is attenuated by absorption through the lower layer such that the flux at the surface is $\tau_3 a_1 B_1$.

Using the fluxes described above and the hydrostatic relation $\partial p/\partial z = -\rho g$, we can write the thermodynamic energy Eq. (60) for the atmospheric layers as

$$\frac{\delta_1 p}{g} c_p \frac{\partial T_1}{\partial t} = (S_o - S_2) + Q_1 \qquad (63)$$

QUANTITATIVE FEEDBACK ANAL

$$\frac{\delta_3 p}{g} c_p \frac{\partial T_3}{\partial t} = (S_2$$

where

$$Q_1 = (1 - \tau_1)\tau_3 B$$

$$= a_1(\tau_3 B_s + a$$

$$Q_3 = (1 - \tau_3)B_s$$

$$= a_3(B_s - 2B_3$$

are the longwave radiation with pressure thicknesses thermodynamic energy equat

$$C_s \frac{\partial T_s}{\partial t} = S_4 + Q_4$$

where

$$Q_4 = - B_s + a_3 B_3$$

is the longwave radiation capacity C_s. In the therm the CO_2 concentration, ∂T_1

$$Q_1 = - (S_0 - S_2)$$

$$Q_3 = - (S_2 - S_4)$$

$$Q_4 = - S_4 < 0 \quad ,$$

and the longwave radiatior negative, that is, a cooli

When the radiative eq of the CO_2 concentration, and (67) become

$$\frac{\delta_1 p}{g} c_p \frac{\partial \Delta T_1}{\partial t} =$$

$$\frac{\delta_3 p}{g} c_p \frac{\partial \Delta T_3}{\partial t} =$$

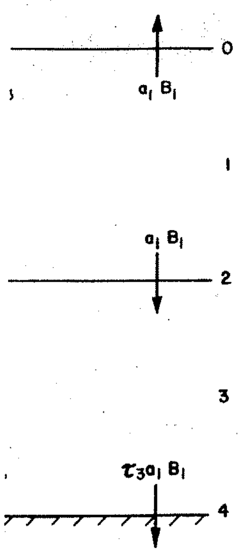

the atmosphere-surface

ity τ_3, and level 4 is the
wave emissivity of unity.
is S_k. Longwave radiation
ic layer. The flux emitted
atmospheric absorption
$= 1 - \tau_3$ such that the flux
tenuated by atmospheric
rptivity $a_1 = 1 - \tau_1$ such
the emissivity ε_3 is equal
he lower layer emits radia-
$a_3 B_3 = a_3 \sigma T_3^4$. The upward
upper layer such that the
er layer emits radiation
$= a_1 \sigma T_1^4$. The downward
lower layer such that the

e hydrostatic relation
energy Eq. (60) for the

(63)

$$\frac{\delta_3 p}{g} c_p \frac{\partial T_3}{\partial t} = (S_2 - S_4) + Q_3 \quad , \tag{64}$$

where

$$Q_1 = (1 - \tau_1)\tau_3 B_s + (1 - \tau_1) a_3 B_3 - 2 a_1 B_1$$

$$= a_1 (\tau_3 B_s + a_3 B_3 - 2 B_1) \tag{65}$$

$$Q_3 = (1 - \tau_3) B_s - 2 a_3 B_3 + (1 - \tau_3) a_1 B_1$$

$$= a_3 (B_s - 2 B_3 + a_1 B_1) \tag{66}$$

are the longwave radiation heating rates for the upper and lower layers with pressure thicknesses $\delta_1 p$ and $\delta_3 p$, respectively. Similarly, the thermodynamic energy equation for the surface is

$$C_s \frac{\partial T_s}{\partial t} = S_4 + Q_4 \quad , \tag{67}$$

where

$$Q_4 = - B_s + a_3 B_3 + \tau_3 a_1 B_1 \tag{68}$$

is the longwave radiation heating rate for the surface with bulk heat capacity C_s. In the thermodynamic equilibrium prior to the change in the CO_2 concentration, $\partial T_1/\partial t = \partial T_3/\partial t = \partial T_s/\partial t = 0$ so that

$$Q_1 = - (S_0 - S_2) < 0 \quad , \tag{69}$$

$$Q_3 = - (S_2 - S_4) < 0 \quad , \tag{70}$$

$$Q_4 = - S_4 < 0 \quad , \tag{71}$$

and the longwave radiation heating of the atmosphere and surface is negative, that is, a cooling.

When the radiative equilibrium is disturbed by the abrupt doubling of the CO_2 concentration, the thermodynamic energy equations (63), (64) and (67) become

$$\frac{\delta_1 p}{g} c_p \frac{\partial \Delta T_1}{\partial t} = \Delta(S_0 - S_2) + \Delta Q_1 \quad , \tag{72}$$

$$\frac{\delta_3 p}{g} c_p \frac{\partial \Delta T_3}{\partial t} = \Delta(S_2 - S_4) + \Delta Q_3 \quad , \tag{73}$$

and

$$C_s \frac{\partial \Delta T_s}{\partial t} = \Delta S_4 + \Delta Q_4 \quad , \tag{74}$$

where by Eqs. (65), (66), (68) and $\Delta\tau_k = -\Delta a_k$,

$$\Delta Q_1 = a_1(\Delta\tau_3 B_s + \Delta a_3 B_3) + \Delta a_1(\tau_3 B_s + a_3 B_3 - 2B_1)$$

$$= -a_1(B_s - B_3)\Delta a_3 + \frac{Q_1}{a_1}\Delta a_1 \quad , \tag{75}$$

$$\Delta Q_3 = a_3 \Delta a_1 B_1 + \Delta a_3(B_s - 2B_3 + a_1 B_1)$$

$$= a_3 B_1 \Delta a_1 + \frac{Q_3}{a_3}\Delta a_3 \quad , \tag{76}$$

and

$$\Delta Q_4 = \Delta a_3 B_3 + \Delta\tau_3 a_1 B_1 + \tau_3 \Delta a_1 B_1$$

$$= (B_3 - a_1 B_1)\Delta a_3 + \tau_3 B_1 \Delta a_1 \quad . \tag{77}$$

Here ΔT_k and ΔQ_k are the temperature and heating perturbations from their respective undisturbed equilibrium values, with Δa_k and $\Delta\tau_k$ the perturbed absorptivity and transmissivity due to the doubled CO_2 concentration. In Eqs. (75)-(77) the temperatures on the right-hand sides in $B_k = \sigma T_k^4$ are held at their undisturbed values so that the direct radiative forcing due to the doubled CO_2 concentration can be determined.

The direct radiative forcing of the stratosphere is given by Eqs. (72) and (75). Because $B_s > B_3$, $\Delta a_3 > 0$, $Q_1 < 0$ and $\Delta a_1 > 0$, both terms on the right-hand side of Eq. (75) are negative, hence $\Delta Q_1 < 0$. Although $\Delta(S_o - S_2) > 0$ in Eq. (72) due to the weak solar absorption bands of CO_2, it is dominated by ΔQ_1 so that the direct radiative forcing acts to cool the stratospheric layer. Figure 5 shows that this cooling tendency occurs primarily because of the greater upward and downward emission from the stratosphere itself.

The direct radiative forcing of the troposphere-surface system is given by Eqs. (73), (74), (76) and (77) as

$$\frac{\delta_3 p}{g} c_p \frac{\partial \Delta T_3}{\partial t} + C_s \frac{\partial \Delta T_s}{\partial t} = \Delta S_2 - \Delta R_2 \quad , \tag{78}$$

where

$$\Delta R_2 = -(B_s - B_3)\Delta a_3 - B_1 \Delta a_1 \tag{79}$$

is the change in the net upward longwave flux at the tropopause. Because $B_s > B_3$, $\Delta a_3 > 0$ and $\Delta a_1 > 0$, then $\Delta R_2 < 0$. Again, although $\Delta S_2 < 0$ in Eq. (78), it is dominated by $-\Delta R_2$ so that the direct radiative forcing acts to warm the troposphere-surface system. Figure 5 and Eq. (79) show that this warming tendency occurs because of both the increased downward flux from the stratosphere and the decreased upward flux from the troposphere.

The direct radiative forcing of the surface is given by Eqs. (74) and (77). Because $B_3 > B_1$, $\Delta a_3 > 0$, and $\Delta a_1 > 0$, both terms on the right-hand side of Eq. (77) are positive, hence $\Delta Q_4 > 0$. Although $\Delta S_4 < 0$, ΔQ_4 dominates ΔS_4 so that the direct radiative forcing acts to warm the surface. As can be seen from Fig. 5, this warming tendency occurs primarily because of the greater downward emission from the troposphere.

Finally, the direct radiative forcing of the troposphere is given by Eqs. (73) and (76). Because $\Delta a_1 > 0$, $Q_3 < 0$ and $\Delta a_3 > 0$, the first term on the right-hand side of Eq. (76) is positive and the second term is negative. Because $\Delta(S_2 - S_4) > 0$ but small, the fact that the direct radiative forcing of the troposphere is a warming tendency (Fig. 4) is seen from Eq. (76) and Fig. 5, as noted by Schneider (1975), to be primarily due to the increased downward flux from the stratosphere.

Kiehl and Ramanathan (1982) have shown that the direct radiative forcing of the surface strongly depends on the water vapor absorption in the 12-18 μm region which overlaps and competes with the 15 μm absorption band of CO_2. However, the direct radiative forcing of the troposphere-surface system does not strongly depend on the water vapor absorption in this spectral region. Kiehl and Ramanathan found that the direct radiative forcing of the surface, ΔR_s, decreased from 1.56 to 0.55 Wm^{-2} when the continuum absorption was added to the line absorption between 12-18 μm. The corresponding change in the direct radiative forcing of the troposphere-surface system, that is, the change in net upward flux at the tropopause ΔR_T, was from 4.18 to 3.99 Wm^{-2}. Consequently, the inclusion of the 12-18 μm continuum absorption increases the direct radiative forcing of the troposphere, $\Delta R_T - \Delta R_s$, from 2.62 to 3.44 Wm^{-2}.

As the stratosphere cools in response to its direct radiative forcing, it is to be expected that the radiation emitted downward into the troposphere will decrease and, in effect, reduce the direct radiative forcing of the troposphere-surface system. However, Ramanathan et al. (1979) found that this effect is negligibly small because most of the contribution to the downward flux at the tropopause comes from the region within 5 km above the tropopause where the final temperature change is small. More recently, Lal and Ramanathan (1984) found that the direct radiative forcing of the troposphere-surface system of 4.1 Wm^{-2} was decreased to 4.0 Wm^{-2} after the stratospheric temperatures alone were allowed to cool to their radiative equilibrium values. Of this 4.0 Wm^{-2}, 2.7 Wm^{-2} was contributed by the reduction in upward flux from the troposphere, 1.55 Wm^{-2} by the increased downward flux from the stratospheric CO_2 increase, and -0.15 Wm^{-2} by the decreased solar flux at the tropopause. In the following we shall consider that the direct radiative forcing of the troposphere-surface system is $\Delta R_T = 4\ Wm^{-2}$.

3.3.2. Response of the climate system without feedbacks to increased CO_2. The response of the climate system to increased CO_2 when only the temperature changes is given by Eq. (18), with f = 0 and $\Delta Q = \Delta R_T$, and Eq. (58b) as

$$(\Delta T_s)_o = G_o \Delta R_T = \frac{T_s(1xCO_2)}{(1-\alpha_p)S_o} \Delta R_T \quad . \qquad (80)$$

Taking $\Delta R_T = 4\ Wm^{-2}$ and $G_o = 0.3°C/(Wm^{-2})$ gives $(\Delta T_s)_o = 1.2°C$. This value is in excellent agreement with the value of $\Delta T_s = 1.22°C$ obtained by Hansen et al. (1981) using an RCM with no feedbacks - that is, with fixed lapse rate (FLR, Table 3), fixed absolute humidity (FAH), fixed cloud altitude (FCA), fixed cloud cover (FCC), fixed cloud optical depth (FOD) and fixed surface albedo (FAL) - and in which $\Delta R_T = 4.0\ Wm^{-2}$. However, since $T_s(1xCO_2)$ was not reported by Hansen et al. (1981), the actual value of G_o may not have been the $0.3°C/(Wm^{-2})$ assumed here. The value of $(\Delta T_s)_o = 1.2°C$ is also in close agreement with the values of $\Delta T_s = 1.33$ and $1.29°C$ obtained respectively by Manabe and Wetherald (1967) and Rowntree and Walker (1978) using different RCMs, but with the same characteristics as those of Hansen et al. (1981) described above. However, the values of ΔR_T were not reported in these earlier studies and so may have been different from the $4\ Wm^{-2}$ assumed here. Therefore, to test the validity of Eq. (80) we have used the 2-layer Oregon State University (OSU) radiative-convective model which has been described by Hall et al. (1982) and has been modified here to include a single cloud layer at 500 mb with a 45% cloud cover. For the zero-feedback configuration described above, this model with $S_o = 1370\ Wm^{-2}$ gives $\alpha_p = 0.3128$, $T_s = 288.38$ K and $\Delta R_T = 4.17\ Wm^{-2}$. Thus, $G_o = 0.306°C/(Wm^{-2})$ by Eq. (58b) and $(\Delta T_s)_o = 1.276°C$ by Eq. (80). Because this value is within 6% of the actual $(\Delta T_s)_o = 1.354°C$, it is seen that Eq. (80) does provide an accurate estimate of $(\Delta T_s)_o$.

3.3.3. Response of the climate system with feedbacks to increased CO_2. The RCM results presented in Table 4 can be characterized in terms of the feedback f by making use of Eqs. (12) and (18) with ΔT_* replaced by ΔT_s to obtain

$$f = 1 - \frac{(\Delta T_s)_o}{\Delta T_s} \qquad (81)$$

and our estimate of $(\Delta T_s)_o = G_o \Delta Q = 1.2°C$ based on $\Delta Q = 4\ Wm^{-2}$ and $G_o = 0.3°C/(Wm^{-2})$. Thus, $-1.5 \le f \le 0.7$. Several physical mechanisms are thought to be the cause of this wide range in the feedback of these models. As T_s increases these mechanisms include: 1) the increase in the amount of water vapor in the atmosphere as a consequence of the quasi-constancy of the relative humidity, 2) the decrease in the temperature lapse rate, 3) the increase in the cloud altitude as the clouds maintain their temperature, 4) the change in cloud amount, 5) the change in the cloud optical depth, and 6) the decrease in surface albedo due to

the decrease in ice and s
mechanisms were all mutua
be equal to the sum of th
contribution of each mech
ally determined and ranke
these ranked feedback mec
wide range in the RCM res
is not equal to the sum o
the feedbacks are depende
should be considered as o
the remaining feedbacks.
mechanism to the total fe
pared as described above.
To investigate the i
we have carried out a qua
two-layer RCM. The resul
$T_s(1xCO_2)$ changes when so
activated, $(\Delta T_s)_o$ is esse
case with no feedback mec
therefore gives a small a
represent the neglected s
will be discounted in the
mechanisms, only that of
a negative feedback. (It
this negative feedback.)
are in decreasing order o
face albedo, cloud optica
sufficiently small in com
the zero-feedback case th
Table 5 shows that the fe
cloud altitude, or surfac
apparent feedback value f
backs are independent. T
back with either the clou
the resultant feedback is
vidual feedbacks. Thus,
variable cloud optical de
act in conjunction with t
Consequently, cloud cover
within an RCM, should be
single feedback mechanism
It is useful to cons
feedback mechanisms of wa
Table 5 shows that these
for the apparent feedback
additional feedback mecha
warming. This value is c
Wang and Stone (1980) us
also simulated for the g
et al. (1984) and Wethera
models (see Schlesinger a

feedbacks to increased
:reased CO_2 when only the
f = 0 and $\Delta Q = \Delta R_T$, and

. (80)

s $(\Delta T_s)_o = 1.2°C$. This
of $\Delta T_s = 1.22°C$ obtained
eedbacks - that is, with
e humidity (FAH), fixed
fixed cloud optical depth
which $\Delta R_T = 4.0\ Wm^{-2}$.
ansen et al. (1981), the
$/(Wm^{-2})$ assumed here. The
ment with the values of
Manabe and Wetherald
fferent RCMs, but with the
(1981) described above.
n these earlier studies
assumed here. Therefore,
the 2-layer Oregon State
ich has been described by
to include a single cloud
he zero-feedback configur-
70 Wm^{-2} gives $\alpha_p = 0.3128$,
$0.306°C/(Wm^{-2})$ by
ecause this value is with-
en that Eq. (80) does pro-

edbacks to increased CO_2.
aracterized in terms of
(18) with ΔT_* replaced

(81)

:d on $\Delta Q = 4\ Wm^{-2}$ and
'eral physical mechanisms
: in the feedback of these
.ude: 1) the increase in
: a consequence of the
:he decrease in the temper-
l altitude as the clouds
:loud amount, 5) the change
se in surface albedo due to

the decrease in ice and snow. If the feedbacks of these individual mechanisms were all mutually independent, then the total feedback would be equal to the sum of the individual feedbacks. In such a case the contribution of each mechanism to the total feedback could be individually determined and ranked. An intercomparison among the models of these ranked feedback mechanisms would then reveal the sources for the wide range in the RCM results. On the other hand, if the total feedback is not equal to the sum of the individual feedbacks, then two or more of the feedbacks are dependent. In this case the dependent feedbacks should be considered as only one feedback such that it is independent of the remaining feedbacks. Then the contribution of each independent mechanism to the total feedback can be determined, ranked and intercompared as described above.

To investigate the independence of the six mechanisms listed above, we have carried out a quantitative feedback evaluation using the OSU two-layer RCM. The results presented in Table 5 show that although $T_s(1xCO_2)$ changes when some of the individual feedback mechanisms are activated, $(\Delta T_s)_o$ is essentially constant and equal to 1.28°C. For the case with no feedback mechanisms, ΔT_s differs from $(\Delta T_s)_o$ by 0.07°C and therefore gives a small apparent feedback. This apparent feedback may represent the neglected second- and higher-order terms in Eq. (3), and will be discounted in the following. Of all the individual feedback mechanisms, only that of the variable (moist adiabatic) lapse rate gives a negative feedback. (It is likely that the two-layer model exaggerates this negative feedback.) The individual positive feedback mechanisms are in decreasing order of magnitude: water vapor, cloud altitude, surface albedo, cloud optical depth and cloud cover. The latter two are sufficiently small in comparison with the small apparent feedback for the zero-feedback case that they can be regarded as essentially zero. Table 5 shows that the feedbacks of water vapor and either lapse rate, cloud altitude, or surface albedo are additive (within the small nonzero apparent feedback value for the zero-feedback case). Thus these feedbacks are independent. This is not the case for the water vapor feedback with either the cloud cover or cloud optical depth feedbacks since the resultant feedback is substantially less than the sum of the individual feedbacks. Thus, it appears that both variable cloud cover and variable cloud optical depth are negative feedback mechanisms when they act in conjunction with the positive water vapor feedback. Consequently, cloud cover and cloud optical depth, when allowed to vary within an RCM, should be considered together with water vapor as a single feedback mechanism.

It is useful to consider here the effect of the three positive feedback mechanisms of water vapor, cloud altitude and surface albedo. Table 5 shows that these feedbacks are essentially independent (allowing for the apparent feedback of the zero-feedback case for each of the two additional feedback mechanisms) and combine to produce a 3.85°C surface warming. This value is close to the 4.2°C maximum warming simulated by Wang and Stone (1980) using an RCM with these feedbacks (Table 4), and also simulated for the global-mean surface air temperature by Hansen et al. (1984) and Wetherald and Manabe (1986) with general circulation models (see Schlesinger and Mitchell, 1985, 1987).

Table 5. Feedback analysis using the Oregon State University two-layer RCM

Feedback Mechanism	$T_s(1xCO_2)$ (°C)	$(\Delta T_s)_o$ [a] (°C)	ΔT_s (°C)	f [b]
None	15.28	1.28	1.35	0.058
Water Vapor [c]	14.53	1.28	1.94	0.340
Lapse Rate [d]	9.53	1.24	0.88	-0.409
Cloud Altitude [e]	15.28	1.28	1.73	0.261
Cloud Cover [f]	15.28	1.28	1.38	0.074
Cloud Optical Depth [g]	15.28	1.28	1.39	0.079
Surface Albedo [h]	15.43	1.28	1.56	0.181
Water Vapor [c] and				
Lapse Rate [d]	9.38	1.25	1.19	-0.043 (-0.069)
Cloud Altitude [e]	14.20	1.28	2.79	0.543 (0.601)
Cloud Cover [f]	15.12	1.29	1.81	0.291 (0.414)
Cloud Optical Depth [g]	15.39	1.28	1.70	0.248 (0.419)
Surface Albedo [h]	14.58	1.28	2.39	0.466 (0.521)
Water Vapor [c], Cloud Altitude [e], and Surface Albedo [h]	14.14	1.28	3.85	0.668 (0.782)

[a] $(\Delta T_s)_o$ is calculated by Eq. (80).

[b] The values in parentheses are the algebraic sum of the individual feedbacks.

[c] With the fixed relative humidity profile of Manabe and Wetherald (1967).

[d] With the moist adiabatic lapse rate.

[e] With fixed cloud temperature prescribed equal to that of the $1xCO_2$ simulation with no feedback.

[f] With variable cloud cover prescribed similarly to that of Wang et al. (1981).

[g] With variable optical depth τ prescribed similarly to that of Wang et al. (1981) and cloud albedo, absorptivity and transmissivity parameterized in terms of τ following Stephens et al. (1984).

[h] With variable surface albedo prescribed as in Wang and Stone (1980).

In the following we sh
individual water vapor, la
feedbacks, and the joint c
depth/water vapor feedback
sider the influence of the
tions in RCMs.

Surface energy flux. In R
induced by increased CO_2 c
face C_s is taken as zero t
tablish equilibrium. The
is then

$$C_s \frac{\partial T_s}{\partial t} = S_s + R_s^{\downarrow}$$

where S_s is the absorbed s
radiation, σT_s^4 is the upw
with temperature T_s, and F
heat. Two treatments or p
RCMs. Manabe and Wethera
where T_a is the surface ai
of the model's lowest laye

$$F_s = S_s + R_s^{\downarrow} - \sigma$$

This is identified as the
in Table 3. In other RCM
F_s is parameterized using
that is,

$$F_s = \rho c_p \, c_D \, V_s (T$$

Here the first term repres
efficient and V_s the surfa
the latent heat flux with
saturation mixing ratio of
water vapor mixing ratio o
mixing ratio of the model'
constrained to be equal to
to prescribe $c_D V_s$.

Do these different tr
account for any of the dif
Only the study by Lindzen
Using their RCM with fixed
of 6.5°C km^{-1} (FLR6.5) and
temperature warming for do
with the BAE and $c_D V_s$ = 0.
moist adiabatic lapse rate

gon State University

	ΔT_s (°C)	f [b]
	1.35	0.058
	1.94	0.340
	0.88	−0.409
	1.73	0.261
	1.38	0.074
	1.39	0.079
	1.56	0.181
	1.19	−0.043 (−0.069)
	2.79	0.543 (0.601)
	1.81	0.291 (0.414)
	1.70	0.248 (0.419)
	2.39	0.466 (0.521)
	3.85	0.668 (0.782)

c sum of the individual

f Manabe and Wetherald

ual to that of the

arly to that of Wang

similarly to that of
ptivity and transmis-
ng Stephens et al.

in Wang and Stone

In the following we shall analyze the RCM results to determine the individual water vapor, lapse rate, cloud altitude and surface albedo feedbacks, and the joint cloud cover/water vapor and cloud optical depth/water vapor feedbacks. However, before doing this we shall consider the influence of the different surface energy flux parameterizations in RCMs.

Surface energy flux. In RCM studies of the equilibrium climate change induced by increased CO_2 concentrations, the heat capacity of the surface C_s is taken as zero to minimize the computer time required to establish equilibrium. The thermodynamic energy equation for the surface is then

$$C_s \frac{\partial T_s}{\partial t} = S_s + R_s^{\downarrow} - \sigma T_s^{\,4} - F_s = 0 \quad , \tag{82}$$

where S_s is the absorbed solar radiation, $R_s^{\downarrow}$ is the downward longwave radiation, $\sigma T_s^{\,4}$ is the upward longwave radiation emitted by the surface with temperature T_s, and F_s is the upward flux of sensible and latent heat. Two treatments or parameterizations of F_s have been used in RCMs. Manabe and Wetherald (1967) and others have assumed that $T_s = T_a$, where T_a is the surface air temperature taken equal to the temperature of the model's lowest layer. In this case, by Eq. (82),

$$F_s = S_s + R_s^{\downarrow} - \sigma T_a^{\,4} \quad . \tag{83}$$

This is identified as the equivalent radiative exchange (ERE) treatment in Table 3. In other RCM studies such as that by Hunt and Wells (1979), F_s is parameterized using the bulk aerodynamic exchange (BAE) method, that is,

$$F_s = \rho c_p \, c_D \, V_s (T_s - T_a) + \rho L \, c_D \, V_s [q^*(T_s) - q_a] \quad . \tag{84}$$

Here the first term represents the sensible heat flux with c_D a drag coefficient and V_s the surface wind speed, and the second term represents the latent heat flux with L the latent heat of vaporization, $q^*(T_s)$ the saturation mixing ratio of water vapor at temperature T_s, and q_a the water vapor mixing ratio of the surface air which is taken equal to the mixing ratio of the model's lowest layer. In using Eq. (84) T_s is not constrained to be equal to T_a as it is in Eq. (83), but it is necessary to prescribe $c_D V_s$.

Do these different treatments of the surface energy flux in RCMs account for any of the differences in the results presented in Table 4? Only the study by Lindzen et al. (1982) investigated this question. Using their RCM with fixed relative humidity (FRH), a fixed lapse rate of 6.5°C km^{-1} (FLR6.5) and no clouds, Lindzen et al. found a surface temperature warming for doubled CO_2 of 1.98°C with the ERE, and 1.93°C with the BAE and $c_D V_s$ = 0.0124 ms^{-1}. Furthermore, in an RCM with FRH, moist adiabatic lapse rate (MALR), fixed cloud altitude (FCA) and the

BAE, Hunt (1981) found that ΔT_s for a CO_2 doubling varied from 1.89 to 1.79°C as V_s varied from 2 to 10 ms^{-1} with $c_D = 1.5 \times 10^{-3}$. Consequently, from these results it appears that the different treatments of the surface energy flux in RCMs has a negligible effect on the CO_2-induced warming of the surface ΔT_s.

Water vapor feedback. In their pioneering RCM study of CO_2-induced climate change, Manabe and Wetherald (1967) argued on the basis of seasonal observations that the atmosphere tends to maintain the climatological distribution of relative humidity RH rather than absolute (specific) humidity q. Accordingly, Manabe and Wetherald (1967) prescribed the vertical profile of relative humidity on the basis of observations to be

$$RH(p) = RH(p_s)\,\frac{p/p_s - 0.02}{1 - 0.02} \quad , \tag{85}$$

where p is pressure, p_s is the surface pressure, and $RH(p_s) = 0.77$, and they calculated the specific humidity from

$$q(T,p) = RH(p)\; q^*(T,p) \quad , \tag{86}$$

where $q^*(T,p)$ is the saturation specific humidity given with the aid of the Clausius-Clapeyron relation as

$$q^*(T,p) = \frac{a}{p}\, e^{-b/T} \quad , \tag{87}$$

where a and b are constants. This fixed relative humidity treatment of water vapor is identified in Table 3 as FRH. For comparison, Manabe and Wetherald (1967) also performed a calculation with fixed absolute humidity (FAH). The results of this study are shown in Table 6 for two cases, one with no clouds (CLR) and the other with three cloud layers with fixed cloud altitude (FCA) and fixed optical depth (FOD). Taking $(\Delta T_s)_o$ for each cloud condition as ΔT_s for the corresponding FAH case, the water vapor feedback for FRH is by Eq. (81) $f_W = 0.534$ for the clear case and $f_W = 0.436$ for the cloudy case.

What is the physical cause of this positive water vapor feedback and why does its value differ for the clear and cloudy cases? These questions can be answered by considering the amount of water vapor per unit horizontal area between two vertical levels k and ℓ,

$$W_{k,\ell} = \int_{z_k}^{z_\ell} q(z)\rho\, dz = \frac{1}{g}\int_{p_\ell}^{p_k} q(p)\, dp \quad , \tag{88}$$

the latter by the hydrostatic equation $dp/dz = -\rho g$. For FAH, $W_{k,\ell}$ is determined solely by the prescribed absolute humidity profile and is constant. For FRH, $W_{k,\ell}$ is given by Eq. (88) with Eqs. (86) and (87) as

$$W_{k,\ell} = \frac{1}{g}\int_{p_\ell}^{p_k} RH(p)$$

and is therefore determined
profile, but also by the te

$$T = T_s(p/p_s)^{R\Gamma/g}$$

for the particular case of
Manabe and Wetherald (1967)
pends on RH(p) and T_s. Con
warming of the surface in r
sults in an increase in $W_{k,}$
the atmospheric absorptivit
(Fig. 5) beyond, and in the
quantities due to the incre
radiative forcing. This ir

Table 6. Water vapor feedt
convective models

Study	Model Attri
Manabe and Wetherald (1967)	ERE;FLR(6. - , - ;FAI
	ERE;FLR(6. FCP(3),FOI
Rowntree and Walker (1978)	BAE;FLR(6 - , - ;FAI
Hansen et al. (1981)	BAE;FLR(6 FCA(1),FO

[a] Surface energy flux; convect
optical depth; surface albed

[b] * indicates the value of (ΔT

[c] $f_W = 1 - (\Delta T_s)_o/\Delta T_s$.

[d] The prescribed relative humi

[e] $(\Delta T_s)_o$ and ΔT_s were obtained

bling varied from 1.89 to
= 1.5 x 10^{-3}.
hat the different treat-
a negligible effect on the

M study of CO_2-induced cli-
ed on the basis of seasonal
ntain the climatological
han absolute (specific)
d (1967) prescribed the
basis of observations to be

(85)

re, and $RH(p_s) = 0.77$, and

(86)

dity given with the aid of

(87)

tive humidity treatment of
For comparison, Manabe and
with fixed absolute humid-
wn in Table 6 for two
with three cloud layers
ical depth (FOD). Taking
e corresponding FAH case,
1) $f_W = 0.534$ for the clear

ive water vapor feedback
nd cloudy cases? These
amount of water vapor per
els k and ℓ,

(88)

= $-\rho g$. For FAH, $W_{k,\ell}$ is
humidity profile and is
with Eqs. (86) and (87) as

$$W_{k,\ell} = \frac{1}{g}\int_{p_\ell}^{p_k} RH(p)\,\frac{a}{p}\,e^{-b/T}dp \tag{89}$$

and is therefore determined not only by the prescribed relative humidity profile, but also by the temperature as well. Because

$$T = T_s(p/p_s)^{R\Gamma/g} \tag{90}$$

for the particular case of a fixed tropospheric lapse rate Γ adopted by Manabe and Wetherald (1967), it can be seen from Eq. (89) that $W_{k,\ell}$ depends on $RH(p)$ and T_s. Consequently, when CO_2 is increased, the initial warming of the surface in response to the direct radiative forcing results in an increase in $W_{k,\ell}$ between any levels k and ℓ. This increases the atmospheric absorptivities and decreases the transmissivities (Fig. 5) beyond, and in the same directions as the changes in these quantities due to the increased CO_2, and thereby acts to enhance the radiative forcing. This in turn leads to further warming of the surface

Table 6. Water vapor feedback f_W determined from selected radiative-convective models

Study	Model Attributes[a]	Water Vapor Treatment	$T_s(1xCO_2)$ (°C)	ΔT_s[b] $2xCO_2-1xCO_2$ (°C)	Estimated Feedback f_W[c]
Manabe and Wetherald (1967)	ERE;FLR(6.5);CLR, –, – ;FAL	FAH[d]	26.89	1.36*	
		FRH	34.04	2.92	0.534
	ERE;FLR(6.5);FCC, FCP(3),FOD;FAL	FAH[d]	17.89	1.33*	
		FRH	15.23	2.36	0.436
Rowntree and Walker (1978)	BAE;FLR(6.5);CLR, –, – ;FAL	FAH[d]		1.29*	
		FRH	32.84	2.76	0.533[e]
Hansen et al. (1981)	BAE;FLR(6.5);FCC, FCA(1),FOD;FAL	FAH[d]		1.22*	
		FRH		1.94	0.371

[a] Surface energy flux; convection; cloud cover, altitude (number of layers), optical depth; surface albedo. See Table 3 for definition of the abbreviations.

[b] * indicates the value of $(\Delta T_s)_o$.

[c] $f_W = 1 - (\Delta T_s)_o/\Delta T_s$.

[d] The prescribed relative humidity profile is given by Eq. (85).

[e] $(\Delta T_s)_o$ and ΔT_s were obtained with $\cos\zeta = 0.225$ and 0.250, respectively.

and further increases in $W_{k,\ell}$ in a feedback loop as shown in Fig. 1. The positive feedback is less than unity hence the amplification of the loop is finite (Fig. 2). However, the feedback increases nonlinearly with increasing T_s due to the $e^{-b/T}$ term in Eq. (89) which arises from the Clausius-Clapeyron relation. This dependence explains, in part, the difference in f_W between the clear and cloudy cases: the $1xCO_2$ surface temperature is lower in the cloudy case than in the clear case because of the larger planetary albedo, hence the feedback is lower in the cloudy case than in the clear case. However, if there is a large lapse rate feedback as in the case of penetrative convection (discussed in the next subsection), ΔT_s may be practically independent of T_s.

Table 6 also shows results from two other RCM studies using the Manabe and Wetherald (1967) prescribed relative humidity profile Eq. (85). The water vapor feedback is seen to range from 0.371 to 0.534. This range is likely due to the dependence of f_W on $T_s(1xCO_2)$ as described above, and the differences in the $T_s(1xCO_2)$ values of the models. This is supported by the fact that $T_s(1xCO_2)$ and f_W of Rowntree and Walker (1978) are nearly the same as those of Manabe and Wetherald (1967). Because the present global-mean surface air temperature is 14.2°C (Jenne, 1975), the results in Tables 5 and 6 suggest a probable value of $f_W \sim 0.3$ to 0.4. This is a moderate positive feedback which, acting alone, would multiply the zero-feedback temperature change by an R_f of about 1.4 to 1.7 (Fig. 2). However, it should be noted that the concept of constant relative humidity is an idealization. If the relative humidity increased with temperature as investigated by Augustsson and Ramanathan (1977) and Rowntree and Walker (1978), f_W would exceed the value above, and f_W would be smaller if the relative humidity decreased with temperature. Interestingly, general circulation model studies of both CO_2- and solar constant-induced climatic changes have shown that the relative humidity is not constant.

Temperature/lapse rate feedback. In the first RCM study of CO_2-induced climate change by Manabe and Wetherald (1967), it was assumed, based on early observations (Brunt, 1933 and Goody, 1964), that the tropospheric temperature lapse rate $\Gamma = -dT/dz$ was 6.5°C km^{-1}. A more recent analysis by Stone and Carlson (1979) using the observations of Oort and Rasmusson (1971) showed that a better estimate of the global-mean tropospheric lapse rate is $\Gamma = 5.1$°C km^{-1}. Is this difference in prescribed critical lapse rate important?

Cess (1975) investigated this question with a PEBM and found that the outgoing infrared flux F and $\partial F/\partial T_s$ were insensitive to Γ in the range 6.0 to 7.0°C km^{-1}. Rowntree and Walker (1978) investigated this question with an RCM and found that varying the fixed lapse rate from 5 to 6.5°C km^{-1} affected the results little. Quantitative results were presented by Chylek and Kiehl (1981), shown in Table 7, who concluded that the choice of the lapse rate within an interval from 5.5 to 6.5°C km^{-1} has no significant effect on the results obtained using radiative-convective models. Nevertheless, Table 7 shows a 12% decrease in ΔT_s for $\Gamma = 5.0$°C km^{-1}. This decrease probably represents a smaller water vapor feedback, although this cannot be verified since the requisite data were not reported.

Table 7. Lapse rate
radiative-conve

Study	Model A
Chylek and Kiehl (1981)	ERE;FR FCA(1)
Hunt and Wells (1979)	BAE;FR FCP(3)
Hummel and Kuhn (1981a)	ERE;FR (500 m
	ERE;FR (800 m
Wang et al. (1981)	BAE;FR FCA(17
Hummel (1982)	ERE;FR FCP(3)
Lindzen et al. (1982)	BAE;FR - , -
Rowntree and Walker (1978)	BAE;FA - , -
Hansen et al. (1981)	BAE;FR FCA(1)

a Surface energy flux cloud layers), opti definition of the a

b ΔT_s for Γ = 6.5 K/k

c BADJ is baroclinic MALR is defined her

d $f_{LR} = 1 - (\Delta T_s)_o/\Delta$

e $f_{LR} = [1 - (\Delta T_s)_o/\Delta$

) as shown in Fig. 1.
:he amplification of the
increases nonlinearly
(89) which arises from
:e explains, in part, the
ises: the $1xCO_2$ surface
the clear case because
ack is lower in the
f there is a large lapse
vection (discussed in the
ndent of T_s.
RCM studies using the
humidity profile
range from 0.371 to
nce of f_W on $T_s(1xCO_2)$ as
$1xCO_2$) values of the
$1xCO_2$) and f_W of Rowntree
of Manabe and Wetherald
e air temperature is
nd 6 suggest a probable
ositive feedback which,
temperature change by an
hould be noted that the
alization. If the rela-
estigated by Augustsson
1978), f_W would exceed
relative humidity
eral circulation model
climatic changes have
t.

RCM study of CO_2-induced
it was assumed, based on
), that the tropospheric
$^{-1}$. A more recent anal-
rvations of Oort and
of the global-mean tropo-
difference in prescribed

h a PEBM and found that
nsensitive to Γ in the
(1978) investigated this
e fixed lapse rate from 5
antitative results were
Table 7, who concluded
terval from 5.5 to
sults obtained using radi-
7 shows a 12% decrease in
y represents a smaller
verified since the requi-

Table 7. Lapse rate feedback f_{LR} determined from selected radiative-convective models

Study	Model Attributes [a]	Convection Treatment	ΔT_s $2xCO_2-1xCO_2$ (°C)	Estimated Feedback f_{LR}
Chylek and Kiehl (1981)	ERE;FRH;FCC; FCA(1);FOD;FAL	FLR(6.5)	100% [b]	
		FLR(6.0)	98%	
		FLR(5.5)	94%	
		FLR(5.0)	88%	
		BADJ [c]	184%	Positive
		MALR [c]	75%	Negative
Hunt and Wells (1979)	BAE;FRH;FCC, FCP(3),FOD;FAL	FLR(6.5)	2.2	
		MALR	1.82	Negative
Hummel and Kuhn (1981a)	ERE;FRH;FCC,FCP(1) (500 mb),FOD;FAL	FLR(6.5)	1.94	
		MALR	0.79	Negative
	ERE;FRH;FCC,FCP(1) (800 mb),FOD;FAL	FLR(6.5)	1.82	
		MALR	1.53	Negative
Wang et al. (1981)	BAE;FRH;FCC, FCA(17),FOD;FAL	FLR(6.5)	2.06	
		MALR	1.49	Negative
Hummel (1982)	ERE;FRH;FCC, FCP(3),FOD;FAL	FLR(6.5)	1.83	
		MALR	1.29	Negative
Lindzen et al. (1982)	BAE;FRH;CLR, - , - ;FAL	FLR(6.5)	1.93	
		MALR	1.51	Negative
		PC	1.46	Negative
Rowntree and Walker (1978)	BAE;FAH;CLR, - , - ;FAL	PC	0.78	-0.654 [d]
Hansen et al. (1981)	BAE;FRH;FCC, FCA(1),FOD;FAL	MALR	1.37	-0.262 [e]

[a] Surface energy flux; water vapor; cloud cover, altitude (number of cloud layers), optical depth; surface albedo. See Table 3 for definition of the abbreviations.

[b] ΔT_s for Γ = 6.5 K/km is taken to be 100%.

[c] BADJ is baroclinic adjustment defined as $d\Gamma/d\Delta T_s = 0.125\ km^{-1}$ and MALR is defined here as $d\Gamma/d\Delta T_s = -0.092\ km^{-1}$.

[d] $f_{LR} = 1 - (\Delta T_s)_o/\Delta T_s$ with $(\Delta T_s)_o$ from Table 6.

[e] $f_{LR} = [1 - (\Delta T_s)_o/\Delta T_s] - f_W$ with $(\Delta T_s)_o$ and f_W from Table 6.

Stone and Carlson (1979) also found that the lapse rate varies systematically with latitude and is governed by the vertical heat transports by cumulus convection and baroclinic eddies. In low latitudes cumulus convection dominates and the lapse rate closely agrees with the moist adiabatic lapse rate

$$\Gamma_m = \Gamma_d \frac{1 + \frac{Lq^*}{RT}}{1 + \frac{Lq^*}{RT}\frac{\varepsilon L}{c_p T}} , \tag{91}$$

where $\Gamma_d = g/c_p \sim 9.8°C\ km^{-1}$ is the dry adiabatic lapse rate, R is the gas constant for dry air, $\varepsilon = 0.622$ and the other symbols have their previously assigned meanings. In high latitudes baroclinic eddies dominate and the lapse rate agrees with the critical lapse rate established by the baroclinic adjustment mechanism (Stone, 1978). Recently, however, Yang and Smith (1985) showed that the lapse rate in the midlatitudes of the Southern Hemisphere follows the critical lapse rate for baroclinic adjustment with a 15 degree latitude lag. Both the moist adiabatic lapse rate (MALR) and the baroclinic adjustment lapse rate (BADJ) depend on temperature and can, therefore, produce a temperature/lapse rate feedback.

Chylek and Kiehl (1981) investigated the feedbacks of the BADJ and MALR lapse rates defined by them as

$$\Gamma_{BADJ} = 6.5 + 0.125\ T,\ °C\ km^{-1} , \tag{92}$$

and

$$\Gamma_{MALR} = 6.5 - 0.092\ T,\ °C\ km^{-1} . \tag{93}$$

Their results are presented in Table 7 and show a positive lapse rate feedback for BADJ and a negative lapse rate feedback for MALR. These lapse rate feedbacks are illustrated schematically in Fig. 6 for the simplified case where ΔT in Eqs. (92) and (93) is taken equal to ΔT_s. In the top panel the critical lapse rate is independent of temperature hence $\Gamma_{1xCO_2} = \Gamma_{2xCO_2} = 6.5°C\ km^{-1}$, and the CO_2-induced warming is uniform throughout the troposphere; in this case there is no lapse rate feedback. In the middle panel the critical lapse rate increases with ΔT_s so that $\Gamma_{2xCO_2} > \Gamma_{1xCO_2} = 6.5°C\ km^{-1}$. If ΔT_s in this case were less than or equal to the ΔT_s of the zero-feedback case, the tropospheric temperatures for doubled CO_2 with feedback would everywhere be colder than the corresponding temperatures without feedback. But then the infrared radiation emitted by the surface and troposphere would be less than the equilibrium values of the zero-feedback case, and the atmosphere/surface system would not be in equilibrium. Therefore, to achieve equilibrium, ΔT_s with this feedback must exceed the ΔT_s without feedback, and the lapse rate feedback with $d\Gamma/dT_s > 0$ is positive. On the other hand, when $d\Gamma/dT_s < 0$ as shown in the bottom panel of Fig. 6,

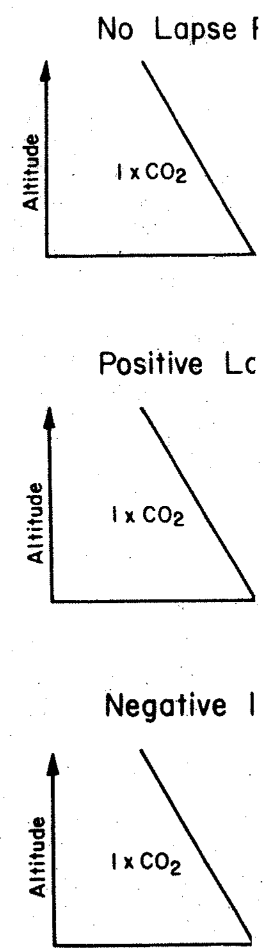

Figure 6. Schematic repr
lapse rate feedback, (B)
lapse rate feedback.

ΔT_s with feedback is less
rate feedback is negative
complex than those shown
MALR vary with altitude.

Because the baroclin
latitudes, while cumulus
should enhance the CO_2-in
and MALR should diminish

the lapse rate varies
by the vertical heat trans-
dies. In low latitudes
te closely agrees with the

(91)

atic lapse rate, R is the
ther symbols have their
des baroclinic eddies dom-
ical lapse rate established
, 1978). Recently, how-
apse rate in the midlati-
critical lapse rate for
de lag. Both the moist
c adjustment lapse rate
re, produce a temperature/

feedbacks of the BADJ and

(92)

(93)

ow a positive lapse rate
eedback for MALR. These
cally in Fig. 6 for the
) is taken equal to ΔT_s.
ndependent of temperature
O_2-induced warming is uni-
there is no lapse rate
apse rate increases with
ΔT_s in this case were less
case, the tropospheric
ıld everywhere be colder
eedback. But then the in-
roposphere would be less
ack case, and the
llibrium. Therefore, to
ıst exceed the ΔT_s without
$/dT_s > 0$ is positive. On
e bottom panel of Fig. 6,

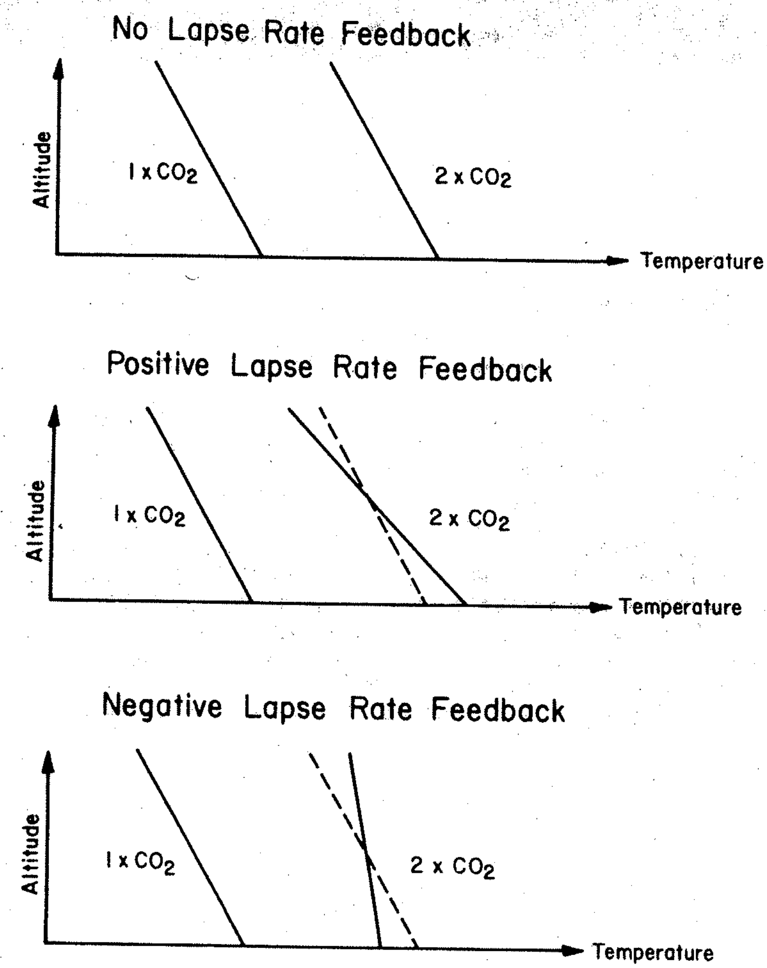

Figure 6. Schematic representation of CO_2-induced warming with (A) no lapse rate feedback, (B) positive lapse rate feedback, and (C) negative lapse rate feedback.

ΔT_s with feedback is less than the ΔT_s without feedback and the lapse rate feedback is negative. The temperature changes are actually more complex than those shown in Fig. 6 because the lapse rates for BADJ and MALR vary with altitude.

Because the baroclinic adjustment process occurs in middle and high latitudes, while cumulus convection is dominant in low latitudes, BADJ should enhance the CO_2-induced middle and high latitude surface warming, and MALR should diminish the surface temperature increase in low latitudes. This latitudinal variation in the surface temperature warming is what is simulated by the general circulation models (Schlesinger and Mitchell, 1985, 1987). Therefore, it is of interest to quantify the feedbacks of the baroclinic adjustment and cumulus convection processes. Unfortunately, we are able to do this from the RCM studies only for cumulus convection.

The moist adiabatic lapse rate Γ_m given by Eq. (91) decreases with increasing temperatures as shown in Fig. 7 due to the increase of q^* with temperature and the fact that $\varepsilon L/c_pT > 1$ for the temperatures in the Earth's atmosphere. Thus, based on the result shown in the bottom panel of Fig. 6, it is expected that the MALR feedback is negative. This is confirmed qualitatively by the studies of Hunt and Wells (1979), Hummel and Kuhn (1981a), Wang et al. (1981), Hummel (1982) and Lindzen et al. (1982) shown in Table 7. A quantitative estimate of this negative feedback can be obtained from the study of Hansen et al. (1981) assuming that the water vapor and lapse rate feedbacks are independent as suggested by the results of Table 5. It is thereby estimated that $f_{MALR} = -0.262$ which, as expected, is smaller than the value given by

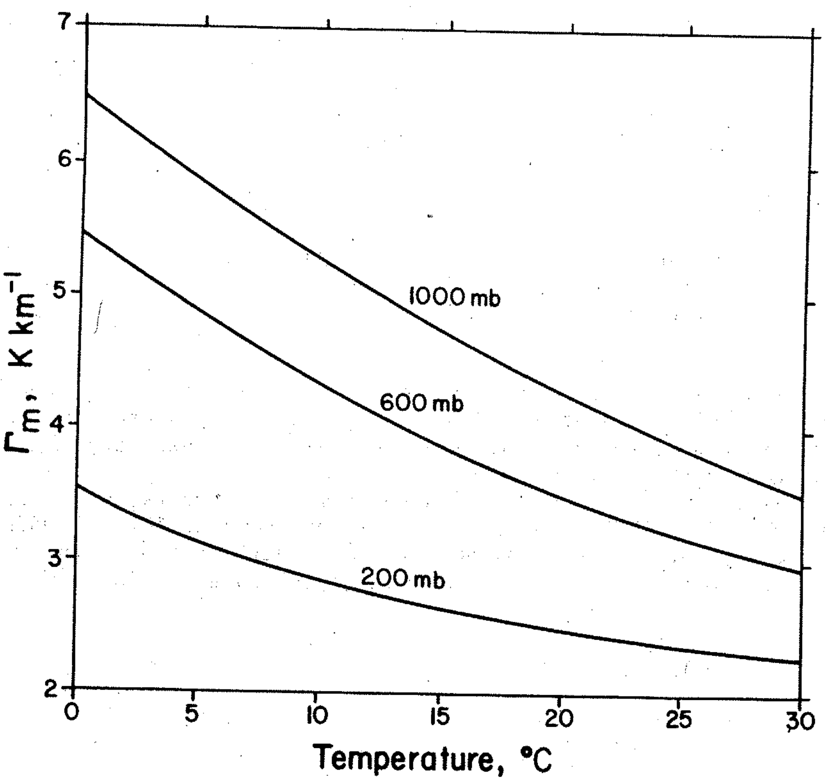

Figure 7. Moist adiabatic lapse rate Γ_m as a function of temperature for selected pressures.

the OSU two-layer RCM (Tal
which, acting alone, woul
by $R_f = 0.79$ (Fig. 2).
In general circulati
change, the physical proc
resolved explicitly and a
form. Two types of cumul
GCMs: moist convective a
abatic lapse rate to the
convection (PC). The PC
convection can take place
which are convectively un
the intervening atmospher
Lindzen et al. (1982) inv
found that f_{PC} is negativ
negative feedback is due
latent heat loss is depos
by a fixed critical lapse
ed to space, and 2) the v
radiative perturbations n
temperature changes witho
lapse rate. However, the
doubled CO_2 for this simp
the MALR (Fig. 8). Rownt
tion of the United Kingdo
1975) and obtained result
is larger in magnitude th
acting alone, would reduc
almost 40%.
In summary it is see
about -0.25 and -0.4, and
on the particular paramet
to give $f_{PC} < f_{MALR} < 0$.

Cloud feedbacks. Changes
clouds induced by a chang
three cloud feedbacks sho
these feedbacks and evalu
from the RCM results.

Cloud altitude feedback.
change, Manabe and Wether
cloud layers at what was
the $1xCO_2$ and $2xCO_2$ simul
altitudes of the clouds h
altitude (FCA). In actua
ers were fixed (FCP) rath
Wetherald (1967) RCM (Wet
for this is that the vert
(1967) RCM is based on th
equal to the pressure p

surface temperature warm-
ation models (Schlesinger
f interest to quantify the
ulus convection processes.
RCM studies only for

y Eq. (91) decreases with
to the increase of q*
for the temperatures in
sult shown in the bottom
feedback is negative.
of Hunt and Wells (1979),
ummel (1982) and Lindzen
e estimate of this nega-
f Hansen et al. (1981)
eedbacks are independent
thereby estimated that
than the value given by

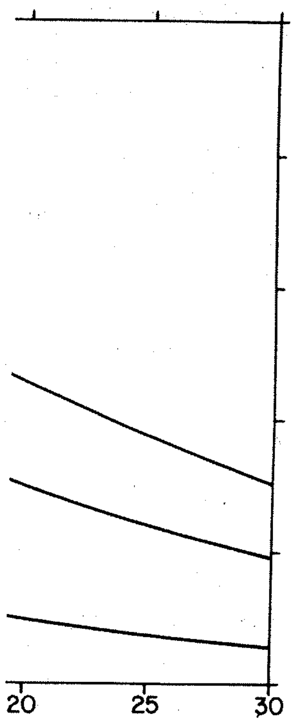

function of temperature

the OSU two-layer RCM (Table 5). This is a moderate negative feedback which, acting alone, would multiply the zero-feedback temperature change by $R_f = 0.79$ (Fig. 2).

In general circulation model studies of CO_2-induced climatic change, the physical processes of cumulus convection are too small to be resolved explicitly and are therefore incorporated in a parameterized form. Two types of cumulus parameterization have been employed in GCMs: moist convective adjustment based on restoring a super moist adiabatic lapse rate to the moist adiabatic lapse rate, and penetrative convection (PC). The PC parameterization differs from the MALR in that convection can take place between two non-contiguous atmospheric layers which are convectively unstable with respect to each other, even though the intervening atmospheric layers are not convectively unstable. Lindzen et al. (1982) investigated a simple PC parameterization and found that f_{PC} is negative (Table 7). These authors concluded that this negative feedback is due to two factors: 1) the surface sensible and latent heat loss is deposited at higher altitudes by cumulus clouds than by a fixed critical lapse rate and is therefore more effectively radiated to space, and 2) the variable lapse rate resulting from the PC allows radiative perturbations near the tropopause to be compensated by local temperature changes without being carried to the surface as by a fixed lapse rate. However, the surface and tropospheric warming induced by doubled CO_2 for this simple PC parameterization is similar to that for the MALR (Fig. 8). Rowntree and Walker (1978) used the PC parameterization of the United Kingdom Meteorological Office 11-layer GCM (Saker, 1975) and obtained results for which $f_{PC} = -0.654$ (Table 7). This value is larger in magnitude than f_{MALR} of the two-layer RCM (Table 5) and, acting alone, would reduce the zero-feedback temperature change by almost 40%.

In summary it is seen that $f_{BADJ} > 0$, $f_{MALR} < 0$ with values between about -0.25 and -0.4, and $f_{PC} < 0$ with values that, although dependent on the particular parameterization of penetrating convection, are likely to give $f_{PC} < f_{MALR} < 0$.

Cloud feedbacks. Changes in the altitude, cover and optical depth of clouds induced by a change in CO_2 concentration can give rise to the three cloud feedbacks shown in Table 5. In this section we describe these feedbacks and evaluate them quantitatively insofar as possible from the RCM results.

Cloud altitude feedback. In the first RCM study of CO_2-induced climate change, Manabe and Wetherald (1967) prescribed the location of three cloud layers at what was stated to be 10, 4.1 and 1.7 to 2.7 km for both the $1xCO_2$ and $2xCO_2$ simulations. Consequently, this treatment of the altitudes of the clouds has come to be known as constant or fixed cloud altitude (FCA). In actuality, however, the pressures of the cloud layers were fixed (FCP) rather than the altitudes in the Manabe and Wetherald (1967) RCM (Wetherald, personal communication). The reason for this is that the vertical structure of the Manabe and Wetherald (1967) RCM is based on the σ-coordinate system which, in this case, is equal to the pressure p divided by the surface pressure p_s. Since the

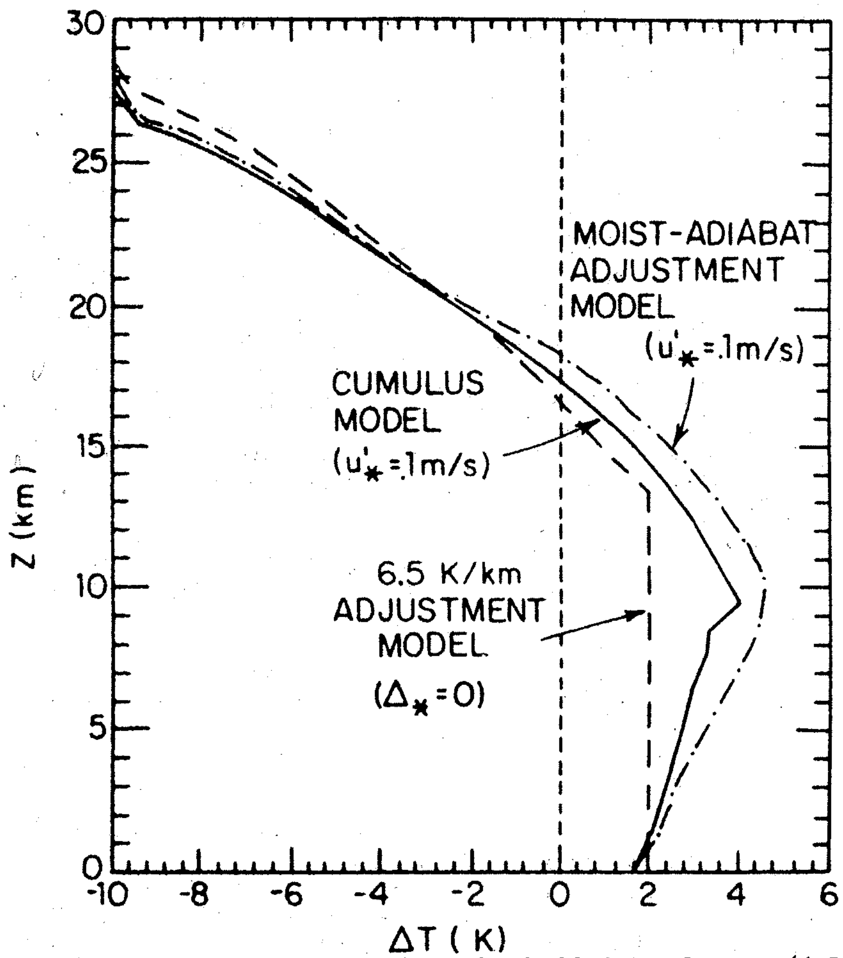

Figure 8. Temperature changes induced by doubled CO_2 for FLR (6.5), MALR and PC (cumulus model) from Lindzen et al. (1982). u_*' is a surface wind parameter used in the calculation of the surface sensible and latent heat fluxes.

clouds were defined at fixed σ-levels and p_s was fixed, the pressures of the cloud layers were fixed. Subsequently, other RCM studies also employed the fixed cloud pressure assumption (e.g., Rowntree and Walker, 1978; Hunt and Wells, 1979; Charlock, 1981; Hummel and Kuhn, 1981a, b; Hummel and Reck, 1981; Hunt, 1981; Hummel, 1982; Lal and Ramanathan, 1984; and Somerville and Remer, 1984), but these studies have also been misinterpreted as employing the FCA assumption. Several RCM studies actually have employed the FCA assumption (e.g., Augustsson and Ramanathan, 1977; Wang and Stone, 1980; Hansen et al., 1981; and Wang et al., 1981) but, as we shall see below, the FCA and FCP assumptions

about the vertical locatic
comparable. Another assum
an examination of the outg
system written as F = c_1 -
$c_1 = c_1(T_s,\Gamma)$, $c_2 = c_2(T_s,$
Cess found that $\partial c_2/\partial T_s$ fc
cloud layers agreed with t
cloud-top temperature was
(FCA).

We can compare the F(
location of clouds by dete
tude, z_c, cloud pressure,
the surface temperature T_s
that the temperature laps

$$T_c = T_s - \Gamma z_c$$

and by integrating the hy
cloud we can obtain

$$p_c = p_s \left(\frac{T_c}{T_s}\right)^{\frac{g}{R\Gamma}}$$

and by Eq. (94)

$$z_c = \frac{1 - (p_c/p_s}{\Gamma}$$

From these expressions we

$$\underline{\text{FCA}} \qquad \frac{\partial z_c}{\partial T_s}$$

$$\frac{\partial p_c}{\partial T_s}$$

and

$$\frac{\partial T_c}{\partial T_s}$$

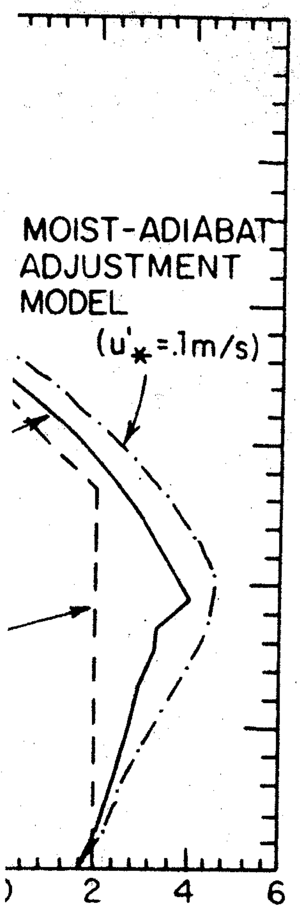

ɔled CO_2 for FLR (6.5),
l. (1982). u_*' is a sur-
f the surface sensible and

vas fixed, the pressures of
ther RCM studies also
(e.g., Rowntree and Walker,
ammel and Kuhn, 1981a, b;
32; Lal and Ramanathan,
ese studies have also been
a. Several RCM studies
g., Augustsson and
a et al., 1981; and Wang
FCA and FCP assumptions

about the vertical location of clouds give results that are not strictly comparable. Another assumption was proposed by Cess (1974, 1975) from an examination of the outgoing infrared flux from the Earth-atmosphere system written as $F = c_1 - c_2A_c$, where A_c is the fractional cloud cover, $c_1 = c_1(T_s,\Gamma)$, $c_2 = c_2(T_s,\Gamma,T_c)$ and T_c is the cloud-top temperature. Cess found that $\partial c_2/\partial T_s$ for either a single effective cloud or for three cloud layers agreed with the empirical findings of Budyko (1969) if the cloud-top temperature was fixed (FCT) rather than the cloud altitude (FCA).

We can compare the FCA, FCP and FCT assumptions about the vertical location of clouds by determining the partial derivatives of cloud altitude, z_c, cloud pressure, p_c, and cloud temperature, T_c, with respect to the surface temperature T_s. This can be done most simply by assuming that the temperature lapse rate Γ is constant. Then

$$T_c = T_s - \Gamma z_c \quad , \tag{94}$$

and by integrating the hydrostatic equation from the surface to the cloud we can obtain

$$p_c = p_s \left(\frac{T_c}{T_s}\right)^{\frac{g}{R\Gamma}} \quad , \tag{95}$$

and by Eq. (94)

$$z_c = \frac{1 - (p_c/p_s)^{\frac{R\Gamma}{g}}}{\Gamma} T_s \quad . \tag{96}$$

From these expressions we can obtain the following:

$$\underline{\text{FCA}} \qquad \frac{\partial z_c}{\partial T_s} = 0 \quad , \tag{97a}$$

$$\frac{\partial p_c}{\partial T_s} = \frac{g z_c}{R T_c} \frac{p_c}{T_s} \quad , \tag{97b}$$

and

$$\frac{\partial T_c}{\partial T_s} = 1 \quad . \tag{97c}$$

$$\underline{\text{FCP}} \qquad \frac{\partial z_c}{\partial T_s} = \frac{1 - (p_c/p_s)^{\frac{R\Gamma}{g}}}{\Gamma} \quad , \tag{98a}$$

$$\frac{\partial p_c}{\partial T_s} = 0 \quad , \tag{98b}$$

and

$$\frac{\partial T_c}{\partial T_s} = \left(\frac{p_c}{p_s}\right)^{\frac{R\Gamma}{g}} \quad . \tag{98c}$$

$$\underline{\text{FCT}} \qquad \frac{\partial z_c}{\partial T_s} = \frac{1}{\Gamma} \quad , \tag{99a}$$

$$\frac{\partial p_c}{\partial T_s} = -\frac{g}{R\Gamma}\left(\frac{T_c}{T_s}\right)^{\frac{g}{R\Gamma}} \frac{p_s}{T_s} \quad , \tag{99b}$$

and

$$\frac{\partial T_c}{\partial T_s} = 0 \quad . \tag{99c}$$

Numerical values for these partial derivatives are shown in Table 8 for the case where p_s = 1000 mb, T_s = 288 K, Γ = 6.5°C km^{-1} and

Table 8. Partial derivatives of cloud altitude, pressure and temperature with respect to surface temperature for the FCA, FCP and FCT assumptions

Cloud Altitude Treatment	$\frac{\partial z_c}{\partial T_s}$ (m°C^{-1})	$\frac{\partial p_c}{\partial T_s}$ (mb°C^{-1})	$\frac{\partial T_c}{\partial T_s}$ (°C °C^{-1})
FCA	0	1.29	1
FCP	19.0	0	0.876
FCT	154	-9.12	0

p_c = 500 mb. Of course ∂z_c FCA, FCP and FCT assumption both T_c and p_c increase as Fig. 9. For the FCP assump es, while for the FCT assum increases. These changes a comparing the three assumpt in surface temperature δT_s

$$0 = (\delta z_c)_A < (\delta z_c$$

$$(\delta p_c)_T < 0 = (\delta p_c$$

and

$$0 = (\delta T_c)_T < (\delta T$$

where $\alpha > 0$ and subscripts and temperature, respective

We can now consider tl the FCP and FCT assumption

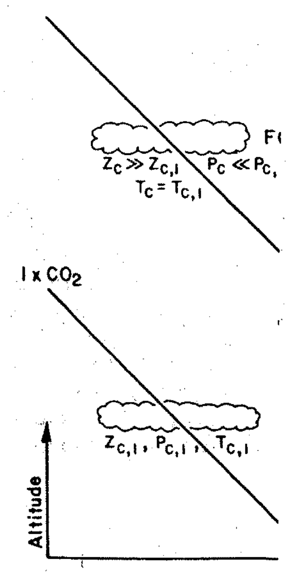

Figure 9. Schematic repre z_c, pressure, p_c, and tem surface temperature, δT_s, pressure (FCP) and fixed

(98a)

(98b)

(98c)

(99a)

(99b)

(99c)

ratives are shown in Table 8
$\Gamma = 6.5°C\ km^{-1}$ and

ltitude, pressure and
temperature for the

$\partial p_c / \partial T_s$ (…$°C^{-1}$)	$\partial T_c / \partial T_s$ ($°C\ °C^{-1}$)
.29	1
0	0.876
.12	0

p_c = 500 mb. Of course $\partial z_c/\partial T_s$, $\partial p_c/\partial T_s$ and $\partial T_c/\partial T_s$ are zero for the FCA, FCP and FCT assumptions, respectively. For the FCA assumption, both T_c and p_c increase as T_s increases. This is shown schematically in Fig. 9. For the FCP assumption, both T_c and z_c increase as T_s increases, while for the FCT assumption, z_c increases and p_c decreases as T_s increases. These changes are also shown schematically in Fig. 9. In comparing the three assumptions, it can be seen that for a small change in surface temperature δT_s

$$0 = (\delta z_c)_A < (\delta z_c)_P < (\delta z_c)_T = \Gamma^{-1}\delta T_s \quad , \tag{100a}$$

$$(\delta p_c)_T < 0 = (\delta p_c)_P < (\delta p_c)_A = \alpha \delta T_s \quad , \tag{100b}$$

and

$$0 = (\delta T_c)_T < (\delta T_c)_P < (\delta T_c)_A = \delta T_s \quad , \tag{100c}$$

where $\alpha > 0$ and subscripts A, P and T denote constant altitude, pressure and temperature, respectively.

We can now consider the feedback of the change in cloud altitude in the FCP and FCT assumptions. First, consider that the cloud altitude is

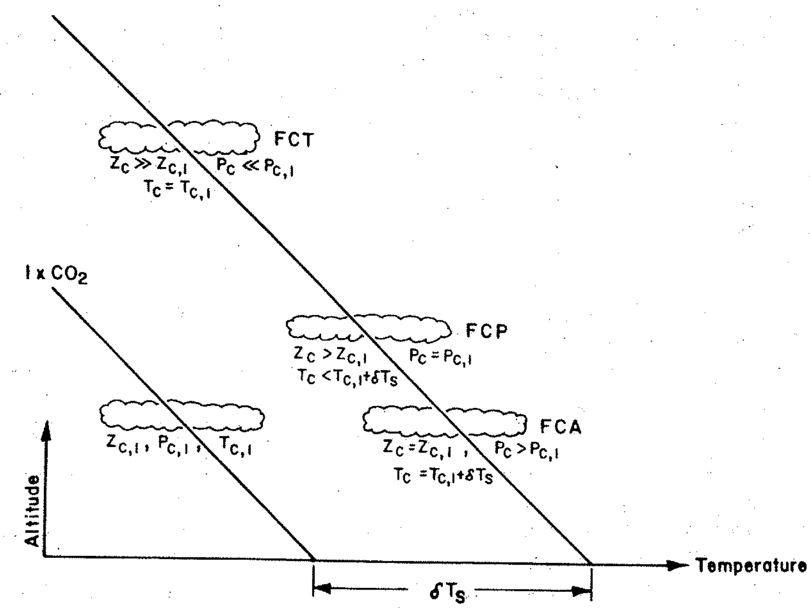

Figure 9. Schematic representation of the changes in cloud altitude, z_c, pressure, p_c, and temperature, T_c, in response to a change in surface temperature, δT_s, for fixed cloud altitude (FCA), fixed cloud pressure (FCP) and fixed cloud temperature (FCT) assumptions.

fixed, the CO_2 concentration is doubled, and the climate system reaches the new equilibrium in which the surface temperature has increased by $(\Delta T_s)_A$ compared with the $1xCO_2$ equilibrium. Then by Eq. (100c), $(\Delta T_c)_A = (\Delta T_s)_A$. Now consider that the cloud temperature is fixed, the CO_2 concentration is doubled, and suppose that the new equilibrium is reached in which $\Delta T_s = (\Delta T_s)_A$. But $(\Delta T_c)_T = 0 < (\Delta T_c)_A$ by Eq. (100c), hence the amount of radiation emitted upward by the cloud for FCT is less than that for FCA; therefore, the climate system with FCT cannot be in equilibrium with $\Delta T_s = (\Delta T_s)_A$. To achieve equilibrium with FCT requires that $(\Delta T_s)_T > (\Delta T_s)_A$. The FCT assumption amplifies the surface temperature change of the FCA assumption and is therefore a positive feedback process. Following similar reasoning it can be seen that the FCP assumption also is a positive feedback process. However, comparison of the $\partial T_c/\partial T_s$ derivatives in Table 8 indicates that the FCP feedback is small compared to the FCT feedback.

A quantitative assessment of the FCT feedback f_{CA} is presented in Table 9. The ratio of ΔT_s with FCT to ΔT_s with FCA or FCP varies from 1.43 to 1.62 in the four studies shown in the table. Because each of these studies was performed with the water vapor feedback of the fixed relative humidity assumption, it is possible to estimate f_{CA} only for the two studies for which f_W can be estimated. The resultant estimated cloud altitude feedback varies from 0.168 to 0.203, which is smaller than the value of 0.261 shown in Table 5.

Table 9. Cloud altitude feedback f_{CA} determined from selected radiative-convective models

Study	Model Attributes [a]	Cloud Altitude Treatment (Layers)	ΔT_s $2xCO_2-1xCO_2$ (°C)	Estimated Feedback f_{CA}
Augustsson and Ramanathan (1977)	ERE;FRH;FLR(6.5); FCC,FOD;FAL	FCA(1) FCT(1)	1.98 3.2	Positive
Wang and Stone (1980)	BAE;FRH;FLR(6.5); FCC,FOD;FAL	FCA(1) FCT(1)	2.00 3.00	Positive
Reck (1979a)	ERE;FRH;FLR(6.5); FCC,FOD;FAL	FCT(3)	1.426 to 1.561 times the response for FCP	0.168 to 0.203 [b]
Hansen et al. (1981)	BAE;FRH;FLR(6.5); FCC,FOD;FAL	FCA(1) FCT(1)	1.94 2.78	0.190 [c]

[a] Surface energy flux; water vapor; lapse rate; cloud cover, optical depth; surface albedo. See Table 3 for definition of abbreviations.

[b] $f_{CA} = [1 - (\Delta T_s)_o/\Delta T_s] - f_W$ with $(\Delta T_s)_o$ and f_W from Table 6 for Manabe and Wetherald (1967) with FCC.

[c] As in footnote b, except values from Hansen et al. (1981).

the climate system reaches
erature has increased by
Then by Eq. (100c),
temperature is fixed, the
it the new equilibrium is
$0 < (\Delta T_C)_A$ by Eq. (100c),
by the cloud for FCT is
e system with FCT cannot be
equilibrium with FCT re-
ion amplifies the surface
is therefore a positive
ig it can be seen that the
ocess. However, comparison
es that the FCP feedback is

dback f_{CA} is presented in
th FCA or FCP varies from
table. Because each of
apor feedback of the fixed
to estimate f_{CA} only for
i. The resultant estimated
0.203, which is smaller

ined from selected

rs)	ΔT_s $2xCO_2$-$1xCO_2$ (°C)	Estimated Feedback f_{CA}
	1.98 3.2	Positive
	2.00 3.00	Positive
	1.426 to 1.561 times the response for FCP	0.168 to 0.203 [b]
	1.94 2.78	0.190 [c]

over, optical depth; surface albedo.

able 6 for

981).

Cloud cover feedback. To begin our discussion of cloud cover feedback it is helpful to reconsider the planetary radiative energy budget given by Eq. (52) as

$$N_o = \frac{1-\alpha_p}{4} S_o - R_o \quad .$$

Following the procedure in Section 2.1, we can write that the change in N_o due to a change in the CO_2 concentration ΔC and the induced surface temperature change $(\Delta T_s)_{\Delta C}$ is

$$\Delta N_o = \frac{\partial N_o}{\partial C}\Delta C + \left(\frac{\partial N_o}{\partial T_s} + \sum_j \frac{\partial N_o}{\partial I_j}\frac{dI_j}{dT_s} + \frac{\partial N_o}{\partial A_c}\frac{dA_c}{dT_s}\right)(\Delta T_s)_{\Delta C}$$

where $\partial N_o/\partial T_s$ is the change in N_o due to the change in T_s when all the internal quantities I_j are constant, $(\partial N_o/\partial A_c)(dA_c/dT_s)$ is the change in N_o due to the change in the internal quantity cloud cover A_c through its dependence on T_s, and $\sum_j (\partial N_o/\partial I_j)(dI_j/dT_s)$ is the change in N_o due to the changes in all the other internal quantities through their dependences on T_s. Setting $\Delta N_o = 0$ in the equation above gives the equilibrium $(\Delta T_s)_{\Delta C}$ as

$$(\Delta T_s)_{\Delta C} = \frac{\frac{\partial N_o}{\partial C}\Delta C}{-\frac{\partial N_o}{\partial T_s} - \sum_j \frac{\partial N_o}{\partial I_j}\frac{dI_j}{dT_s} - \frac{\partial N_o}{\partial A_c}\frac{dA_c}{dT_s}} \tag{101a}$$

or

$$(\Delta T_s)_{\Delta C} = \frac{G_o}{1 - \sum_j f_j - f_{CC}} \frac{\partial N_o}{\partial C}\Delta C \quad , \tag{101b}$$

where $G_o = -\left(\frac{\partial N_o}{\partial T_s}\right)^{-1}$, $f_j = G_o \frac{\partial N_o}{\partial I_j}\frac{dI_j}{dT_s}$, and the cloud cover feedback f_{CC} is given by

$$f_{CC} = \delta \frac{dA_c}{dT_s} G_o \quad , \tag{102}$$

with

$$\delta = \frac{\partial N_o}{\partial A_c} = -\frac{S_o}{4}\frac{\partial \alpha_p}{\partial A_c} - \frac{\partial R_o}{\partial A_c} \quad , \tag{103}$$

as first defined by Schneider (1972). From Eq. (102) it can be seen that cloud cover feedback depends on the three quantities: δ, dA_c/dT_s and G_o. Assuming that

$$\alpha_p = (1-A_c)\alpha_s + A_c\,\alpha_c \quad , \tag{104}$$

where α_s is the clear-sky albedo and α_c the albedo with cloud cover, Eq. (103) can be written as

$$\delta = -\frac{S_o}{4}\left(\alpha_c - \alpha_s\right) - \frac{\partial R_o}{\partial A_c} \quad . \tag{105}$$

Because $\alpha_c > \alpha_s$ in the global mean, the change in albedo due to a change in cloud cover contributes negatively to δ. On the other hand, $\partial R_o/\partial A_c < 0$ because the upward emission from clouds is less than that from the warmer ground. Thus, the change in longwave radiation due to a change in cloud cover contributes positively to δ. If $\delta > 0$ the longwave radiation effect dominates the albedo effect, and vice versa if $\delta < 0$. This is summarized in Table 10, together with the dependence of the sign of the cloud cover feedback on dA_c/dT_s.

Only one CO_2 study has been performed with an RCM in which the cloud cover has been a predicted quantity. (We shall describe this study subsequently.) In all the other RCM CO_2 studies, $dA_c/dT_s = 0$; hence, as shown in Table 10, $f_{CC} = 0$. However, a few non-CO_2 studies have been carried out to determine the effects of prescribed changes in cloud cover. In these studies A_c is an external quantity, hence

$$\Delta N_o = \frac{\partial N_o}{\partial A_c}\Delta A_c + \left(\frac{\partial N_o}{\partial T_s} + \sum_j \frac{\partial N_o}{\partial I_j}\frac{dI_j}{dT_s}\right)(\Delta T_s)_{\Delta CL} \quad ,$$

Table 10. Characteristics of cloud cover feedback, f_{CC}

$\frac{dA_c}{dT_s}$	δ	Dominant Effect	f_{CC}
+	+	longwave	+
	0	neither	0
	−	albedo	−
0	+	longwave	0
	0	neither	0
	−	albedo	0
−	+	longwave	−
	0	neither	0
	−	albedo	+

:q. (102) it can be seen
e quantities: δ, dA_c/dT_s

(104)

albedo with cloud cover,

(105)

ge in albedo due to a change
On the other hand,
clouds is less than that
longwave radiation due to a
to δ. If $\delta > 0$ the long-
ffect, and vice versa if
ther with the dependence of
dT_s.
ith an RCM in which the
(We shall describe this
O_2 studies, $dA_c/dT_s = 0$;
er, a few non-CO_2 studies
ts of prescribed changes in
rnal quantity, hence

$(\Delta T_s)_{\Delta CL}$,

er feedback, f_{CC}

ant ct	f_{CC}
ave	+
er	0
o	-
ave	0
er	0
o	0
ave	-
er	0
o	+

and the equilibrium $(\Delta T_s)_{\Delta CL}$ is then

$$(\Delta T_s)_{\Delta CL} = \frac{\delta \Delta A_c}{-\frac{\partial N_o}{\partial T_s} - \sum_j \frac{\partial N_o}{\partial I_j}\frac{dI_j}{dT_s}} \quad . \tag{106}$$

This can be written by Eq. (6) as

$$(\Delta T_s)_{\Delta CL} = G_f \, \delta \, \Delta A_c \quad . \tag{107}$$

Thus, δ can be determined from

$$\delta = \frac{(\Delta T_s)_{\Delta CL}}{G_f \, \Delta A_c} \quad , \tag{108}$$

if G_f for the model is known. In addition, a few RCM studies have been performed in which both the CO_2 concentration and the fractional cloudiness were changed. In this case

$$\Delta N_o = \frac{\partial N_o}{\partial C} \Delta C + \delta \, \Delta A_c + \left(\frac{\partial N_o}{\partial T_s} + \sum_j \frac{\partial N_o}{\partial I_j}\frac{dI_j}{dT_s}\right) (\Delta T_s)_{\Delta C,\Delta CL} \quad .$$

Setting $\Delta N_o = 0$ at equilibrium and solving for $(\Delta T_s)_{\Delta C,\Delta CL}$ then gives

$$(\Delta T_s)_{\Delta C,\Delta CL} = \frac{\frac{\partial N_o}{\partial C} \Delta C + \delta \Delta A_c}{-\frac{\partial N_o}{\partial T_s} - \sum_j \frac{\partial N_o}{\partial I_j}\frac{dI_j}{dT_s}} \tag{109}$$

and

$$(\Delta T_s)_{\Delta C,\Delta CL} = (\Delta T_s)_{\Delta C} + G_f \, \delta \, \Delta A_c \quad , \tag{110}$$

the latter by Eq. (101a) with $dA_c/dT_s = 0$ and the definition of G_f (Eq. (16)). Thus, δ can be determined from

$$\delta = \frac{(\Delta T_s)_{\Delta C,\Delta CL} - (\Delta T_s)_{\Delta C}}{G_f \, \Delta A_c} \tag{111}$$

if G_f for the model is known.

An analysis of δ based on either Eq. (108) or Eq. (111) has been made for six RCM studies, and the necessary input data and results are presented in Table 11 together with the attributes and cloud characteristics of the models. These results are categorized in Table 12 in

Table 11. Analysis of $\delta = \partial N_o/\partial A_c$ from RCM simulations of $(\Delta T_s)_{\Delta CL}$ and $(\Delta T_s)_{\Delta C,\Delta CL}$

Study	Model Attributes [a]	Cloud Altitude (km)	Cloud Emissivity	Cloud Albedo	Cloud Absorptivity	ΔA_c	G_f (°C/(Wm^{-2}))	$(\Delta T_s)_{\Delta CL}$ or $(\Delta T_s)_{\Delta C,\Delta CL}$, and $(\Delta T_s)_{\Delta C}$ (°C)	δ (Wm^{-2})
Manabe and Strickler (1964)	ERE; FAH; FLR(6.5); FOD; FAL;	20	0.5	0.21	0.005	1	0.34 [b]	- 5	14.7 [c]
		11	0.5	0.21	0.005	1	0.34 [b]	- 5	14.7 [c]
		7.5	1	0.21	0.005	1	0.34 [b]	- -2	-5.9 [c]
		3.7	1	0.48	0.02	1	0.34 [b]	- -22	-65 [c]
		1.4-2.0	1	0.69	0.035	1	0.34 [b]	- -50	-147 [c]
Manabe and Wetherald (1967)	ERE; FRH; FLR(6.5); FOD; FAL	10	0.5	0.20	0	1	0.73 [d]	4	5.5 [c]
		10	1	0.20	0	1	0.73 [d]	39	53 [c]
		4.1	1	0.48	0	1	0.73 [d]	-39	-53 [c]
		1.7-2.7	1	0.69	0	1	0.73 [d]	-82	-112 [c]
Reck (1979b)	ERE; FRH; FLR(6.5);	10	1	0.20	0	-0.05	0.425 [e]	0, 1.7	80 [f]
	FOD; FAL	1.7-2.7	1	0.69	0	0.03	0.425 [e]	0, 1.7	-133 [f]
Hummel and Reck (1981)	ERE; FRH; MALR; FOD; FAL	3.5-5.5	1	0.32	0	-0.212	0.512 [g]	2.56, 2.05	-4.7 [f]
		3.5-5.5	1	0.32	0	0.176	0.512 [g]	1.89, 2.05	-1.8 [f]
Hunt (1981)	BAE, FRH, FLR(6.5); FOD; FAL	10	1	0.21	0.005	0.018	0.455 [h]	2.19, 1.82	45 [f]
		4.1	1	0.48	0.020	0.008	0.455 [h]	1.59, 1.82	-63 [f]
		1.7-2.7	1	0.69	0.035	0.030	0.455 [h]	0.01, 1.82	-133 [f]
Stephens and Webster (1981)	ERE; FRH; FLR(6.5); FOD; FAL	7.5-9	IWP = 20 g m^{-2} [i]			1	0.52 [j]	16	31 [f]
		3.75-5	LWP = 140 g m^{-2} [i]			1	0.52 [j]	-22	-42 [f]
		0.75-1.5	LWP = 140 g m^{-2} [i]			1	0.52 [j]	-40	-77 [f]

[a] Surface energy flux; water vapor; convection; cloud optical depth; surface albedo. See Table 3 for definition of the abbreviations.

[b] $G_f = (\Delta T_s)_{2xCO_2}/\Delta Q$ with $(\Delta T_s)_{2xCO_2} = 1.36°C$ from Table 6 for Manabe and Wetherald (1967) with CLR and FAH, and assumed $\Delta Q = 4\ Wm^{-2}$.

[c] Determined from Eq. (108).

[d] As in footnote b, except with $(\Delta T_s)_{2xCO_2} = 2.92°C$ from Table 6 for Manabe and Wetherald (1967) with CLR and FRH.

[e] As in footnote b, except with $(\Delta T_s)_{2xCO_2} = 1.7°C$.

[f] Determined from Eq. (111).

[g] As in footnote b, except with $(\Delta T_s)_{2xCO_2} = 2.05°C$.

[h] As in footnote b, except with $(\Delta T_s)_{2xCO_2} = 1.82°C$.

[i] Cloud emissivity, albedo and absorptivity determined from the cloud liquid water and ice water paths (LWP and IWP) shown, based on Stephens (1978) and Stephens and Webster (1981), respectively.

[j] $G_f = \beta/(S_o(1-\alpha_p)/4)$ with $\alpha_p = 0.3$, $S_o = 1370\ Wm^{-2}$, and $\beta = S_o(\Delta T_s/\Delta S_o) = 125°C$ from Stephens and Webster (1981).

Table 12. $\delta = \partial N_o/\partial A_c$ (Wm^{-2}) for low, middle and high cloud summarized from the analysis of Table 11

Study	Low Cloud (0.75, 2.7 km) [a]	Middle Cloud (3.5, 5.5 km) [a]	High Cloud [b] (7.5, 11 km) [a]
Manabe and Strickler (1964)	-147	-65	14.7 (0.5)
Manabe and Wetherald (1967)	-112	-53	5.5 (0.5) 53 (1.0)
Reck (1979b)	-133		80 (0.5)
Hummel and Reck (1981)		-4.7, -1.8 [c]	
Hunt (1981)	-133	-63	45 (1.0)
Stephens and Webster (1981)	-77	-42	31 (0.86)
Hummel (1982)	-143	-50	36 (1.0)

[a] Altitude bounds between which the particular cloud type is located.

[b] The cloud emissivity is shown in parentheses.

[c] For $\Delta A_c = -0.212$ and 0.176, respectively.

terms of the vertical location of the clouds, that is, low, middle and high clouds defined within the altitude bounds of 0.75 and 2.7 km, 3.5 and 5.5 km, and 7.5 and 11 km, respectively. It can be seen that these RCMs give negative values of δ for low and middle clouds, with more negative values for the low clouds than for the middle clouds, and positive values of δ for high clouds. Thus, from Table 10, the albedo effect dominates the longwave effect for low and middle clouds, while the opposite is true for high clouds. From Eq. (105) it can be seen that the dominance of the albedo effect over the longwave effect in low and middle clouds occurs because α_c is large (Table 11) and $\partial R_o/\partial A_c$ is small (and negative), the latter because the cloud-top temperature is not much colder than the ground. However, as the cloud altitude increases, the difference between the cloud-top and ground temperatures grows and $\partial R_o/\partial A_c$ becomes more negative. Also α_c decreases as the optical thickness of the cloud decreases with increasing altitude (Table 11). Both of these effects cause δ to increase with increasing altitude and eventually to become positive for the high clouds. For the latter, α_c is small and close to α_s, so that the value of δ is largely determined by

a Surface energy flux; water vapor; convection; cloud optical depth; surface albedo. See Table 3 for definition of the abbreviations.

b $G_f = (\Delta T_s)_{2xCO_2}/\Delta Q$ with $(\Delta T_s)_{2xCO_2} = 1.36°C$ from Table 6 for Manabe and Wetherald (1967) with CLR and FAH, and assumed $\Delta Q = 4\ Wm^{-2}$.

c Determined from Eq. (108).

d As in footnote b, except with $(\Delta T_s)_{2xCO_2} = 2.92°C$ from Table 6 for Manabe and Wetherald (1967) with CLR and FRH.

e As in footnote b, except with $(\Delta T_s)_{2xCO_2} = 1.7°C$.

f Determined from Eq. (111).

g As in footnote b, except with $(\Delta T_s)_{2xCO_2} = 2.05°C$.

h As in footnote b, except with $(\Delta T_s)_{2xCO_2} = 1.82°C$.

i Cloud emissivity, albedo and absorptivity determined from the cloud liquid water and ice water paths (LWP and IWP) shown, based on Stephens (1978) and Stephens and Webster (1981), respectively.

j $G_f = \beta/[S_o(1-\alpha_p)/4)$ with $\alpha_p = 0.3$, $S_o = 1370\ Wm^{-2}$, and $\beta = S_o(\Delta T_s/\Delta S_o) = 125°C$ from Stephens and Webster (1981).

$\partial R_o/\partial A_c$. This, in turn, depends on the emissivity ε of the high cloud as well as on the difference between the cloud-top and ground temperatures. Because $\partial R_o/\partial A_c$ increases in magnitude with increasing ε, δ increases with ε for high clouds as generally shown in Table 12.

The values of δ shown in Table 12 for each cloud differ among the models for several reasons including differences in the atmospheric composition of the models, other feedback processes, the actual location of clouds within the altitude bounds of low, middle and high clouds, and, probably most importantly, the cloud optical properties of the models. With regard to the latter, all of the models except that of Stephens and Webster (1981) prescribe the optical properties of the clouds on the basis of limited and nonsimultaneous observations. On the other hand, Stephens and Webster (1981) calculate all of the cloud optical properties in a consistent manner for the prescribed cloud liquid water path (LWP) or ice water path (IWP) and the solar zenith angle from parameterizations of multiple scattering calculations. Figure 10 shows $(\Delta T_s)_{\Delta CL}$ as a function of the LWP or IWP for the three cloud layers of Stephens and Webster (1981) defined in Table 11. Because δ is related to $(\Delta T_s)_{\Delta CL}$ by Eq. (108), in this case for which $\Delta A_c = 1$ and $G_f = = 0.52$ (Table 11), $\delta \simeq 2(\Delta T_s)_{\Delta CL}$. Therefore, Fig. 10 shows that δ decreases with increasing LWP and IWP. As shown by Stephens and Webster (1981) and Eq. (105), this occurs because α_c increases with LWP(IWP), but ε rapidly reaches unity for small LWP(IWP) and thereafter cannot increase with increasing LWP. Figure 10 also shows that δ increases with altitude for fixed LWP(IWP), as was also shown in Table 12, and increases with latitude in winter for fixed LWP(IWP) and altitude. The latter occurs because of the dependence of δ on insolation and the decrease of insolation with latitude in the winter hemisphere. It can be concluded from the above that the feedback effect of a CO_2-induced change in cloud cover depends on the latitude, altitude, LWP(IWP) - or equivalently optical depth - of the clouds, and on the sign and magnitude of dA_c/dT_s.

We now consider the RCM study by Wang et al. (1981) in which the cloud cover is a predicted quantity. The cloud model is based on the conservation equation for the cloud liquid water mixing ratio ℓ,

$$\frac{\partial \ell}{\partial t} = C - P \quad , \tag{112}$$

where C and P are the condensation and precipitation rates per unit mass of air. The precipitation rate is parameterized as

$$P = f_1 \ell \quad , \tag{113}$$

where f_1^{-1} is a prescribed conversion time (~ 2 h) of cloud droplets to precipitation. The condensation is obtained from

$$(1 + B)LC = H_c \quad , \tag{114}$$

where H_c is the convective heating rate given by the convective adjustment. This is equal to the latent heating rate, LC, plus the sensible heating rate, B(LC), where B is the Bowen ratio of the sensible

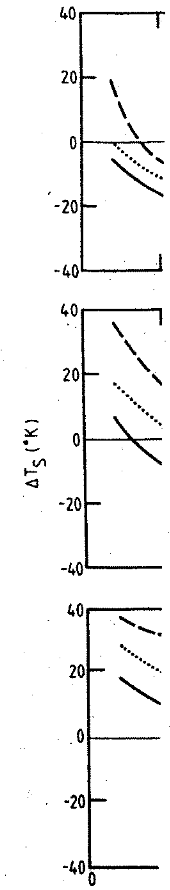

Figure 10. Change in su
different latitudes as a
(LWP and IWP) for high (
(0.75-1.5 km) clouds. S

and latent heating rates
$\partial\ell/\partial t = 0$ for equilibriu

$$\ell = \frac{H_c}{f_1(1 + B)L}$$

The Bowen ratio is taker
vertically-integrated cc
the relative humidity is

ivity ε of the high cloud
d-top and ground
agnitude with increasing ε,
ly shown in Table 12.
ch cloud differ among the
ces in the atmospheric
cesses, the actual location
middle and high clouds,
ical properties of the
e models except that of
ical properties of the
neous observations. On the
late all of the cloud op-
he prescribed cloud liquid
the solar zenith angle from
ulations. Figure 10 shows
the three cloud layers of
11. Because δ is related
ich $\Delta A_c = 1$ and G_f = = 0.52
0 shows that δ decreases
phens and Webster (1981)
es with LWP(IWP), but ε
thereafter cannot increase
at δ increases with alti-
Table 12, and increases
d altitude. The latter
lation and the decrease of
here. It can be concluded
CO_2-induced change in cloud
IWP) - or equivalently
n and magnitude of dA_c/dT_s.
al. (1981) in which the
ud model is based on the
ater mixing ratio ℓ,

(112)

itation rates per unit mass
ized as

(113)

2 h) of cloud droplets to
from

(114)

n by the convective
ting rate, LC, plus the sen-
wen ratio of the sensible

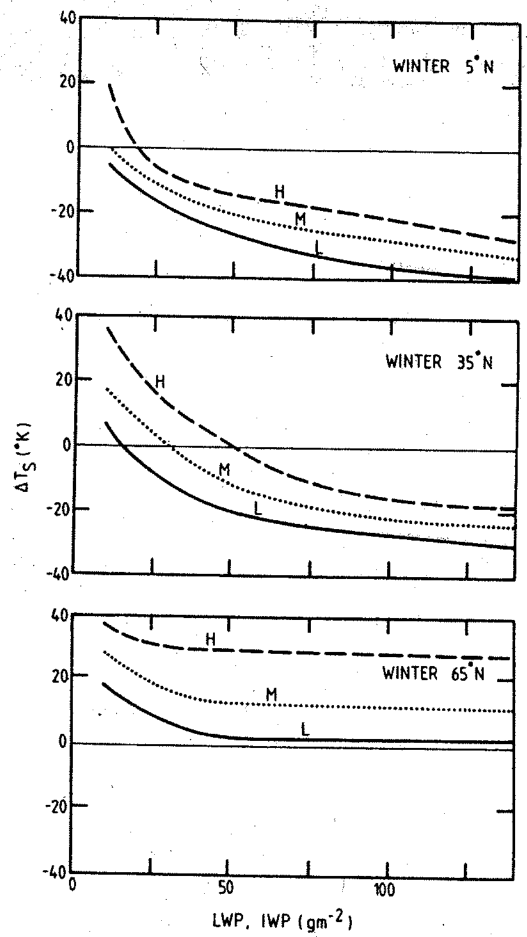

Figure 10. Change in surface temperature $(\Delta T_s)_{\Delta C}$ for $\Delta A_c = 1$ at different latitudes as a function of liquid water and ice water path (LWP and IWP) for high (7.5-9 km), middle (3.75-5 km) and low (0.75-1.5 km) clouds. Source: Stephens and Webster (1981).

and latent heating rates. Combining Eqs. (112)-(114) and setting $\partial \ell / \partial t = 0$ for equilibrium gives

$$\ell = \frac{H_c}{f_1(1 + B)L} \quad . \tag{115}$$

The Bowen ratio is taken to be independent of altitude to satisfy the vertically-integrated conservation of water substance and energy, and the relative humidity is assumed fixed (FRH). The Bowen ratio is then given by the surface value

$$B = \frac{\frac{1}{4}\frac{c_p}{L}}{RH_s \left(\frac{\partial q^*}{\partial T}\right)_{T_s}} \quad , \tag{116}$$

where the derivative of saturation mixing ratio q^* with respect to temperature is evaluated at the surface temperature, and the factor 1/4 is introduced to match the global mean value of B given by Budyko (1956). Finally, it is assumed that the cloud cover A_c increases with increasing precipitation rate, hence

$$A_c = \ell / f_2 \quad , \tag{117}$$

where f_2 is a typical mixing ratio for precipitating cloud systems (5.5×10^{-4}). Combining Eqs. (115) and (117) gives

$$A_c = \frac{H_c}{f_1 f_2 (1 + B) L} \tag{118}$$

from which

$$\frac{dA_c}{dT_s} = \frac{1}{f_1 f_2 L (1 + B)} \left(\frac{dH_c}{dT_s} - \frac{H_c}{1+B}\frac{dB}{dT_s}\right) \quad . \tag{119}$$

Because B decreases with increasing T_s, the last term in Eq. (119) contributes positively to dA_c/dT_s. However, because dH_c/dT_s can be either positive or negative, dA_c/dT_s can also be of either sign.

The RCM of Wang et al. (1981) has 17 vertical layers from the surface to 50 km altitude with attributes of ERE, FRH, FLR(6.5), FCA, FOD and FAL (Table 3). Thus, the results with and without cloud cover feedback also include water vapor feedback, and a precise evaluation of f_{CC} cannot be obtained because $(\Delta T_s)_o$ is not known. The optical depth in the experiments discussed below was fixed with values of 16, 6 and 2 for the altitude ranges 0-3 km, 3-8 km, and above 8 km, respectively.

Results from Wang et al. (1981) are shown in Table 13 for both a CO_2 doubling and a 2% increase in the solar constant S_o. For fixed cloud cover, these different external forcings give comparable surface warmings of about 2°C. Both external forcings give nearly the same increase in the total cloud cover of about 0.02 on a scale from 0 (no clouds) to 1 (overcast). Since ΔT_s is also positive, dA_c/dT_s is positive for both forcings. However, ΔT_s for the CO_2 doubling increases with the increased cloud cover, but ΔT_s for the increased solar constant decreases with the increased cloud cover. Table 13 shows an estimate of the cloud cover feedback defined as $\tilde{f}_{CC} = 1 - (\Delta T_s)_{\Delta CL=0}/(\Delta T_s)_{\Delta CL\neq 0}$. This parameter is different from the actual cloud feedback f_{CC} because

Table 13. Cloud cover fe (1981)

External Forcing
$\Delta C/C = 1$
$\Delta S_o/S_o = 0.02$

a $\tilde{f}_{CC} = 1 - \frac{(\Delta T_s)_{\Delta CL =}}{(\Delta T_s)_{\Delta CL \neq}}$

both $(\Delta T_s)_{\Delta CL=0}$ and $(\Delta T_s)_{\Delta C}$ that f_{CC} is positive for th able magnitude for the incr

To understand these ap the vertical distribution c

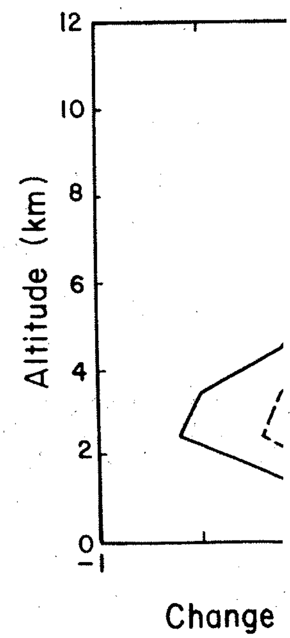

Figure 11. Change in pres a 2% increase in the sola concentration. Source: W

(116)

ɔ q* with respect to tem-
ce, and the factor 1/4 is
given by Budyko (1956).
increases with increasing

(117)

cating cloud systems
gives

(118)

. (119)

st term in Eq. (119)
ecause dH_c/dT_s can be
be of either sign.
ical layers from the
RE, FRH, FLR(6.5), FCA,
and without cloud cover
d a precise evaluation of
nown. The optical depth
ith values of 16, 6 and 2
ove 8 km, respectively.
in Table 13 for both a
nstant S_o. For fixed
give comparable surface
give nearly the same in-
on a scale from 0 (no
sitive, dA_c/dT_s is posi-
CO_2 doubling increases
e increased solar constant
le 13 shows an estimate of
$(\Delta T_s)_{\Delta CL=0}/(\Delta T_s)_{\Delta CL\neq 0}$.
oud feedback f_{CC} because

Table 13. Cloud cover feedback analysis for the study by Wang et al. (1981)

External Forcing	ΔA_c	ΔT_s (°C)	$\tilde{f}_{CC}$ [a]
$\Delta C/C = 1$	0	1.96	
	0.0178	2.68	0.269
$\Delta S_o/S_o = 0.02$	0	2.28	
	0.021	1.87	−0.219

[a] $\tilde{f}_{CC} = 1 - \frac{(\Delta T_s)_{\Delta CL = 0}}{(\Delta T_s)_{\Delta CL \neq 0}}$

both $(\Delta T_s)_{\Delta CL=0}$ and $(\Delta T_s)_{\Delta CL\neq 0}$ have water vapor feedback. It is seen that f_{CC} is positive for the CO_2 doubling and is negative and of comparable magnitude for the increased solar constant.

To understand these apparently contradictory results, Fig. 11 shows the vertical distribution of the changes in cloud cover for both

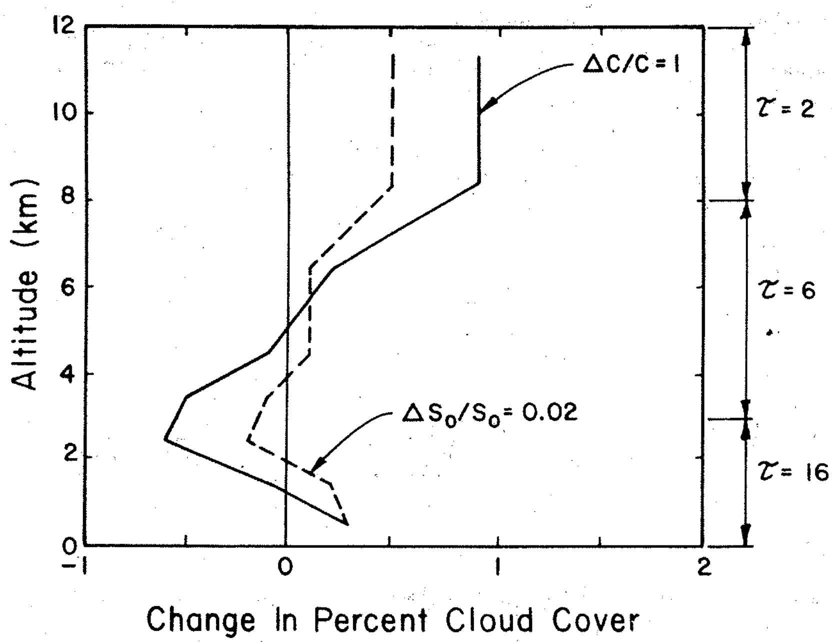

Figure 11. Change in present cloud cover as a function of altitude for a 2% increase in the solar constant and a doubling of the CO_2 concentration. Source: Wang et al. (1981).

external forcings. This figure shows cloud cover increases below about 2 km and above about 5 km, with cloud cover decreases between these altitudes. The changes in cloud cover of both signs are generally larger in magnitude for the CO_2 doubling than for the solar constant increase. In Table 14 we present an estimate of the contribution of these changes in cloud cover to the feedback f_{CC}. For this purpose we have estimated the values of δ for the three layers of constant τ (0-3 km, 3-8 km, and above 8 km) based on the results of Manabe and Wetherald (1967) shown in Table 12. The values of ΔA_c are estimated from Fig. 11 for each of these constant τ layers. Table 14 shows that both the increased high cloud cover and decreased low cloud cover give positive contributions to the positive cloud cover feedback of the CO_2 doubling, with the contribution from the low cloud being about twice that of the high cloud, and no contribution from the middle cloud. On the other hand, the increased low and middle cloud cover in the increased solar constant forcing give negative contributions to the cloud cover feedback which dominate the positive contribution from the increased high cloud.

Table 14. Contributions to f_{CC} by the changes in the low, middle and high clouds in the study by Wang et al. (1981)

External Forcing	Cloud	τ	δ (Wm^{-2}) [a]	ΔA_c [b]	f_{CC} [c]
$\Delta C/C = 1$	High ($z > 8$ km)	2	6	0.01	0.0090
	Middle ($3 < z < 8$ km)	6	-50	0	0
	Low ($z < 3$ km)	16	-100	-0.0015	0.0225
	Total effect				0.0315
$\Delta S_o/S_o = 0.02$	High ($z > 8$ km)	2	6	0.005	0.0045
	Middle ($3 < z < 8$ km)	6	-50	0.002	-0.0150
	Low ($z < 3$ km)	16	-100	0.0007	-0.0105
	Total effect				-0.0210

[a] Based on the study of Manabe and Wetherald (1967) shown in Table 12.

[b] Estimated from Fig. 11.

[c] $f_{CC} = \delta(\Delta A_c/\Delta T_s)G_o$ with ΔT_s taken as 2°C based on Table 13 and $G_o = 0.3°C/(Wm^{-2})$.

:over increases below about
lecreases between these
:h signs are generally
ı for the solar constant
ə of the contribution of
f_{CC}. For this purpose we
layers of constant τ
e results of Manabe and
ues of ΔA_c are estimated
yers. Table 14 shows that
eased low cloud cover give
cover feedback of the CO_2
cloud being about twice
from the middle cloud. On
cloud cover in the increas-
ributions to the cloud cover
ution from the increased

.ges in the low, middle and
.. (1981)

τ	δ[a] (Wm^{-2})	ΔA_c[b]	f_{CC}[c]
2	6	0.01	0.0090
6	-50	0	0
l6	-100	-0.0015	0.0225
			0.0315
2	6	0.005	0.0045
6	-50	0.002	-0.0150
16	-100	0.0007	-0.0105
			-0.0210

rald (1967) shown in

.°C based on Table 13 and

These results from the study performed by Wang et al. (1981) clearly show that it is the vertical integral throughout the atmosphere of $\delta\Delta A_c$ which determines the sign and magnitude of the cloud cover feedback. Because this integral includes the changes in the vertical location of clouds through the vertical distribution of ΔA_c, it is seen that cloud altitude feedback is subsumed in cloud cover feedback.

Cloud optical depth feedback. We now consider the third and final feedback mechanism of clouds, namely, that due to the change in cloud optical depth, τ_c. As in the preceding section it is useful to consider this feedback from the viewpoint of the planetary radiative energy budget. Doing so we can obtain

$$(\Delta T_s)_{\Delta C} = \frac{G_o}{1 - \sum_j f_j - f_{OD}} \frac{\partial N_o}{\partial C} \Delta C \quad , \tag{120}$$

where the cloud optical depth feedback f_{OD} is given by

$$f_{OD} = \phi \frac{d\tau_c}{dT_s} G_o \quad , \tag{121}$$

and

$$\phi = \frac{\partial N_o}{\partial \tau_c} = - \frac{S_o}{4} \frac{\partial \alpha_p}{\partial \tau_c} - \frac{\partial R_o}{\partial \tau_c} \quad . \tag{122}$$

These three equations are analogous to Eqs. (101b)-(103) from which they may be obtained by replacing f_{CC} by f_{OD} and A_c by τ_c. Equation (121) shows the f_{OD}, like f_{CC}, depends on three quantities: ϕ, $d\tau_c/dT_s$ and G_o. As in the preceding section we assume that

$$\alpha_p = (1 - A_c)\alpha_s + A_c\alpha_c \quad ,$$

and we also assume that R_o can be approximated as

$$R_o \doteq (1 - A_c)R_{o,s} + A_c[R_{o,s}(1 - \varepsilon_c) + \varepsilon_c\sigma T_c^4] \quad , \tag{123}$$

where $R_{o,s}$ is the clear-sky value of R_o, ε_c is the upward effective cloud emissivity (Stephens, 1978), and T_c is the cloud top temperature. Substituting Eqs. (104) and (123) into Eq. (122) then gives

$$\phi = - A_c\left[\frac{S_o}{4} \frac{\partial \alpha_c}{\partial \tau_c} + (\sigma T_c^4 - R_{o,s}) \frac{\partial \varepsilon_c}{\partial \tau_c}\right] \quad . \tag{124}$$

This shows that ϕ, like δ, has both an albedo effect and a longwave radiation effect, and depends on the cloud cover A_c. Since $\partial\varepsilon_c/\partial\tau_c = 0$ for black clouds, while $\partial\alpha_c/\partial\tau_c > 0$, $\phi < 0$ for most low and middle clouds. On the other hand, because $\partial\varepsilon_c/\partial\tau_c > 0$ for nonblack clouds and σT_c^4 can be smaller than $R_{o,s}$, ϕ may be either negative or positive for cirrus clouds. Thus, if $d\tau_c/dT_s > 0$ for the reasons described below, the cloud optical depth feedback f_{OD} is negative for low and middle clouds, and may be either negative or positive for cirrus clouds.

Because τ_c depends on the LWP and IWP for water and ice (cirrus) clouds, respectively (e.g. Stephens, 1978; Stephens et al., 1984), we also can write Eqs. (121) and (124) as

$$f_{OD} = \tilde{\phi}\,\frac{dWP}{dT_s}\,G_o \quad , \tag{125}$$

$$\tilde{\phi} = -\,A_c\left[\frac{S_o}{4}\,\frac{\partial\alpha_c}{\partial WP} + (\sigma T_c^4 - R_{o,s})\,\frac{\partial\varepsilon_c}{\partial WP}\right] \quad , \tag{126}$$

where WP represents LWP or IWP. Following the development of the preceding section leading to Eq. (108), we can then write that

$$\tilde{\phi} = \frac{(\Delta T_s)_{\Delta WP}}{G_f\,\Delta WP} \quad . \tag{127}$$

Estimates of $\tilde{\phi}$ for low and high clouds can be obtained from the results by Charlock (1982) using a RCM (Fig. 12) and $G_f \sim 0.5°C/(Wm^{-2})$ based on the 2.253°C warming obtained by Charlock (1981) for a CO_2 doubling with an assumed $\Delta N_o = 4$ Wm^{-2}. For low cloud with $A_c = 0.2$, Fig. 12 and Eq. (127) show that $\tilde{\phi}$ varies from about -0.1 Wm^{-2}/gm^{-2} for WP between 50 and 100 gm^{-2} to about -0.003 Wm^{-2}/gm^{-2} for WP between 400 and 800 gm^{-2}. For high cloud with $A_c = 0.2$, $\tilde{\phi}$ varies from about $+0.8$ Wm^{-2}/gm^{-2} for WP between 10 and 20 gm^{-2} to about -0.05 Wm^{-2}/gm^{-2} for WP between 50 and 100 gm^{-2}. This transition from positive to negative values of $\tilde{\phi}$ with increasing WP represents the dominance of the longwave effect in Eq. (126) for thin cirrus clouds and the dominance of the albedo effect in thick cirrus clouds, the latter because $\partial\varepsilon_c/\partial WP$ becomes zero once ε_c becomes unity.

Three RCM studies of the effect of variable cloud optical depth or cloud water path on CO_2-induced temperature change have been performed by Wang et al. (1981), Charlock (1982) and Somerville and Remer (1984). The results of these studies are shown in Table 15 along with the characteristics of the RCMs used therein. The optical depth feedback defined as $\tilde{f}_{OD} = 1 - (\Delta T_s)_{FOD}/(\Delta T_s)_{VOD}$ ranges from essentially zero to about -1.3. These values depend not only on ϕ, as previously discussed, but also on $d\tau_c/dT_s$ or dWP/dT_s as shown by Eqs. (121) and (127). Each of the three studies parameterized these latter quantities differently as described below.

Wang et al. (1981) used the model described in the preceding subsection with cloud cover A_c prescribed instead of computed by

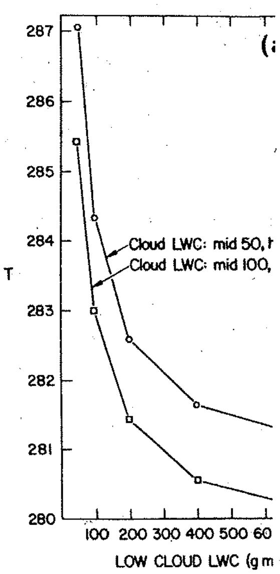

Figure 12. Surface tempe
liquid water content LWC
two different altitudes.
Source: Charlock (1982).

Eq. (117), and τ_c given b

$$\tau_c = f_3\ell \quad ,$$

with $f_3 = 3.09\times10^4$ (z < 3
(z ≥ 8 km). Substituting

$$\tau_c = \frac{f_3 H_c}{f_1(1+B)L}$$

from which we can obtain

$$\frac{d\tau_c}{dT_s} = \frac{f_3}{f_1 L(1+B)}$$

This has the same form as
like dA_c/dT_s, can be eit
of the change in τ_c for
constant is shown in Fig.
prescribed cloud cover.

A_c. Since $\partial\varepsilon_c/\partial\tau_c = 0$
ost low and middle
for nonblack clouds and
gative or positive for
sons described below,
for low and middle
or cirrus clouds.
ater and ice (cirrus)
ens et al., 1984), we

(125)

(126)

,

development of the pre-
n write that

(127)

btained from the results
$\sim 0.5°C/(Wm^{-2})$ based on
for a CO_2 doubling with
$= 0.2$, Fig. 12 and
$^{-2}/gm^{-2}$ for WP between 50
between 400 and 800 gm^{-2}.
out $+0.8\ Wm^{-2}/gm^{-2}$ for WP
for WP between 50 and
gative values of $\tilde{\jmath}$ with
longwave effect in
ance of the albedo effect
$/\partial WP$ becomes zero once ε_c

le cloud optical depth or
ange have been performed
erville and Remer (1984).
e 15 along with the char-
ical depth feedback de-
om essentially zero to
, as previously discussed,
. (121) and (127). Each
r quantities differently

ed in the preceding
ead of computed by

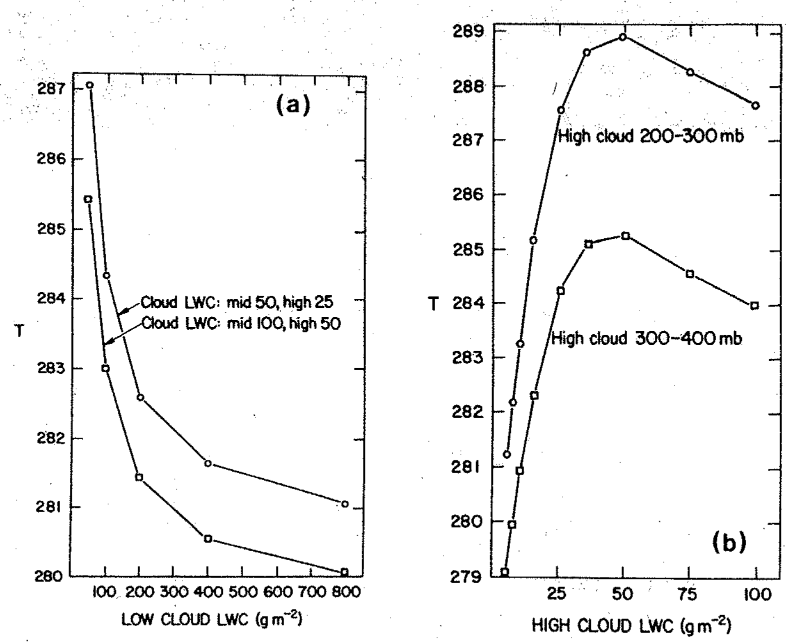

Figure 12. Surface temperature T(K) as a function of (A) low cloud liquid water content LWC and (B) high cloud LWC with the high cloud at two different altitudes. Fractional area of each cloud type is 0.20. Source: Charlock (1982).

Eq. (117), and τ_c given by

$$\tau_c = f_3 \ell \quad , \tag{128}$$

with $f_3 = 3.09\times10^4$ ($z < 3$ km), 1.15×10^4 ($3 \le z < 8$ km) and 2.75×10^3 ($z \ge 8$ km). Substituting Eq. (115) into Eq. (128) then gives

$$\tau_c = \frac{f_3 H_c}{f_1(1+B)L} \quad , \tag{129}$$

from which we can obtain

$$\frac{d\tau_c}{dT_s} = \frac{f_3}{f_1 L(1+B)} \left(\frac{dH_c}{dT_s} - \frac{H_c}{1+B}\frac{dB}{dT_s}\right) \quad . \tag{130}$$

This has the same form as dA_c/dT_s given by Eq. (119), hence $d\tau_c/dT_s$, like dA_c/dT_s, can be either positive or negative. The vertical profile of the change in τ_c for both a CO_2 doubling and a 2% increase in solar constant is shown in Fig. 13, together with the vertical profile of the prescribed cloud cover. This figure shows that τ_c increased at both low

Table 15. Cloud optical depth feedback f_{OD} determined from selected radiative convective models

Study	Model Attributes[a]	Cloud Optical Depth Treatment	ΔT_s $2xCO_2-1xCO_2$ (°C)	Estimated Feedback $\tilde{f}_{OD}$ [b]
Wang et al. (1981)	BAE;FRH;FLR(6.5); FCC,FCA(17);FAL	FOD VOD	2.06 2.08	0.0096
	BAE;FRH;FLR(MA)[c] FCC;FCA(17);FAL	FOD VOD	2.26 2.09	-0.08
Charlock (1981)	ERE;VRH[d];FLR(6.5); FCC;FCA(3);FAL	FOD VOD	2.253 1.579	-0.427
Somerville and Remer (1984)	BAE;FRH,MALR; FCC;FCA(1);FAL	FOD VOD	1.74 0.85 to 0.75	-1.05 to -1.32 [e]

a Surface energy flux; water vapor; lapse rate; cloud cover, altitude (number of cloud layers); surface albedo. See Table 3 for definition of abbreviations.

b $\tilde{f}_{OD} = 1 - \frac{(\Delta T_s)_{FOD}}{(\Delta T_s)_{VOD}}$.

c Lapse rate fixed equal to the moist adiabatic value for the initial conditions.

d From Charlock (1982), $RH(p) = RH(p_s)[(p/p_s - 0.02)/(1 - 0.02)]^{\Omega}$ with $RH(p_s) = 0.77$ and $\Omega = 1 - 0.03\ (T_s - 288)$.

e See Fig. 14.

and high altitudes, and decreased at middle altitudes, for both the CO_2 and solar constant increases. If we assume that $\phi < 0$ for the low, middle and high clouds, then $\phi d\tau_c/dT_s$ is negative at low and high altitudes, and positive at middle altitudes. It is not possible to evaluate the vertical integral of $\phi d\tau_c/dT_s$ quantitatively, but the zero value of f_{OD} in Table 15 does not appear to be inconsistent with the profile shown in Fig. 13 for the CO_2 doubling. Furthermore, the larger increase of τ_c at low altitudes in the 2% solar constant increase experiment indicates that f_{OD} for this experiment should be smaller than that for the CO_2 doubling experiment, that is, that it should be negative. Indeed, such a negative value was obtained by Wang et al. (1981) because ΔT_s for the 2% solar constant increase experiment decreased from 2.26°C to 1.95°C when τ_c was changed from a prescribed to a predicted quantity. These results from Wang et al. (1981) show that, as for the cloud cover etermined from selected

l	ΔT_s $2xCO_2$-$1xCO_2$ (°C)	Estimated Feedback f_{OD} b
	2.06	
	2.08	0.0096
	2.26	
	2.09	-0.08
	2.253	
	1.579	-0.427
	1.74	
	0.85 to	-1.05 to
	0.75	-1.32 e

te; cloud cover, altitude
See Table 3 for definition

tic value for the initial

$- 0.02)/(1 - 0.02)]^{\Omega}$ with

ltitudes, for both the CO_2
hat $\phi < 0$ for the low, mid-
e at low and high
It is not possible to
antitatively, but the zero
e inconsistent with the
. Furthermore, the larger
ar constant increase exper-
should be smaller than that
t it should be negative.
Wang et al. (1981) because
ment decreased from 2.26°C
ed to a predicted quantity.
at, as for the cloud cover

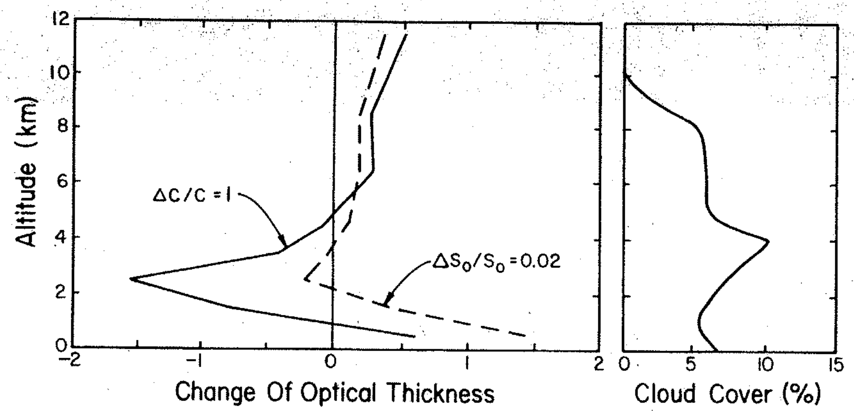

Figure 13. Change in the optical thickness (left) for prescribed cloud cover (right) as a function of altitude for a 2% increase in the solar constant ($\Delta S_o/S_o = 0.02$) and a doubling of the CO_2 concentration ($\Delta C/C = 1$). Adapted from Wang et al. (1981).

feedback, the cloud optical depth feedback depends on the vertical integral of $\phi d\tau_c/dT_s$ throughout the atmosphere.

Charlock (1981) used a simpler model than Wang et al. (1981) to compute the change in the cloud water path WP induced by doubling CO_2,

$$\frac{\Delta WP}{WP} = \frac{\Delta q}{q} \quad , \tag{131}$$

where q is the water vapor mixing ratio. Charlock prescribed the relative humidity profile as

$$RH(p) = RH(p_s)\left(\frac{p/p_s - 0.02}{1 - 0.02}\right)^{\Omega} \tag{132}$$

with

$$\Omega = 1 - 0.03(T_s - 288) \quad . \tag{133}$$

Thus, RH(p) increases slightly with T_s, q and WP increase rapidly with increasing T_s, and $dWP/dT_s > 0$ everywhere. Furthermore, since Charlock assumed $\partial\epsilon_c/\partial WP = 0$, $\tilde{\phi} < 0$ (see Eq. (126)). Consequently, $\tilde{\phi} dWP/dT_s < 0$ for each of the three cloud layers in Charlock's study, with the result that $\tilde{f}_{OD} < 0$ as shown in Table 15.

Somerville and Remer (1984) also used a simple model for the change in the cloud optical thickness,

$$\Delta\tau_c = \mu\Delta T \quad , \tag{134}$$

where

$$\mu = \frac{1}{\rho_c}\frac{\partial\rho_c}{\partial T} \quad , \tag{135}$$

and ρ_c is the cloud water density. Somerville and Remer assumed μ to be a positive constant, hence $\partial\tau_c/\partial T > 0$. Furthermore, they assumed their single cloud to be black, $\varepsilon_c = 1$, hence $\partial\varepsilon_c/\partial\tau_c = 0$ and $\phi < 0$ by Eq. (122). Consequently, $f_{OD} = \phi(d\tau_c/dT)G_o = \phi\mu G_o$ is negative as shown in Fig. 14. From this figure it appears that $\phi = -87.7\ Wm^{-2}$. If μ is as large as 0.1, then $\Delta T_s = 0.48°C$. This is the minimum surface air temperature warming shown in Table 4 for all the radiative-convective models. This minimum warming is the result of both the large negative cloud optical depth feedback and the negative lapse rate feedback which results from the MALR used in this model (see Table 15). However, based on Soviet observations of $\rho_c(T)$ as summarized by Feigelson (1978), Somerville and Remer conclude that $\mu \approx 0.04$ to 0.05. Thus, as shown in Fig. 14 and Table 15, this range (labelled OBS) gives $\Delta T_s = 0.75$ to 0.85°C.

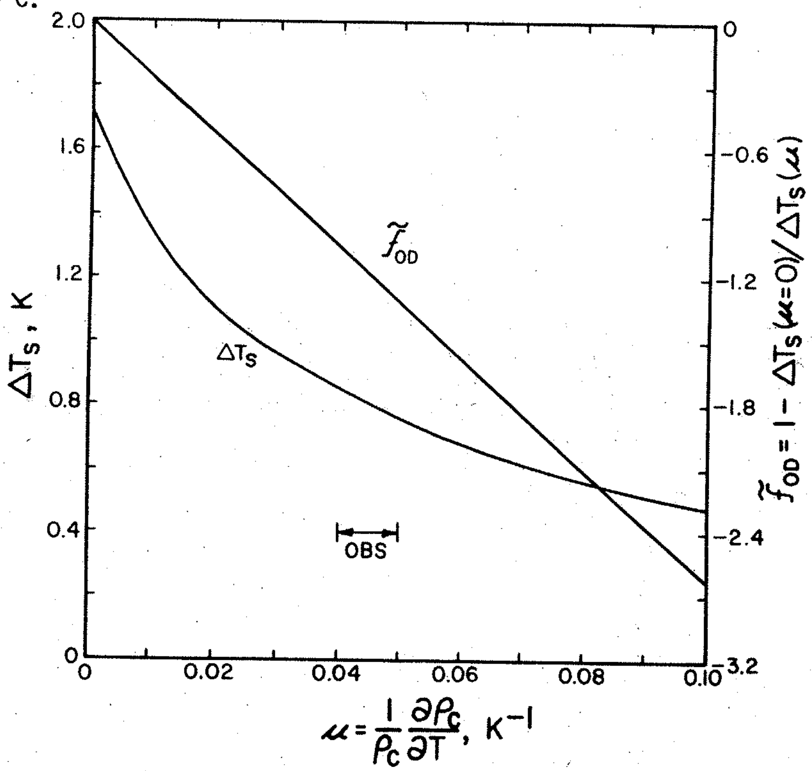

Figure 14. Surface temperature change and cloud optical depth feedback for CO_2 doubling versus the prescribed cloud parameter μ based on the study by Somerville and Remer (1984).

Surface albedo feedback. CO_2-induced climate chan sea ice, land ice and sn in the preceding two sub feedback from the viewpo

$(\Delta T_s)_{\Delta C} = \frac{}{1 -}$

where the surface albedo

$f_{SA} = \psi \frac{d\alpha_s}{dT_s} G_o$

and

$\psi = \frac{\partial N_o}{\partial \alpha_s} = -\frac{S_o}{4}$

or

$\psi = -\frac{S_o}{4}\frac{\partial\alpha_p}{\partial\alpha_s}$

the latter because $\partial R_o/\partial$ Wang and Stone (198 feedback on CO_2-induced assumed that the annual represented by

$T_s(x) - \overline{T}_s + 1$

where x is the sine of temperature, P_2 is the -32.1. The latter is cl edge is $x_s = 0.95$ at T_s $\overline{T}_s = 14.2°C$. Assuming change, Eq. (139) can b

$x_s = (d + e\overline{T}_s$

where d = 0.6035 and e

(135)

le and Remer assumed μ to be
hermore, they assumed their
$\partial\tau_c = 0$ and $\phi < 0$ by
$= \phi\mu G_o$ is negative as shown
$\phi = -87.7$ Wm^{-2}. If μ is
the minimum surface air
the radiative-convective
of both the large negative
lapse rate feedback which
Table 15). However, based
by Feigelson (1978),
to 0.05. Thus, as shown in
S) gives $\Delta T_s = 0.75$ to

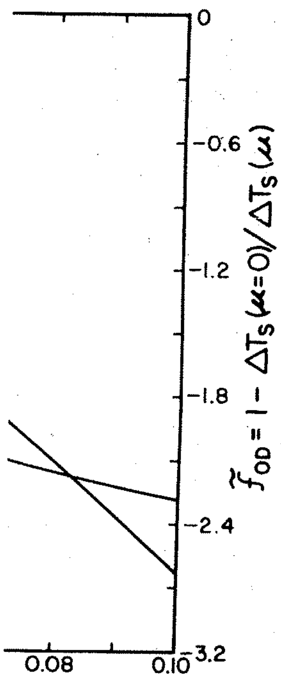

oud optical depth feedback
parameter μ based on the

Surface albedo feedback. Surface albedo feedback can occur during a CO_2-induced climate change as a result of alterations in the amount of sea ice, land ice and snow, or in the amount and type of vegetation. As in the preceding two subsections, we can analyze this surface albedo feedback from the viewpoint of the planetary energy budget and obtain

$$(\Delta T_s)_{\Delta C} = \frac{G_o}{1 - \sum_j f_j - f_{SA}} \frac{\partial N_o}{\partial C} \Delta C \quad , \tag{136}$$

where the surface albedo feedback f_{SA} is given by

$$f_{SA} = \psi \frac{d\alpha_s}{dT_s} G_o \quad , \tag{137}$$

and

$$\psi = \frac{\partial N_o}{\partial \alpha_s} = -\frac{S_o}{4}\frac{\partial \alpha_p}{\partial \alpha_s} - \frac{\partial R_o}{\partial \alpha_s}$$

or

$$\psi = -\frac{S_o}{4}\frac{\partial \alpha_p}{\partial \alpha_s} \quad , \tag{138}$$

the latter because $\partial R_o/\partial \alpha_s = 0$.

Wang and Stone (1980) investigated the effect of ice albedo feedback on CO_2-induced warming. Following North (1975), Wang and Stone assumed that the annual mean, zonal mean surface air temperature can be represented by

$$T_s(x) - \overline{T}_s + T_2 P_2(x) = \overline{T}_s + \frac{T_2}{2}(3x^2 - 1) \quad , \tag{139}$$

where x is the sine of the latitude, $\overline{T}_s$ is the global mean surface air temperature, P_2 is the Legendre polynomial of degree two, and $T_2 = -32.1$. The latter is chosen so that the sine of the latitude of the ice edge is $x_s = 0.95$ at $T_s(x_s) = -13°C$ for the current climate for which $\overline{T}_s = 14.2°C$. Assuming that $T_s(x_s) = -13°C$ is invariant under a climatic change, Eq. (139) can be solved for x_s to obtain

$$x_s = (d + e\overline{T}_s)^{1/2} \quad , \tag{140}$$

where d = 0.6035 and e = 0.02078. Then assuming that

$$\alpha_s = \begin{cases} a, & 0 \leq x < x_s \\ b, & x_s \leq x \leq 1 \end{cases} , \tag{141}$$

where a = 0.087 is the ice-free zonal mean surface albedo and b = 0.55 is the ice-covered zonal mean surface albedo, and that the surface insolation has the same latitudinal distribution as the insolation at the top of the atmosphere given by

$$S(x) = \left[1 + \frac{S_2}{2}(3x^2 - 1)\right]\overline{S} , \tag{142}$$

where $\overline{S}$ is the global mean, $S_2 = -0.482$ and the global mean albedo is given by

$$\overline{\alpha}_s = b(1 - x_s) + ax_s + \frac{S_2}{2}(b - a)(x_s - x_s^3) . \tag{143}$$

From Eqs. (140) and (143) it can be shown that

$$\frac{d\overline{\alpha}_s}{d\overline{T}_s} = -\frac{(b - a)e}{2} \; \frac{1 + \frac{S_2}{2}[1 - 3(d + e\overline{T}_s)]}{(d + e\overline{T}_s)^{1/2}} . \tag{144}$$

Combining this with Eq. (137) gives

$$\frac{f_{SA}}{\partial\alpha_p/\partial\alpha_s} = \left[\frac{S_o}{4}\,\frac{(b - a)e}{2}\;\frac{1 + \frac{S_2}{2}[1 - 3(d + e\overline{T}_s)]}{(d + e\overline{T}_s)^{1/2}}\right]G_o . \tag{145}$$

This is shown plotted in Fig. 15 versus $\overline{T}_s$ and the ice edge latitude x_s for an assumed value of $G_o = 0.3°C/(Wm^{-2})$. Because $\partial\alpha_p/\partial\alpha_s > 0$, $f_{SA} > 0$. If $\partial\alpha_p/\partial\alpha_s$ is independent of $\overline{T}_s$, then f_{SA} decreases with increasing temperature as the ice edge of the control climate retreats toward the pole. This effect has been demonstrated in the GCM study of Spelman and Manabe (1984). However, in the formulation of Wang and Stone, f_{SA} does not approach zero as the ice edge retreats to the pole and the ice disappears.

The results of Wang and Stone (1980) are summarized in Table 16. Although we cannot estimate f_{SA} for this study because $(\Delta T_s)_o$ is not known, the feedback $f_{SA} = 1 - (\Delta T_s)_{FAL}/(\Delta T_s)_{VAL}$ is positive. In fact, the case with fixed cloud top temperature (FCT), along with fixed relative humidity (FRH), produces the maximum warming of all the RCMs shown in Table 4. Because this 4.2°C warming is also the maximum global mean surface air temperature increase simulated by GCMs for a CO_2 doubling

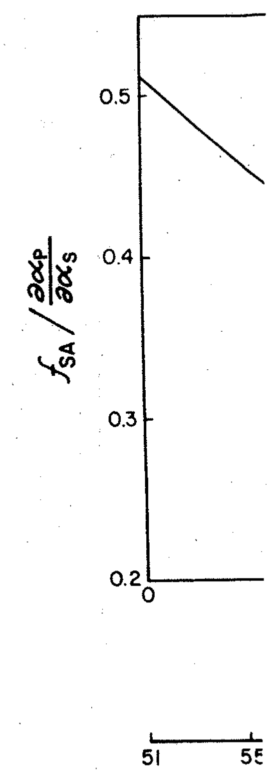

Figure 15. Surface albed
versus the surface air te
based on the study by War

(Schlesinger and Mitchell
feedback is important in
Finally, Hansen et a
apparently with the ice-a
(1980). Because we have
Hansen et al. (see Table
shown in Table 16, f_{SA} ~
$f_{SA} = 0.135$ that one obt
0.45 obtained from the O
of $f_{SA} = 0.181$ obtained
result of Hansen et al.

(141)

:ace albedo and b = 0.55
ınd that the surface inso-
; the insolation at the

(142)

e global mean albedo is

$- x_s^3)$. (143)

that

$\overline{T}_s)]$. (144)

$3(d + e\overline{T}_s)]$ $]G_o$. (145)
$_s)^{1/2}$

ı the ice edge latitude x_s
ecause $\partial\alpha_p/\partial\alpha_s > 0$,
en f_{SA} decreases with in-
ontrol climate retreats
trated in the GCM study of
ormulation of Wang and
edge retreats to the pole

summarized in Table 16.
y because $(\Delta T_s)_o$ is not
AL is positive. In fact,
T), along with fixed rela-
ming of all the RCMs shown
so the maximum global mean
GCMs for a CO_2 doubling

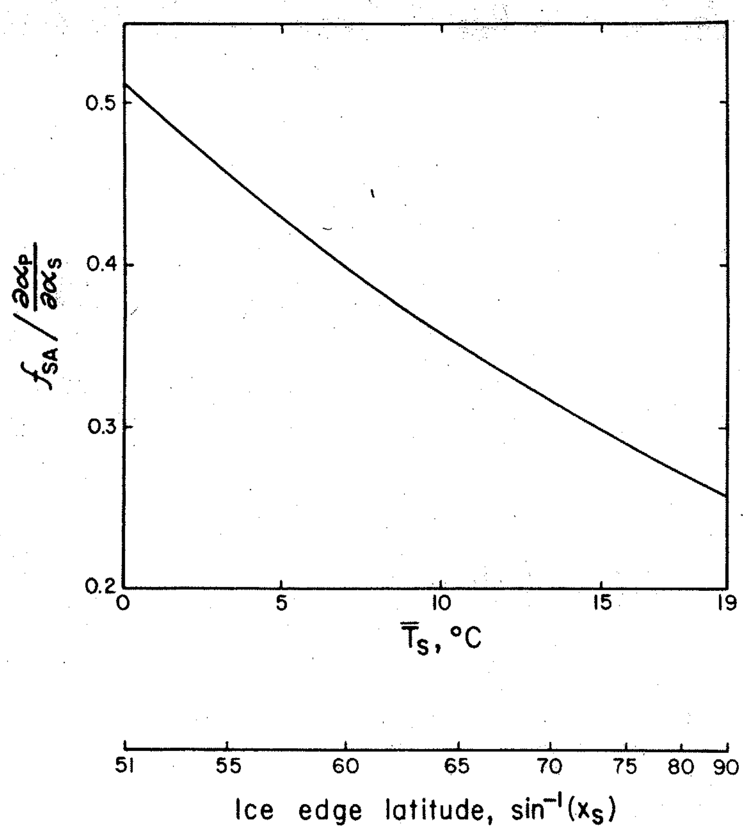

Figure 15. Surface albedo feedback divided by $\partial\alpha_p/\partial\alpha_s$ for CO_2 doubling versus the surface air temperature and ice edge latitude of the control based on the study by Wang and Stone (1980).

(Schlesinger and Mitchell, 1985, 1987), it appears that ice albedo-feedback is important in GCM simulations of CO_2-induced climatic change.

Finally, Hansen et al. (1981) also studied the ice-albedo effect, apparently with the ice-albedo parameterization of Wang and Stone (1980). Because we have an estimate of $(\Delta T_s)_o$ and f_W for the RCM of Hansen et al. (see Table 6), we can estimate f_{SA} for this model. As shown in Table 16, $f_{SA} \sim 0.141$ to 0.193. This is close to the value of $f_{SA} = 0.135$ that one obtains from Fig. 15 at $\overline{T}_s = 15°C$ using $\partial\alpha_p/\partial\alpha_s = 0.45$ obtained from the Oregon State University two-layer RCM. The value of $f_{SA} = 0.181$ obtained from that model (Table 5) also agrees with the result of Hansen et al. (1981).

Table 16. Surface albedo feedback f_{SA} from selected radiative-convective models

Study	Model Attributes [a]	Surface Albedo Treatment	ΔT_s $2xCO_2$-$1xCO_2$ (°C)	Estimated Feedback $\tilde{f}_{SA}$ [b]	Estimated Feedback f_{SA}
Wang and Stone (1980)	BAE;FRH;FLR(6.5); FCC,FCA(3),FOD	FAL	2.00		
		VAL	2.51	0.203	
	BAE;FRH;FLR(6.5); FCC,FCT(3),FOD	FAL	3.00		
		VAL	4.20	0.286	
Hansen et al. (1981)	BAE;FRH;FLR(6.5); FCC,FCA(3),FOD	FAL	1.94		
		VAL	2.5-2.8	0.224-0.307	0.141-0.193 [c]

a Surface energy flux; water vapor; lapse rate; cloud cover, cloud layer, altitude (number of cloud layers), optical depth. See Table 3 for definition of abbreviations.

b $\tilde{f}_{SA} = 1 - \dfrac{(\Delta T_s)_{FAL}}{(\Delta T_s)_{VAL}}$.

c $f_{SA} = 1 - \dfrac{(\Delta T_s)_o}{(\Delta T_s)_{VAL}} - f_W$ with $(\Delta T_s)_o = 1.22$°C and $f_W = 0.371$ from Table 6.

3.4. Summary

The pioneering RCM study of Manabe and Wetherald (1967) showed that doubling the CO_2 concentration results in a warming of the surface and the troposphere, and a cooling of the stratosphere above 20 km. This and other RCM studies give a surface temperature warming induced by doubled CO_2 which ranges from 0.48 to 4.2°C. These CO_2-induced surface temperature changes can be understood in terms of the direct radiative forcing, the response to this forcing in the absence of feedbacks, and the amplification and damping of the response that results from positive and negative feedbacks, respectively.

The direct radiative forcing occurs predominantly in the longwave radiation and is characterized by a decrease in the net upward flux at the surface and throughout the atmosphere. The decrease at the surface acts to warm the surface. In the troposphere the magnitude of the decrease in the net upward longwave flux increases with altitude which acts to warm the troposphere. In the stratosphere the magnitude of the decrease in the net upward longwave flux decreases with altitude which acts to cool the stratosphere. This cooling tendency occurs primarily because of the greater upward and downward emission from the strato-

sphere itself. The warmi
to the increased downward
tendency of the surface o
emission from the troposp
The surface temperat
feedbacks to the radiativ
characterized by a zero-f
$G_o \Delta R_T$, where G_o is the cl
estimated from a planetar
$(\Delta T_s)_o = 1.2$°C for the no
$(\Delta T_s)_o$ is in good agreeme
without feedbacks.
The surface temperat
feedback can be character

$$\Delta T_s = \frac{G_o}{1 - f} \Delta R_T$$

where f is the feedback w
of CO_2-induced climate ch
to this range include, as
water vapor in the atmosp
the relative humidity; th
cloud altitude, cloud cov
surface albedo.
A study with the Ore
performed to determine th
study shows that the indi
and surface albedo are po
optical depth feedbacks a
adiabatic lapse rate feed
the feedbacks of water va
surface albedo are addit
This is not the case for
cover or cloud optical de
variable optical depth ac
in conjunction with the
A positive water va
is held fixed because th
with increasing temperatu
the increased water vapo
enhances the CO_2 greenho
was obtained by the Oreg
to 0.533 were obtained b
depending upon the tempe
sphere was clear or clou
dependencies is $f_W \approx 0.3$
(smaller) than this if t
stead increased (decreas
Radiative-convectiv

lected radiative-

CO_2	Estimated Feedback f_{SA} [b]	Estimated Feedback f_{SA}
	0.203	
	0.286	
8	0.224-0.307	0.141-0.193 [c]

ate; cloud cover, cloud
optical depth. See

2°C and f_W = 0.371 from

ıld (1967) showed that
ırming of the surface and
ıhere above 20 km. This
ıre warming induced by
These CO_2-induced surface
of the direct radiative
ıbsence of feedbacks, and
that results from positive

ıminantly in the longwave
n the net upward flux at
ıe decrease at the surface
the magnitude of the de-
ses with altitude which
here the magnitude of the
ases with altitude which
endency occurs primarily
ssion from the strato-

sphere itself. The warming tendency of the troposphere is primarily due to the increased downward flux from the stratosphere, and the warming tendency of the surface occurs primarily because of the greater downward emission from the troposphere.

The surface temperature response of the climate system without feedbacks to the radiative forcing due to increased CO_2, ΔR_T, can be characterized by a zero-feedback surface temperature change $(\Delta T_s)_o = G_o \Delta R_T$, where G_o is the climate system gain without feedbacks. G_o can be estimated from a planetary energy balance model as $0.3°C/(Wm^{-2})$. Thus, $(\Delta T_s)_o = 1.2°C$ for the nominal value of $\Delta R_T = 4\ Wm^{-2}$. This estimate of $(\Delta T_s)_o$ is in good agreement with several RCM studies that were made without feedbacks.

The surface temperature response of the climate system with feedback can be characterized by

$$\Delta T_s = \frac{G_o}{1 - f} \Delta R_T \quad ,$$

where f is the feedback which varies from -1.5 to 0.7 in the RCM studies of CO_2-induced climate change. The physical mechanisms that contribute to this range include, as T_s increases: the increase in the amount of water vapor in the atmosphere as a consequence of the quasi-constancy of the relative humidity; the decrease in the lapse rate; the changes in cloud altitude, cloud cover and cloud optical depth; and the decrease in surface albedo.

A study with the Oregon State University two-layer RCM was performed to determine the independence of the above feedbacks. This study shows that the individual feedbacks of water vapor, cloud altitude and surface albedo are positive, the individual cloud cover and cloud optical depth feedbacks are essentially zero, and the individual moist adiabatic lapse rate feedback is negative. This study also shows that the feedbacks of water vapor and either lapse rate, cloud altitude or surface albedo are additive, hence these feedbacks are independent. This is not the case for the water vapor feedback with either the cloud cover or cloud optical depth feedbacks. Both variable cloud cover and variable optical depth act as negative feedback mechanisms when they act in conjunction with the positive water vapor feedback.

A positive water vapor feedback occurs when the relative humidity is held fixed because then the absolute humidity increases nonlinearly with increasing temperature due to the Clausius-Clapeyron relation, and the increased water vapor reduces the atmospheric transmissivity which enhances the CO_2 greenhouse effect. A positive feedback of $f_W = 0.340$ was obtained by the Oregon State University RCM, and values from 0.371 to 0.533 were obtained by the other RCMs, with their actual values depending upon the temperatures of the control and whether the atmosphere was clear or cloudy. A reasonable estimate allowing for these dependencies is $f_W \simeq 0.3$ to 0.4. The value of f_W would be larger (smaller) than this if the relative humidity were not constant and instead increased (decreased) with increasing temperature.

Radiative-convective model studies have shown that the CO_2-induced warming decreases by 12% as the prescribed temperature lapse rate is decreased from 6.5 to 5.0 K/km. When the lapse rate is allowed to vary, a lapse rate feedback is obtained. A positive feedback is found for the baroclinic adjustment lapse rate which should be applicable in middle and high latitudes were baroclinic adjustment is prevalent. From Table 7 we can estimate $f_{BADJ} = 1 - 1/1.84 - f_W \sim 0.15$ if $f_W = 0.3$. A negative feedback is found for the moist adiabatic lapse rate with values of -0.409 and -0.262 from the Oregon State University and other RCMs, respectively. Since the former value is probably an overestimate by the two-layer RCM, a reasonable estimate of this feedback is $f_{MALR} \sim -0.25$ to -0.4. A negative feedback is also found when the lapse rate is determined by penetrative convection with a value of $f_{PC} = -0.654$ given by one RCM. One or both of these negative feedbacks is likely to be found in the tropics where cumulus convection is prevalent.

Cloud feedback can occur from changes in cloud altitude, cloud cover and cloud optical depth. Three treatments of cloud altitude have been used in RCMs, namely, fixed cloud altitude (FCA), fixed cloud pressure (FCP) and fixed cloud temperature (FCT). Fixed cloud altitude and fixed cloud pressure have frequently been taken to be synonymous even though this is strictly not the case. For FCA the cloud temperature increases by the same amount as the surface temperature and there is no feedback. For FCP the cloud temperature increases less than the surface temperature, hence to achieve equilibrium the CO_2-induced surface temperature warming must be greater with FCP than with FCA. Therefore, FCP is a positive feedback process; however, there is insufficient information to evaluate it quantitatively. For FCT the cloud temperature does not change with a change in the surface temperature, hence its CO_2-induced surface temperature warming must be even larger than that for FCP to achieve equilibrium. The FCT feedback f_{CA} is 0.261 from the Oregon State University RCM and 0.168 to 0.203 from another RCM, the latter in comparison with the FCP case. Thus, a reasonable range of f_{CA} is perhaps from 0.15 to 0.30.

The feedback due to changes in cloud cover A_c depends in part on the quantity $\delta = -\frac{S_o}{4}\frac{\partial \alpha_p}{\partial A_c} - \frac{\partial R_o}{\partial A_c}$, which itself depends on the competing effects of changes in the planetary albedo, α_p, and in the net upward longwave flux at the top of the atmosphere, R_o. An analysis of several RCM studies shows that $\delta \simeq -100$ Wm^{-2} for low clouds, $\delta \simeq -50$ Wm^{-2} for middle clouds, and $\delta \simeq 5$ to 80 Wm^{-2} for high clouds, the latter generally increasing with cloud emissivity. Thus, for the case $dA_c/dT_s > 0$, low and middle clouds make a positive contribution to the cloud cover feedback f_{CC}, and high clouds make a negative contribution, while the sign of these contributions reverses for $dA_c/dT_s < 0$. A single RCM study of cloud cover feedback gave a positive value of f_{CC} for the case of doubled CO_2, but a negative value for the case of a 2% solar constant increase. These seemingly contradictory findings can be understood on the basis of the changes in the vertical cloud cover profile which demonstrates that it is the vertical integral of $\delta \Delta A_c$ that determines the sign and magnitude of the cloud cover feedback. Because of this, cloud altitude feedback is subsumed in cloud cover feedback.

The feedback due to changes in cloud optical depth τ_c depends in

emperature lapse rate is de-
e rate is allowed to vary, a
feedback is found for the
d be applicable in middle
t is prevalent. From
$f_W \sim 0.15$ if $f_W = 0.3$. A
abatic lapse rate with val-
te University and other
is probably an overestimate
of this feedback is
is also found when the lapse
with a value of f_{PC} =
se negative feedbacks is
lus convection is prevalent.
n cloud altitude, cloud
ents of cloud altitude have
ude (FCA), fixed cloud pres-
. Fixed cloud altitude and
ken to be synonymous even
CA the cloud temperature
temperature and there is no
reases less than the surface
e CO_2-induced surface tem-
an with FCA. Therefore, FCP
re is insufficient informa-
the cloud temperature does
erature, hence its CO_2-
even larger than that for
k f_{CA} is 0.261 from the
03 from another RCM, the
s, a reasonable range of f_{CA}

ver A_c depends in part on
f depends on the competing

α_p, and in the net upward
R_o. An analysis of several
clouds, $\delta \simeq -50$ Wm^{-2} for
clouds, the latter gener-
, for the case $dA_c/dT_s > 0$,
bution to the cloud cover
e contribution, while the
$/dT_s < 0$. A single RCM
e value of f_{CC} for the case
case of a 2% solar constant
dings can be understood on
ud cover profile which
l of $\delta\Delta A_c$ that determines
edback. Because of this,
cover feedback.
tical depth τ_c depends in

part on the quantity $\phi = -\frac{S_o}{4}\frac{\partial\alpha_p}{\partial\tau_c} - \frac{\partial R_o}{\partial\tau_c}$, which also depends on the competing albedo and longwave effects. For black clouds, $\partial R_o/\partial\tau_c = 0$ and $\phi < 0$. For non-black clouds, $\partial R_o/\partial\tau_c < 0$ and ϕ may be positive or negative. Thus, for the case of $d\tau_c/dT_s > 0$, low and middle clouds make a negative contribution to the cloud optical depth feedback f_{OD}, and high clouds can make either a positive or negative contribution, while the sign of these contributions reverses for $d\tau_c/dT_s < 0$. Two RCM studies, each with a single cloud layer, found that f_{OD} was negative with values of -0.427 and -1.05 to -1.32. Another study found that f_{OD} was essentially zero for doubled CO_2, but was negative for the case of a 2% solar constant increase. This latter study, as that above for the cloud cover feedback, showed that the cloud optical depth feedback depends on the vertical integral of $\phi d\tau_c/dT_s$ throughout the atmosphere.

Finally, the feedback due to changes in the extent of ice depends in part on $-\frac{S_o}{4}\frac{\partial\alpha_p}{\partial\alpha_s}\frac{d\alpha_s}{dT_s}$. Since the amount of ice decreases as the surface temperature increases, $d\alpha_s/dT_s < 0$. Consequently, because $\partial\alpha_p/\partial\alpha_s > 0$, the ice-albedo feedback f_{SA} is positive. A single RCM study gives values of f_{SA} from 0.141 to 0.193.

Based on the RCM studies reviewed in this section we can summarize our knowledge about water vapor, lapse rate, cloud altitude, cloud cover, cloud optical depth, and surface albedo feedbacks as

$$
\begin{aligned}
f_W &\simeq 0.3 \text{ to } 0.4,\\
f_{BADJ} &\simeq 0.15,\\
f_{MALR} &= -0.25 \text{ to } -0.4,\\
f_{PC} &\simeq -0.65,\\
f_{CA} &\simeq 0.15 \text{ to } 0.30,\\
f_{CC} &= \text{unknown},\\
f_{OD} &\simeq 0 \text{ to } -1.32 \text{ and}\\
f_{SA} &= 0.14 \text{ to } 0.19.
\end{aligned}
$$

However, we cannot have a high degree of confidence in these quantitative results because RCMs are not models of the global climate system and, more importantly, because RCMs of necessity prescribe the behavior of much of that system. In particular, water vapor feedback is predicted on the basis of constant relative humidity, lapse rate feedback generally on the basis of baroclinic or moist adiabatic adjustment, cloud feedbacks on the basis of greatly simplified cloud models, and surface albedo on the basis of assumed constant temperature of the position of the equatorward position of the ice extent. However, the relative humidity may not be constant, the lapse rate may differ from those given by baroclinic and moist adiabatic adjustment, the altitude of clouds may not conform to FCA, FCP or FCT, the cloud cover and cloud optical depth may vary vertically in a complex manner, and the change in surface albedo depends on snow and ice, neither of whose extent may have a constant dependence on temperature. These changes can be predicted credibly only by a physically-based global model that includes the essential dynamical and thermodynamical processes in addition to radiative transfer. Nevertheless, RCMs are extremely valuable because their comparative simplicity permits a more complete understanding of their feedbacks than the more comprehensive, and therefore more complex, GCMs.

4. GENERAL CIRCULATION MODELS

Many aspects of climate such as the horizontal transport of heat and land/sea contrasts are omitted in radiative-convective models and are inadequately treated in one- and two-dimensional energy balance models. Consequently, considerable effort has been devoted to the development of atmospheric general circulation models (AGCMs) and a hierarchy of ocean models that range from the swamp ocean model with no heat capacity or heat transport to the oceanic general circulation model (Gates, 1988; Simmonds and Bengtsson, 1988; Han, 1988; and Schlesinger, 1984). In this section we present and analyze the studies of CO_2-induced equilibrium climate change that have been made with AGCMs coupled to models of the oceanic mixed layer in which the mixed layer depth and oceanic heat transport are prescribed.

4.1. Simulation of CO_2-induced Surface Temperature Change

The first simulation of the seasonal variation of CO_2-induced climate change with a model in which sea surface temperatures and sea ice were predicted was carried out by Manabe and Stouffer (1979, 1980). In their study the GFDL AGCM was coupled to a fixed depth mixed layer ocean model with no horizontal and vertical heat transports, whose 68 m depth was chosen to give the best fit to the observed annual cycle of sea surface temperatures. To increase the statistical significance of their results, Manabe and Stouffer investigated the climatic changes induced by a CO_2 quadrupling. More recently three simulations of the equilibrium climatic change for doubled CO_2 have been performed by Hansen et al. (1984), Washington and Meehl (1984), and Wetherald and Manabe (1986) with, respectively, the GISS (Goddard Institute for Space Studies), NCAR (National Center for Atmospheric Research) and GFDL (Geophysical Fluid Dynamics Laboratory) AGCMs coupled to mixed layer ocean models. These more recent studies are summarized in Table 17 in terms of the annual global mean surface air temperature. This table shows that these models simulate a warming of the surface air temperature of about 3.5 to 4.2°C for a CO_2 doubling.

It is of interest to contrast these results with those obtained from the earlier studies with AGCM/simplified ocean models (see Schlesinger and Mitchell, 1985, 1987). An earlier version of the GISS model with computed clouds and annual mean insolation (Hansen, 1979) obtained a 3.9°C warming, while the current GISS model with computed clouds and the annual insolation cycle obtained 4.2°C. The NCAR model with computed clouds and annual mean insolation (Washington and Meehl, 1983) obtained a 1.3°C warming, while the NCAR model with computed clouds and the annual insolation cycle obtained 3.5°C. From this it is seen that both the GISS and NCAR models with the annual insolation cycle produce a larger $2xCO_2$-induced warming than these models with annual mean insolation. These results are in contrast to what was found by Wetherald and Manabe (1981) from a model with idealized geography and

Table 17. CO_2-indu temperature, Δ with the annua

Study
Manabe and Stouff (1979, 1980) an Manabe et al. (
Hansen et al. (19
Washington and Meehl (1984) d,
Wetherald and Manabe (1986) b

a Annual mean val

b Slab ocean mode transport. Sea dynamic sea ice

c Slab ocean mode based on observ 63 m. Meridion simulation with ice thickness p model.

d As in footnote

e Fixed clouds.

f Computed clouds

g The 3.5°C globa NCAR model was years of the 1x Washington and had not reached ments because c the time. The and the $2xCO_2$ w $1xCO_2$ global me ing at about 0. (1984) results were extended l showed a smalle (e.g., 0.3°C pe $1xCO_2$ and $2xCO_2$

: understanding of their
:refore more complex, GCMs.

: transport of heat and
›nvective models and are
ıal energy balance models.
voted to the development of
› and a hierarchy of ocean
vith no heat capacity or
:ion model (Gates, 1988;
Schlesinger, 1984). In
:s of CO_2-induced
: with AGCMs coupled to
: mixed layer depth and

:ature Change

ı of CO_2-induced climate
:ratures and sea ice were
fer (1979, 1980). In their
›th mixed layer ocean model
:s, whose 68 m depth was
ınual cycle of sea surface
ynificance of their re-
limatic changes induced by
ıtions of the equilibrium
formed by Hansen et al.
:rald and Manabe (1986)
:e for Space Studies), NCAR
ı GFDL (Geophysical Fluid
ıyer ocean models. These
7 in terms of the annual
›le shows that these models
:ure of about 3.5 to 4.2°C

lts with those obtained
ocean models (see
:lier version of the GISS
solation (Hansen, 1979)
ISS model with computed
:d 4.2°C. The NCAR model
›n (Washington and Meehl,
R model with computed
:d 3.5°C. From this it is
:he annual insolation cycle
ıese models with annual
:t to what was found by
idealized geography and

Table 17. CO_2-induced changes in the global mean surface air temperature, ΔT_s, simulated by AGCM/mixed layer ocean models with the annual insolation cycle

Study	X CO_2	Clouds	ΔT_s [a] (°C)
Manabe and Stouffer (1979, 1980) and Manabe et al. (1981) [b,e]	4	Fixed	4.1
Hansen et al. (1984) [c,f]	2	Computed	4.2
Washington and Meehl (1984) [d,f,g]	2	Computed	3.5
Wetherald and Manabe (1986) [b,f]	2	Computed	4.0

[a] Annual mean values.

[b] Slab ocean model with depth of 68 m and no horizontal heat transport. Sea ice thickness predicted based on thermodynamic sea ice model.

[c] Slab ocean model with prescribed seasonally-varying depth based on observations but constrained to be less than 63 m. Meridional heat transport prescribed based on AGCM simulation with prescribed sea surface temperatures. Sea ice thickness predicted based on thermodynamic sea ice model.

[d] As in footnote b except with depth of 50 m.

[e] Fixed clouds.

[f] Computed clouds.

[g] The 3.5°C global mean surface air temperature warming of the NCAR model was determined by averaging over the last three years of the $1xCO_2$ and $2xCO_2$ simulations. However, as noted by Washington and Meehl (1984), the $2xCO_2$ and $1xCO_2$ simulations had not reached quasi-equilibrium by the end of these experiments because of the lack of computing resources available at the time. The $1xCO_2$ experiment was cooling at 0.4°C per year and the $2xCO_2$ was cooling at 0.21°C per year. Thus the $2xCO_2$-$1xCO_2$ global mean surface air temperature warming was increasing at about 0.19°C per year. After the Washington and Meehl (1984) results were published, the $1xCO_2$ and $2xCO_2$ experiments were extended by five years and two years, respectively, and showed a smaller secular cooling trend in both experiments (e.g., 0.3°C per year in the $1xCO_2$ experiment). Therefore, the $1xCO_2$ and $2xCO_2$ results from the NCAR model should be viewed as

underestimates of the equilibrium response to a doubling of CO_2. Nevertheless, an examination of the geographical patterns of the three-year and seven-year averages shown in Washington and Meehl (1984) reveals similar results. Consequently, the $2xCO_2$-$1xCO_2$ results from the NCAR model may be comparable qualitatively with the corresponding results from the GISS and GFDL models. (Washington, 1987, personal communication.)

---

fixed clouds, namely, that the $4xCO_2$-induced warming with the annual insolation cycle was less than that with annual mean insolation.

In the case of the GISS model the contradiction may be due to the differences between the versions of the model used by Hansen (1979) and Hansen et al. (1984). Furthermore, the GISS models were global with realistic geography and predicted clouds, while the GFDL model used by Wetherald and Manabe (1981) was a sector of the Earth with idealized geography and fixed clouds. These latter differences may also contribute to the contradiction with the NCAR model. However, a more likely explanation lies in the ice-albedo feedback mechanism and the fact that both the GFDL simulations were performed with a mixed layer ocean model, while a mixed layer ocean model was used in the seasonal NCAR simulation and a swamp ocean model in the annual NCAR simulation. The $1xCO_2$ annual simulation with the GFDL model is colder than the $1xCO_2$ seasonal simulation and likely has a larger sea ice extent; this would produce a larger CO_2-induced ice-albedo feedback and larger warming. The $1xCO_2$ annual simulation with the NCAR model is also colder than the $1xCO_2$ seasonal NCAR simulation, and so would also be expected to have a larger warming. The fact that it does not may indicate that there is less sea ice in the $1xCO_2$ annual simulation with the swamp ocean model than there is in the warmer $1xCO_2$ seasonal simulation with the mixed layer ocean model. Perhaps this is due to the fact that the sea ice in the swamp model is diagnostically determined and can thus change to open ocean (and vice versa) in a single time step, while the sea ice in the mixed layer model is prognostically determined and is therefore more slowly changing. Clearly, further analyses of the simulations are required to clarify the contradiction between the studies of Hansen (1979), Wetherald and Manabe (1981), Washington and Meehl (1983, 1984), and Hansen et al. (1984).

It is also of interest to compare the results of the Wetherald and Manabe (1986) study with those of Manabe and Stouffer (1980). Table 17 shows that the 4.0°C warming obtained by Wetherald and Manabe (1986) for a CO_2 doubling is virtually the same as the 4.1°C warming obtained by Manabe and Stouffer for a CO_2 quadrupling. Because the only difference between the models used by Manabe and Stouffer (1980) and Wetherald and Manabe (1986) is that clouds are prescribed in the former and predicted in the latter, these results indicate that clouds are of extreme importance in CO_2-induced climate change. But this is a contradiction to the findings of Manabe and Wetherald (1975, 1980) and Washington and Meehl (1983) which indicate virtually no difference between the CO_2-induced temperature changes with prescribed and predicted clouds. The explanation of this contradiction remains to be determined.

4.2. Feedback Analysis of

Hansen et al. (1984) have
the feedbacks in the GISS
$2xCO_2$-$1xCO_2$ global mean su
for this analysis is a mod
essentially the same as th
have by Eq. (16) with ΔT_*

$$f = 1 - \frac{(\Delta T_s)_o}{\Delta T_s} =$$

$$= \frac{(\Delta T_s)_{feedbac}}{\Delta T_s}$$

$$= \sum_{i=1}^{M} f_i \ ,$$

where M is the number of

$$f_i = \frac{(\Delta T_s)_i}{\Delta T_s} \ ,$$

and

$$\Delta T_s = \sum_{j=0}^{M} (\Delta T_s)$$

This analysis assumes tha
that the total temperatur
change $(\Delta T_s)_o$ and the cha
The validity of the
which was obtained by mak
convective model. In the
concentration without any
the second column the eff
simulated by the GCM was
level of the RCM by 33%.
below, the CO_2 concentra
permitted. The result t
of the change in the ver
the GCM, the latter was
ture change was decrease
termine the effect of th

onse to a doubling of
the geographical patterns
ges shown in Washington
ts. Consequently, the
l may be comparable qual-
ts from the GISS and GFDL
ommunication.)

rming with the annual
mean insolation.
ction may be due to the
sed by Hansen (1979) and
dels were global with
the GFDL model used by
Earth with idealized
rences may also contrib-
However, a more likely
hanism and the fact that
mixed layer ocean model,
seasonal NCAR simulation
lation. The $1xCO_2$ annual
he $1xCO_2$ seasonal simula-
is would produce a larger
ing. The $1xCO_2$ annual
han the $1xCO_2$ seasonal
to have a larger warming.
re is less sea ice in the
del than there is in the
l layer ocean model.
e in the swamp model is
o open ocean (and vice
in the mixed layer model
more slowly changing.
re required to clarify the
979), Wetherald and Manabe
Hansen et al. (1984).
ilts of the Wetherald and
touffer (1980). Table 17
rald and Manabe (1986) for
1°C warming obtained by
cause the only difference
(1980) and Wetherald and
the former and predicted
uds are of extreme import-
is a contradiction to the
and Washington and Meehl
between the CO_2-induced
ted clouds. The explana-
mined.

4.2. Feedback Analysis of the GISS Model

Hansen et al. (1984) have used a radiative-convective model to analyze the feedbacks in the GISS general circulation model simulation of the $2xCO_2$-$1xCO_2$ global mean surface air temperature difference. The basis for this analysis is a model of the climate system feedback which is essentially the same as that developed in Section 2. From the latter we have by Eq. (16) with ΔT_* replaced by ΔT_s

$$f = 1 - \frac{(\Delta T_s)_o}{\Delta T_s} = \frac{\Delta T_s - (\Delta T_s)_o}{\Delta T_s}$$

$$= \frac{(\Delta T_s)_{feedbacks}}{\Delta T_s} = \frac{\sum_{i=1}^{M} (\Delta T_s)_i}{\Delta T_s}$$

$$= \sum_{i=1}^{M} f_i \quad , \tag{146}$$

where M is the number of feedback mechanisms,

$$f_i = \frac{(\Delta T_s)_i}{\Delta T_s} \quad , \tag{147}$$

and

$$\Delta T_s = \sum_{j=0}^{M} (\Delta T_s)_j \quad . \tag{148}$$

This analysis assumes that the feedback mechanisms are independent so that the total temperature change ΔT_s is the sum of the zero-feedback change $(\Delta T_s)_o$ and the changes $(\Delta T_s)_i$ due to the feedbacks.

The validity of the above assumption is demonstrated by Fig. 16 which was obtained by making the indicated changes in the radiative-convective model. In the first column the effect of doubling the CO_2 concentration without any feedbacks is shown to be $(\Delta T_s)_o = 1.2°C$. In the second column the effect of the 33% increase in total water vapor simulated by the GCM was estimated by increasing the water vapor at each level of the RCM by 33%. In this RCM experiment, and those described below, the CO_2 concentration was not doubled, nor were any feedbacks permitted. The result then is $(\Delta T_s)_1 = 1.85°C$. To determine the effect of the change in the vertical distribution of water vapor simulated by the GCM, the latter was inserted into the RCM and the resulting temperature change was decreased by $(\Delta T_s)_1$ to obtain $(\Delta T_s)_2 = 0.90°C$. To determine the effect of the change in lapse rate simulated by the GCM, the

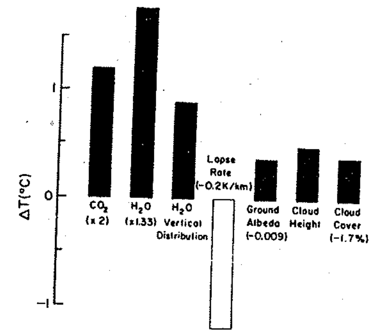

Figure 16. Contributions to the global mean $2xCO_2$-$1xCO_2$ temperature rise as estimated by inserting the changes obtained in the GCM experiment into a radiative-convective model. Source: Hansen et al., 1984.

latter was inserted into the RCM and gave $(\Delta T_s)_3 = -1.1°C$. Similarly, for the GCM-simulated change in surface albedo, $(\Delta T_s)_4 = 0.38°C$. The total cloud effect on temperature was obtained by changing the cloud amounts at all levels in the RCM in proportion to the changes obtained in the GCM. The effect of changing only cloud cover, $(\Delta T_s)_6 = 0.42°C$, was obtained by inserting a uniform cloud change in the RCM equal to the total change in the GCM. The effect of the cloud altitude change, $(\Delta T_s)_5 = 0.51°C$, was obtained by subtracting $(\Delta T_s)_6$ from the total cloud effect. Summing these individual changes gives $\Delta T_s = 4.16°C$ which agrees with the GCM-simulated value.

The results of the feedback analysis using Eqs. (146)-(148) are presented in Table 18. The feedback due to the changes in water vapor amount and vertical distribution is $f_W = 0.661$. This is considerably larger than the $f_W = 0.3$ to 0.4 given by the RCMs reviewed in Section 3. The much larger f_W estimated for the GISS GCM indicates that the relative humidity increased with doubled CO_2 in that model, unlike the constant relative humidity assumed by the RCMs; indeed, Hansen et al. (1984) state that the average relative humidity increased by 1.5% with a maximum of 6% at the 200 mb level. The estimated lapse rate feedback, $f_{LR} = -0.264$, lies at the smaller limit given by the RCMs of Section 3 for the moist adiabatic lapse rate case, perhaps because the change in lapse rate of −0.2°C/km is less than the change in the moist adiabatic value of −0.5°C/km. The cloud height feedback, $f_{CA} = 0.123$, also lies at the lower limit given by the RCMs of Section 3. The cloud cover feedback estimated for the GCM is positive. Because it appears from the results of Hansen et al. (1984) that the global mean cloudiness

Table 18. Radiative-
the GISS general
temperature chan

Feedback Mechan
None
Water Vapor Amount
Water Vapor Distri
Lapse Rate
Ground Albedo
Cloud Height
Cloud Cover
Total

a $f_i = (\Delta T_s)_i / \sum_{j=1}^{7} (\Delta T$

decreased, $dA_c/dT_s < 0$, Ta
fective $\delta < 0$. This indic
the longwave effect which,
clouds as shown in Table 1
largely to reduced sea ice
what smaller than the esti
total feedback estimated f
feedback, $f_W = 0.661$, is t
followed by cloud feedback
$f_{SA} = 0.091$, with the laps
tive contribution.

Hansen et al. (1984)
implied from the $4xCO_2$ sin
GFDL model, namely 2°C, is
the GISS model because the
since the clouds were pres
presumably smaller since t
estimated. However, the i

$2xCO_2-1xCO_2$ temperature
:ained in the GCM
Source: Hansen et al.,

$)_3$ = -1.1°C. Similarly,
', $(\Delta T_s)_4$ = 0.38°C. The
l by changing the cloud
. to the changes obtained
. cover, $(\Delta T_s)_6$ = 0.42°C,
ge in the RCM equal to the
oud altitude change,
$\Delta T_s)_6$ from the total cloud
s ΔT_s = 4.16°C which

g Eqs. (146)-(148) are
e changes in water vapor
. This is considerably
CMs reviewed in Section 3.
indicates that the rela-
at model, unlike the con-
ndeed, Hansen et al.
y increased by 1.5% with a
ted lapse rate feedback,
by the RCMs of Section 3
ps because the change in
e in the moist adiabatic
, f_{CA} = 0.123, also lies
n 3. The cloud cover
ecause it appears from the
l mean cloudiness

Table 18. Radiative-convective model analysis of the feedbacks in the GISS general circulation model simulation of $2xCO_2-1xCO_2$ temperature change. Based on Hansen et al., 1984

Feedback Mechanism	Column in Fig. 16 i	$(\Delta T_s)_{i-1}$ (°C)	f_i [a]
None	1	1.2	0
Water Vapor Amount	2	1.85	0.445
Water Vapor Distribution	3	0.90	0.216
Lapse Rate	4	-1.10	-0.264
Ground Albedo	5	0.38	0.091
Cloud Height	6	0.51	0.123
Cloud Cover	7	0.42	0.101
Total		4.16	0.712

[a] $f_i = (\Delta T_s)_i / \sum_{j=1}^{7} (\Delta T_s)_{j-1}$ for $i = 2, \ldots, 7$

decreased, $dA_c/dT_s < 0$, Table 10 shows that $f_{CC} > 0$ implies that the effective $\delta < 0$. This indicates the dominance of the albedo effect over the longwave effect which, in turn, is expected for low and middle clouds as shown in Table 12. Finally, the surface albedo feedback, due largely to reduced sea ice, is estimated as f_{SA} = 0.091 which is somewhat smaller than the estimates given by the RCMs in Section 3. The total feedback estimated for the GCM is f = 0.712, of which water vapor feedback, f_W = 0.661, is the single most important positive contributor, followed by cloud feedback, f_C = 0.224, and surface albedo feedback, f_{SA} = 0.091, with the lapse rate feedback, f_{LR} = -0.264, making a negative contribution.

Hansen et al. (1984) attribute the fact that the $2xCO_2$ warming implied from the $4xCO_2$ simulation of Manabe and Stouffer (1980) with the GFDL model, namely 2°C, is smaller than the 4.2°C warming simulated by the GISS model because there is no cloud feedback in the GFDL model since the clouds were prescribed, and the surface albedo feedback was presumably smaller since the extent of the $1xCO_2$ sea ice was underestimated. However, the feedback analysis shown in Table 18 suggests that perhaps the large water vapor feedback in the GISS model also contributes to the difference between the GISS and GFDL model's sensitivities.

5. CONCLUSION

In this chapter we have reviewed the projections of equilibrium temperature change to increased CO_2 concentration that have been made with a hierarchy of climate models that includes surface and planetary EBMs, RCMs, and GCMs. The energy balance models compute only the surface temperature, and the radiative-convective models only the vertical profile of temperature. The results of both EBMs and RCMs are determined only at one point which may, under some circumstances, be interpreted as the global average. Only the GCMs determine other climatic quantities such as precipitation, soil water and clouds, and only the GCMs determine the geographical distributions of these and other climatic quantities.

We have seen that each of the climate models (EBMs, RCMs and GCMs) is limited by its treatment of the physical processes that are not explicitly resolved by the model. In EBMs these unresolved processes include all the processes that do not occur at the energy balance level; that is, all the atmospheric processes for surface balance models and, in addition, all the surface processes in planetary energy balance models. Because of this, EBMs have given a wide range of projections of CO_2-induced surface temperature change and must be used, therefore, only in a qualitative sense with great caution.

In RCMs the unresolved physical processes include those having to do with the horizontal variations of the temperature, such as advection, and those having to do with any quantity other than temperature, such as water vapor, sea ice and clouds. Nevertheless, these models are useful for preliminary hypothesis testing and for understanding some of the results simulated by the GCMs.

Although the GCMs do include many climatic quantities other than temperature, and resolve many of the physical processes that are not resolved by the RCMs and EBMs, they nevertheless do not resolve all of the physical processes that may be of importance to climate and climatic change which span the 14 orders of magnitude from the planetary scale (10^7 m) to the cloud microphysical scale (10^{-6}m). In fact, contemporary computers permit the resolution of physical processes over only two orders of magnitude, and even a thousand-fold increase in computer speed, which is not projected to occur within this century, would allow the resolution of only one more order of magnitude! Clearly, even the GCMs are, and will continue to be, critically dependent on their treatments and parameterizations of the physical processes that occur on the unresolved or subgrid scales.

Keeping these limitations and dependencies in mind, how can we be or become confident in the GCM projections of CO_2-induced equilibrium climate change? To have confidence in the GCM simulations of a potential future climate requires that these models correctly simulate at least one known equilibrium climate, with the present climate being the best choice because of the quantity, quality and global distribution of contemporary instrumental observations. However, an evaluation of the fidelity of a GCM in simulating the present climate is not simple for a variety of reasons, including how well the simulated and observed climates represent their corresponding equilibrium climates, and the poor quality of the observations of many climatic quantities such as precipitation over the ocean and soil moisture. However, forgetting these difficulties for the moment, suppose that a GCM simulates the present climate perfectly. How then can we gain confidence in its ability to simulate another climate different from that of the present? In the case of weather forecasting, this question can and has been answered by making thousands of forecasts and comparing them with the actual observed weather. Unfortunately, this cannot be done for climate because only a few paleoclimatic reconstructions have been made, and these may or may not be of sufficient quality to provide a meaningful assessment of the GCM's capability. Thus, there is an inherent limitation on our ability to validate the accuracy of GCM simulations of CO_2-induced climate change.

However, the state of the art is that GCMs simulate the present climate imperfectly. Yet these models frequently employ treatments of dubious merit, including prescribing the oceanic heat flux, ignoring the oceanic heat flux, and using incorrect values of the solar constant. Such approximations indicate that the models are physically incomplete and/or have errors in the included physics. Furthermore, the state of the art is that the CO_2-induced climatic changes simulated by GCMs show many quantitative and even qualitative differences; thus, we know that not all of these simulations can be correct, but all could be wrong. Therefore, it is not productive now to dwell on the inherent limitation in establishing the confidence of the GCM simulations of equilibrium climate change. Rather, we must concentrate on understanding the differences and similarities of the most recent simulations and develop more-comprehensive models of the climate system. The actions required to meet these two goals are elaborated below.

5.1. Understanding the Contemporary GCM Simulations

Four simulations of CO_2-induced climate change using atmospheric GCM/mixed layer ocean models that include the annual solar cycle have been performed, namely, the CO_2 quadrupling study by Manabe and Stouffer (1980) with the GFDL model, and the CO_2 doubling studies by Hansen et al. (1984) with the GISS model, Washington and Meehl (1984) with the NCAR model, and Wetherald and Manabe (1986) with the GFDL model. Among these four simulations there is a factor of two difference in the global mean surface air temperature warming, and among the latter three, which have predicted clouds, there is a factor of two difference in the tropical surface air temperature changes. To understand these differences, an estimate of the feedbacks in each GCM should be obtained with a compatible RCM following the feedback analysis performed by Hansen et al. (1984). An intercomparison of these feedback analyses for the GCMs will allow ranking of the feedbacks in terms of magnitude, and thereby illuminate the likely parameterized physical processes responsible for the differences.

GCM sensitivity studies should then be performed to verify the findings of the RCM feedback analysis. For example, if it is indicated that cloudiness or ice albedo feedback is dominant, then a pair of $1xCO_2$ and $2xCO_2$ GCM simulations should be made with noninteractive clouds or sea ice and compared with the existing simulations with interactive clouds or sea ice. On the other hand, if water vapor feedback is dominant, then simulations with a different parameterization of cumulus convection may be warranted. Because these sensitivity studies may involve many reruns of the models, each for a period of several decades, it may be more economical to employ the adjoint sensitivity method described by Hall (1985). Having established by RCM feedback analyses and GCM sensitivity studies which of the parameterized physical processes are most important for the CO_2-induced climate changes, how can we determine which of the contemporary parameterizations, if any, is correct? The answer is described below.

5.2. Validation of Physical Process Parameterizations

In the past, simple parameterizations of the unresolved or subgrid-scale physical processes have been developed. The simplicity of the parameterization has been justified because the processes are extremely complex and our understanding of them is small. This in fact was the justification for parameterizing cumulus convection by moist adiabatic adjustment (Manabe <u>et al</u>., 1965). Yet it is clear that this parameterization ignores penetrative convection and, therefore, produces a different vertical profile of heating from a parameterization that includes penetrative convection. Furthermore, there is circumstantial evidence that these differences in the convective vertical heating profile may be responsible for the differences in the tropical profiles of CO_2-induced temperature changes in the most recent GCM simulations (Schlesinger and Mitchell, 1985, 1987).

Accordingly, it is now time to begin the very difficult task of systematically validating the GCM parameterizations of subgrid-scale processes. Fortunately, a prototype validation procedure has been developed and is currently being carried out, in this case for the parameterization of radiative transfer under the Intercomparison of Radiation Codes in Climate Models (ICRCCM, see Luther, 1984). Following this prototype program, scientists worldwide would be invited to intercompare results from their parameterizations for specifically agreed upon cases. However, to reduce the possibility that the parameterizations may all agree and yet be incorrect, it is essential to have corresponding results from highly detailed models that actually resolve the physical processes whose parameterizations are being intercompared, and to have actual observations to validate these highly detailed models. Such a program, for example, the Intercomparison of Parameterizations in Climate Models (ICPCM), should investigate all of the parameterized physical processes in the order of importance indicated by the previously described feedback analysis and sensitivity studies.

ACKNOWLEDGEMENTS

I would like to thank Syuku
Geophysical Fluid Dynamics
Lacis and David Rind of the
Warren Washington and Geral
Atmospheric Research for ma
their discussions of those
and Dean Vickers for perfor
herein, to Larry Holcomb an
Dee Dee Reynolds, Leah Rile
manuscript. I would like t
Yves Fouquart for their car
This study was supported by
number DE-AC03-76SF00098, a
U.S. Department of Energy u

REFERENCES

Augustsson, T., and V. Rama
study of the CO_2 clima
Bode, H. W., 1975: <u>Network</u>
Krieger, New York, 577
Brunt, D., 1933: 'The adiab
<u>Quart. J. Roy. Meteor.</u>
Budyko, M. I., 1956: <u>Heat</u>
Gidrometeoizdat, <u>Lenin</u>
N. A. Steanova, MGA 13
11B-25.
Budyko, M. I., 1969: 'The e
climate of the earth.'
Callendar, G. S., 1938: 'Th
its influence on tempe
223-240.
Cess, R. D., 1974: 'Radiati
Global considerations
<u>Spectros. Radiat. Tran</u>
Cess, R. D., 1975: 'Global
atmospheric feedback n
Charlock, T. P., 1981: 'Clc
climate change.' J. A
Charlock, T. P., 1982: 'Clc
a radiative-convective
Chylek, P., and J. T. Kiehl
climate models.' J. A
Elliott, W. P., L. Machta a
biotic contribution tc
measurements at Mauna
3741-3746.
Feigelson, E. M., 1978: 'Pr

erformed to verify the
xample, if it is indicated
inant, then a pair of $1xCO_2$
noninteractive clouds or
tions with interactive
er vapor feedback is domin-
terization of cumulus con-
itivity studies may involve
of several decades, it may
itivity method described by
ack analyses and GCM sensi-
ical processes are most
, how can we determine
if any, is correct? The

rizations

nresolved or subgrid-scale
implicity of the paramet-
esses are extremely complex
in fact was the justifica-
moist adiabatic adjustment
his parameterization ig-
roduces a different ver-
ion that includes penetra-
nstantial evidence that
eating profile may be
l profiles of CO_2-induced
nulations (Schlesinger and

very difficult task of
tions of subgrid-scale
n procedure has been dev-
this case for the paramet-
rcomparison of Radiation
984). Following this pro-
invited to intercompare
fically agreed upon
t the parameterizations
ntial to have correspond-
ctually resolve the phys-
ng intercompared, and to
hly detailed models. Such
Parameterizations in
. of the parameterized
indicated by the
sitivity studies.

ACKNOWLEDGEMENTS

I would like to thank Syukuro Manabe and Richard Wetherald of the Geophysical Fluid Dynamics Laboratory, James Hansen, Gary Russel, Andrew Lacis and David Rind of the Goddard Institute for Space Studies, and Warren Washington and Gerald Meehl of the National Center for Atmospheric Research for making their results available to me, and for their discussions of those results. I express my gratitude to Jai-Ho Oh and Dean Vickers for performing some of the calculations and graphics herein, to Larry Holcomb and John Stark for drafting, and to Monica Cox, Dee Dee Reynolds, Leah Riley and especially Naomi Weidner for typing the manuscript. I would like to thank B. Henderson-Sellers and Yves Fouquart for their careful and constructive reviews of the chapter. This study was supported by the Department of Energy under contract number DE-AC03-76SF00098, and by the National Science Foundation and the U.S. Department of Energy under grants ATM 82-05992 and ATM 85-11889.

REFERENCES

Augustsson, T., and V. Ramanathan, 1977: 'A radiative-convective model study of the CO_2 climate problem.' J. Atmos. Sci., **34**, 448-451.

Bode, H. W., 1975: Network Analysis and Feedback Amplifier Design. Krieger, New York, 577 pp.

Brunt, D., 1933: 'The adiabatic lapse rate for dry and saturated air.' Quart. J. Roy. Meteor. Soc., **59**, 351-360.

Budyko, M. I., 1956: Heat Balance of the Earth's Surface. Gidrometeoizdat, Leningrad [in Russian], 266 pp. Translation by N. A. Steanova, MGA 13E-286, U.S. Weather Bureau, Washington, D.C., 11B-25.

Budyko, M. I., 1969: 'The effect of solar radiation variations on the climate of the earth.' Tellus, **21**, 611-619.

Callendar, G. S., 1938: 'The artificial production of carbon dioxide and its influence on temperature.' Quart. J. Roy. Meteor. Soc., **64**, 223-240.

Cess, R. D., 1974: 'Radiative transfer due to atmospheric water vapor: Global considerations of the earth's energy balance.' J. Quant. Spectros. Radiat. Transfer, **14**, 861-871.

Cess, R. D., 1975: 'Global climate change: An investigation of atmospheric feedback mechanisms.' Tellus, **27**, 193-198.

Charlock, T. P., 1981: 'Cloud optics as a possible stabilizing factor in climate change.' J. Atmos. Sci., **38**, 661-663.

Charlock, T. P., 1982: 'Cloud optical feedback and climate stability in a radiative-convective model.' Tellus, **34**, 245-254.

Chylek, P., and J. T. Kiehl, 1981: 'Sensitivity of radiative-convective climate models.' J. Atmos. Sci., **38**, 1105-1110.

Elliott, W. P., L. Machta and C. D. Keeling, 1985: 'An estimate of the biotic contribution to the atmospheric CO_2 increase based on direct measurements at Mauna Loa Observatory.' J. Geophys. Res., **90**, 3741-3746.

Feigelson, E. M., 1978: 'Preliminary radiation model of a cloudy atmosphere, 1, Structure of clouds and solar radiation.' Beitr. Phys. Atmos., **51**, 203-229.

Gates, 1988: 'Climate and the climate system.' In Physically-Based Modelling and Simulation of Climate and Climatic Change, Vol. I, M. E. Schlesinger, ed., Kluwer Academic Publishers, 3-21.

Goody, R. M., 1964: Atmospheric Radiation, Vol.I. Clarendon Press, 436 pp.

Hall, M. C. G., 1985: 'Estimating the reliability of climate model projections - steps toward a solution.' In The Potential Climatic Effects of Increasing Carbon Dioxide, eds., M. C. MacCracken and F. M. Luther, DOE/ER-0237, U.S. Department of Energy, Washington, D.C., available from NTIS, Springfield, Virginia.

Hall, M. C. G., D. G. Cacuci and M. E. Schlesinger, 1982: 'Sensitivity analysis of a radiative-convective model by the adjoint method.' J. Atmos. Sci., **39**, 2038-2050.

Han, 1988: 'Modelling and simulation of the general circulation of the ocean.' In Physically-Based Modelling and Simulation of Climate and Climatic Change, Vol. I, M. E. Schlesinger, ed., Kluwer Academic Publishers, 465-508.

Hansen, J., 1979: Results presented in Carbon Dioxide and Climate: A Scientific Assessment, Report of an Ad Hoc Study Group on Carbon Dioxide and Climate. Climate Res. Board, Natl. Acad. Sci., Washington, D.C.

Hansen, J., D. Johnson, A. Lacis, S. Lebedeff, P. Lee, D. Rind and G. Russell, 1981: 'Climate impact of increasing atmospheric carbon dioxide.' Science, **213**, 957-966.

Hansen, J., A. Lacis, D. Rind, G. Russell, P. Stone, I. Fung, R. Ruedy and J. Lerner, 1984: 'Climate sensitivity: Analysis of feedback mechanisms.' In Climate Processes and Climate Sensitivity, Maurice Ewing Series, 5, eds., J. E. Hansen and T. Takahashi, American Geophysical Union, Washington, D.C., 130-163.

Hummel, J. R., 1982: 'Surface temperature sensitivities in a multiple cloud radiative-convective model with a constant and pressure dependent lapse rate.' Tellus, **34**, 203-208.

Hummel, J. R., and W. R. Kuhn, 1981a: 'Comparison of radiative-convective models with constant and pressure-dependent lapse rates.' Tellus, **33**, 254-261.

Hummel, J. R., and W. R. Kuhn, 1981b: 'An atmospheric radiative-convective model with interactive water vapor transport and cloud development.' Tellus, **33**, 372-381.

Hummel, J. R., and R. A. Reck, 1981: 'Carbon dioxide and climate: The effects of water transport in radiative-convective models.' J. Geophys. Res., **86**, 12,035-12,038.

Hunt, B. G., 1981: 'An examination of some feedback mechanisms in the carbon dioxide climate problem.' Tellus, **33**, 78-88.

Hunt, B. G., and N. C. Wells, 1979: 'An assessment of the possible future climatic impact of carbon dioxide increases based on a coupled one-dimensional atmospheric-oceanic model.' J. Geophys. Res., **84**, 787-791.

Idso, S. B., 1980: 'The climatological significance of a doubling of

earth's atmospheric ca
1462-1463.

Jenne, R. L., 1975: 'Data s
NCAR-TN/IA-111, Nation
CO, 194 pp.

Kiehl, J. T., and V. Ramana
increased CO_2: The ro
region.' J. Atmos. Sc

Lal, M., and V. Ramanathan,
water vapor radiative
Atmos. Sci., **41**, 2238-

Lindzen, R. S., A. Y. Hou a
convective model choic
doubling CO_2.' J. Atm

Luther, F. M., 1984: 'The I
Models (ICRCCM): Long
Research Programme, WC
Unions and World Meteo
37 pp.

Manabe, S., 1971: 'Estimate
of carbon dioxide conc
the Climate, eds., W.
MIT Press, Cambridge,

Manabe, S., and R. J. Stouf
with a mathematical mo
491-493.

Manabe, S., and R. J. Stouf
model to an increase o
Geophys. Res., **85**, 552

Manabe, S., and R. F. Stric
atmosphere with a conv
361-385.

Manabe, S., and R. T. Wethe
atmosphere with a give
Atmos. Sci., **24**, 241-2

Manabe, S., and R. T. Wethe
concentration on the c
Atmos. Sci., **32**, 3-15.

Manabe, S., and R. T. Wethe
change resulting from
atmosphere.' J. Atmos

Manabe, S., J. Smagorinsky
climatology of a gener
cycle.' Mon. Wea. Rev

McClatchey, R. A., R. W. Fe
Garing, 1971: 'Optical
AFCRL-71-0279, Air For
MA, 85 pp.

Möller, F., 1963: 'On the i
air on the radiative b
climate.' J. Geophys.

olar radiation.' Beitr.

' In Physically-Based
Climatic Change, Vol. I,
Publishers, 3-21.
ol.I. Clarendon Press,

lity of climate model
In The Potential Climatic
s., M. C. MacCracken and
nt of Energy, Washington,
Virginia.
inger, 1982: 'Sensitivity
by the adjoint method.'

eneral circulation of the
nd Simulation of Climate
singer, ed., Kluwer Academic

n Dioxide and Climate: A
oc Study Group on Carbon
, Natl. Acad. Sci.,

, P. Lee, D. Rind and
reasing atmospheric carbon

Stone, I. Fung, R. Ruedy
y: Analysis of feedback
limate Sensitivity, Maurice
T. Takahashi, American
-163.
sitivities in a multiple
constant and pressure
208.
ison of radiative-
sure-dependent lapse

ospheric radiative-
vapor transport and cloud

dioxide and climate: The
convective models.' J.

edback mechanisms in the
, **33**, 78-88.
sment of the possible
increases based on a
nic model.' J. Geophys.

icance of a doubling of

earth's atmospheric carbon dioxide concentration.' Science, **207**, 1462-1463.

Jenne, R. L., 1975: 'Data sets for meteorological research.' NCAR-TN/IA-111, National Center for Atmospheric Research, Boulder, CO, 194 pp.

Kiehl, J. T., and V. Ramanathan, 1982: 'Radiative heating due to increased CO_2: The role of H_2O continuum absorption in the 12-μm region.' J. Atmos. Sci., **39**, 2923-2926.

Lal, M., and V. Ramanathan, 1984: 'The effects of moist convection and water vapor radiative processes on climate sensitivity.' J. Atmos. Sci., **41**, 2238-2249.

Lindzen, R. S., A. Y. Hou and B. F. Farrell, 1982: 'The role of convective model choice in calculating the climate impact of doubling CO_2.' J. Atmos. Sci., **39**, 1189-1205.

Luther, F. M., 1984: 'The Intercomparison of Radiation Codes in Climatic Models (ICRCCM): Longwave Clear-Sky Calculations.' World Climate Research Programme, WCP-93, International Council of Scientific Unions and World Meteorological Organization, Geneva, Switzerland, 37 pp.

Manabe, S., 1971: 'Estimate of future changes in climate due to increase of carbon dioxide concentration in the air.' In Man's Impact on the Climate, eds., W. H. Mathews, W. W. Kellogg and G. D. Robinson, MIT Press, Cambridge, MA, 249-264.

Manabe, S., and R. J. Stouffer, 1979: 'A CO_2-climate sensitivity study with a mathematical model of the global climate.' Nature, **282**, 491-493.

Manabe, S., and R. J. Stouffer, 1980: 'Sensitivity of a global climate model to an increase of CO_2 concentration in the atmosphere.' J. Geophys. Res., **85**, 5529-5554.

Manabe, S., and R. F. Strickler, 1964: 'Thermal equilibrium of the atmosphere with a convective adjustment.' J. Atmos. Sci., **21**, 361-385.

Manabe, S., and R. T. Wetherald, 1967: 'Thermal equilibrium of the atmosphere with a given distribution of relative humidity.' J. Atmos. Sci., **24**, 241-259.

Manabe, S., and R. T. Wetherald, 1975: 'The effects of doubling the CO_2 concentration on the climate of a general circulation model.' J. Atmos. Sci., **32**, 3-15.

Manabe, S., and R. T. Wetherald, 1980: 'On the distribution of climate change resulting from an increase in CO_2-content of the atmosphere.' J. Atmos. Sci., **37**, 99-118.

Manabe, S., J. Smagorinsky and R. F. Strickler, 1965: 'Simulated climatology of a general circulation model with a hydrological cycle.' Mon. Wea. Rev., **93**, 769-798.

McClatchey, R. A., R. W. Fenn, J. E. A. Selby, F. E. Volz and J. S. Garing, 1971: 'Optical properties of the atmosphere.' AFCRL-71-0279, Air Force Cambridge Research Laboratories, Bedford, MA, 85 pp.

Möller, F., 1963: 'On the influence of changes in CO_2 concentration in air on the radiative balance of the earth's surface and on the climate.' J. Geophys. Res., **68**, 3877-3886.

Newell, R. E., and T. G. Dopplick, 1979: 'Questions concerning the possible influence of anthropogenic CO_2 on atmospheric temperature.' J. Appl. Meteor., **18**, 822-825.

Nordhaus, W. D., and G. W. Yohe, 1983: 'Future paths of energy and carbon dioxide emissions.' In Changing Climate, National Academy of Sciences, Washington, D.C., 87-153.

North, G. R., 1975: 'Theory of energy-balance climate models.' J. Atmos. Sci., **32**, 2033-2043.

Oort, A. H., and E. Rasmusson, 1971: 'Atmospheric Circulation Statistics.' NOAA Prof. Paper No. 5, 323 pp.

Plass, G. N., 1956: 'The influence of the 15μ carbon-dioxide band on the atmospheric infra-red cooling rate.' Quart. J. Roy. Meteor. Soc., **82**, 310-324.

Privett, D. W., 1960: 'The exchange of energy between the atmosphere and the oceans of the Southern Hemisphere.' Geophys. Memo, **13**, No. 104, United Kingdom Meteorological Office, London, 61 pp.

Ramanathan, V., M. S. Lian and R. D. Cess, 1979: 'Increased atmospheric CO_2: Zonal and seasonal estimates of the effects on the radiation energy balance and surface temperature.' J. Geophys. Res., **84**, 4949-4958.

Rasool, S. I., and S. H. Schneider, 1971: 'Atmospheric carbon dioxide and aerosols: Effects of large increases on global climate.' Science, **173**, 138-141.

Reck, R. A., 1979a: 'Comparison of fixed cloud-top temperature and fixed cloud-top altitude approximations in the Manabe-Wetherald radiative-convective atmospheric model.' Tellus, **31**, 400-405.

Reck, R. A., 1979b: 'Carbon dioxide and climate: Comparison of one- and three-dimensional models.' Environment International, **2**, 387-391.

Rotty, R. M., 1983: 'Distribution of and changes in industrial carbon dioxide production.' J. Geophys. Res., **88**, 1301-1308.

Rowntree, P. R., and J. Walker, 1978: 'The effects of doubling the CO_2 concentration on radiative-convective equilibrium.' In Carbon Dioxide, Climate and Society, ed., J. Williams, Pergamon, Oxford, 181-191.

Saker, N. J., 1975: 'An 11-layer general circulation model.' Met 020 Tech. Note No. II/30, United Kingdom Meteorological Office, Bracknell.

Schlesinger, M. E., 1984: 'Atmospheric general circulation model simulations of the modern Antarctic climate.' In Environment of West Antarctica: Potential CO_2-Induced Change, National Research Council, National Academy Press, Washington, D.C., 155-196.

Schlesinger, M. E., and J. F. B. Mitchell, 1985: 'Model projections of the equilibrium climatic response to increased CO_2.' In The Potential Climatic Effects of Increasing Carbon Dioxide, eds., M. C. MacCracken and F. M. Luther, DOE/ER-0237, U.S. Department of Energy, Washington, D.C., 81-147. (Available from NTIS, Springfield, Virginia.)

Schlesinger, M. E., and J. F. B. Mitchell, 1987: 'Climate model simulations of the equilibrium climatic response to increased carbon dioxide.' Rev. of Geophys., **25**, 760-798.

Schneider, S. H., 1972: 'Cloudiness as a global climatic feedback

mechanism: The effec
temperature of variat
1413-1422.
Schneider, S. H., 1975: 'O
Atmos. Sci., **32**, 2060-
Sellers, W. D., 1969: 'A g
balance of the earth-
392-400.
Simmonds and Bengtsson, 19
Their design and use
Modelling and Simulat
M. E. Schlesinger, ed
Somerville, R. C. J., and
feedbacks in the CO_2
9668-9672.
Spelman, M. J., and S. Man
transport upon the se
Res., **89**, 571-586.
Stephens, G. L., 1978: 'Ra
Parameterization sche
Stephens, G. L., and P. J.
Sensitivity of simple
Stephens, G. L., S. Ackerm
parameterization revi
Sci., **41**, 687-690.
Stone, P. H., 1978: 'Baroc
561-571.
Stone, P. H., and J. H. Ca
and their parameteriz
Wang, W.-C., and P. H. Sto
global sensitivity in
model.' J. Atmos. Sc
Wang, W.-C., W. B. Rossow,
sensitivity of a one-
cloud feedback.' J.
Washington, W. M., and G.
experiments on the cl
quadrupling of carbon
88, 6600-6610.
Washington, W. M., and G.
the climate sensitivi
spheric general circu
ocean model.' J. Geo
Wetherald, R. T., and S. M
upon the sensitivity
1194-1204.
Wetherald, R. T., and S. M
change in response to
Yang, S.-K., and G. L. Smi
rate regimes.' J. At

mechanism: The effects on the radiation balance and surface temperature of variations in cloudiness.' J. Atmos. Sci., **29**, 1413-1422.

Schneider, S. H., 1975: 'On the carbon dioxide-climate confusion.' J. Atmos. Sci., **32**, 2060-2066.

Sellers, W. D., 1969: 'A global climate model based on the energy balance of the earth-atmosphere system.' J. Appl. Meteor., **8**, 392-400.

Simmonds and Bengtsson, 1988: 'Atmospheric general circulation models: Their design and use for climate studies.' In Physically-Based Modelling and Simulation of Climate and Climatic Change, Vol. I, M. E. Schlesinger, ed., Kluwer Academic Publishers, 23-76.

Somerville, R. C. J., and L. A. Remer, 1984: 'Cloud optical thickness feedbacks in the CO_2 climate problem.' J. Geophys. Res., **89**, 9668-9672.

Spelman, M. J., and S. Manabe, 1984: 'Influence of oceanic heat transport upon the sensitivity of a model climate.' J. Geophys. Res., **89**, 571-586.

Stephens, G. L., 1978: 'Radiation profiles in extended water clouds, 2, Parameterization schemes.' J. Atmos. Sci., **35**, 2123-2132.

Stephens, G. L., and P. J. Webster, 1981: 'Clouds and climate: Sensitivity of simple systems.' J. Atmos. Sci., **38**, 235-247.

Stephens, G. L., S. Ackerman and E. A. Smith, 1984: 'A shortwave parameterization revised to improve cloud absorption.' J. Atmos. Sci., **41**, 687-690.

Stone, P. H., 1978: 'Baroclinic adjustment.' J. Atmos. Sci., **35**, 561-571.

Stone, P. H., and J. H. Carlson, 1979: 'Atmospheric lapse rate regimes and their parameterizations.' J. Atmos. Sci., **36**, 415-423.

Wang, W.-C., and P. H. Stone, 1980: 'Effect of ice-albedo feedback on global sensitivity in a one-dimensional radiative-convective model.' J. Atmos. Sci., **37**, 545-552.

Wang, W.-C., W. B. Rossow, M. S. Yao and M. Wolfson, 1981: 'Climate sensitivity of a one-dimensional radiative-convective model with cloud feedback.' J. Atmos. Sci., **38**, 1167-1178.

Washington, W. M., and G. A. Meehl, 1983: 'General circulation model experiments on the climatic effects due to a doubling and quadrupling of carbon dioxide concentration.' J. Geophys. Res., **88**, 6600-6610.

Washington, W. M., and G. A. Meehl, 1984: 'Seasonal cycle experiment on the climate sensitivity due to a doubling of CO_2 with an atmospheric general circulation model coupled to a simple mixed-layer ocean model.' J. Geophys. Res., **89**, 9475-9503.

Wetherald, R. T., and S. Manabe, 1981: 'Influence of seasonal variation upon the sensitivity of a model climate.' J. Geophys. Res., **86**, 1194-1204.

Wetherald, R. T., and S. Manabe, 1986: 'An investigation of cloud cover change in response to thermal forcing.' Climatic Change, **8**, 5-23.

Yang, S.-K., and G. L. Smith, 1985: 'Further study on atmospheric lapse rate regimes.' J. Atmos. Sci., **42**, 961-965.

DISCUSSION

Simonot

I have a question about cloud cover feedback. When you use Eq. (101b) you make the assumption that the f_j are independent of the f_{CC}, but then you tell us that cloud altitude feedback is in fact subsumed in the cloud cover feedback. This means that the cloud altitude feedback can't be contained in the f_j. But what about the correlation of f_{CC} with other feedbacks?

Schlesinger

In Section 3.3.3 of the chapter I presented Table 5 where I've examined the dependence or independence of each of the individual feedback processes using a radiative-convective model. In that kind of analysis if you find two feedback processes that are not independent, then you have to combine them into a single feedback process.

Dalfes

I think that when you are considering the optical depth feedback we have in fact two optical depths, one for solar radiation and one for longwave radiation. So it might be better to formulate that feedback in terms of cloud liquid water content.

Schlesinger

Indeed, that has been done in the chapter.

Mysak

Again getting to this question of the coupling between feedbacks, could you use other types of functions in Eq. (18) rather than just 1 - f, such as transcendental functions, in which the zeros of your denominator don't couple so simply?

Schlesinger

Equation (18) is the equation obtained from the classical analysis of feedbacks in engineering systems, and also arises quite naturally from the energy balance condition given by Eq. (1). In Eq. (18) the functional form of the individual f_j is not yet determined, and the denominator has a zero only in the unphysical case where all the feedbacks sum to unity.

Crowley

Given that the greatest uncertainty in a negative feedback has to do with clouds, can you give your own opinion as to what would be some

of the examples of resear
down the uncertainty?

Schlesinger

We need to make clou
variables so that we can
interactive way and then
that Yves Fouquart talked
models that predict cloud
ative field at the top of
lite observations. Then
eterization within the GC
a simulation of CO_2-induc
have with clouds is their
our understanding we can
ship between the scales w

Fouquart

With respect to the
points which are relative
fractional cloud cover ar
satellite observations to
liquid water content beco
lot of study can be done
archive the spectral data
determination of the stat
clouds. In recent years
field. For example, we k
cumulus clouds depends st
itself. So some process-
be done in the upcoming y
radiative-convective stud
in which she also generat
of using the hypothesis o
clouds used by Wang, we n
between clouds at differe
from those that Wang obta
about the horizontal dist
distribution of clouds a

Schlesinger

You are right, natu

Williams

You didn't mention
our modelling isn't good
being driven by changes

back. When you use
are independent of the
feedback is in fact sub-
s that the cloud altitude
hat about the correlation

ted Table 5 where I've
ch of the individual
ve model. In that kind of
hat are not independent,
eedback process.

e optical depth feedback we
r radiation and one for
formulate that feedback in

er.

oupling between feedbacks,
. (18) rather than just
which the zeros of your

from the classical analysis
o arises quite naturally
q. (1). In Eq. (18) the
yet determined, and the
l case where all the feed-

a negative feedback has to
n as to what would be some

of the examples of research we have to do in the future to really narrow down the uncertainty?

Schlesinger

We need to make cloud liquid water and cloud ice prognostic variables so that we can calculate the cloud optical properties in an interactive way and then use the radiative transfer parameterization that Yves Fouquart talked about in his lecture. We can validate these models that predict clouds by comparing their simulated cloud and radiative field at the top of the atmosphere with the corresponding satellite observations. Then we can use this physically-based cloud parameterization within the GCM to assess the cloud optical depth feedback in a simulation of CO_2-induced climatic change. However, a problem that we have with clouds is their fractional cloud cover. To make advances in our understanding we can use mesoscale models to determine the relationship between the scales we resolve and the fractional cloud cover.

Fouquart

With respect to the impacts of clouds on climate, there are two points which are relatively important. The first one is the problem of fractional cloud cover and how we can use both mesoscale models and satellite observations to try to understand much more about the way the liquid water content becomes distributed in the horizontal. I think a lot of study can be done directly from satellite observations if we archive the spectral data with a horizontal resolution that allows the determination of the statistics of the spatial distribution of the clouds. In recent years a lot of very good work has been done in this field. For example, we know that the fractional cloud cover for stratocumulus clouds depends strongly on the properties of the boundary layer itself. So some process-oriented satellite observations can and should be done in the upcoming years. The second point is illustrated by the radiative-convective study carried out by Laura Smith of our Laboratory in which she also generated clouds using the Wang model. But, instead of using the hypothesis of nonoverlapping clouds or maximum overlapping clouds used by Wang, we made the hypothesis of random overlapping between clouds at different levels. We obtained quite different results from those that Wang obtained. That means that we must know not only about the horizontal distribution of clouds, but also about the vertical distribution of clouds as well.

Schlesinger

You are right, nature has not presented us a simple problem here.

Williams

You didn't mention any feedbacks from the ocean. Was that because our modelling isn't good enough, or do you feel the whole process is being driven by changes in the atmosphere?

Schlesinger

I don't believe it is being driven only by changes in the atmosphere. Kirk Bryan has done some work at GFDL showing the feedbacks due to the change in the ocean circulation and the impact on the sea ice, so very definitely there are feedbacks in the ocean. However, there is a problem in evaluating the feedbacks from general circulation model simulations. One GCM simulation has been analyzed in terms of feedbacks by using a radiative-convective model. However, what we need to do is develop a method of determining the feedbacks directly from the GCM's themselves. That's a completely open problem.

Simonot

I think there is a methodology that you did not mention, namely, the adjoint method.

Schlesinger

You're right. There is a technique that has been developed largely at Oak Ridge Laboratory using what is called the adjoint method. That method has been tested in radiative-convective models to determine the feedback and it works quite well. Serious thought should be given to using the adjoint method to determine the feedbacks in general circulation model simulations.

Ghan

The feedback as you defined it is restricted between negative infinity and one, and that implies that if the CO_2 forcing is positive you can only get a surface warming. It seems to me that somehow the clouds might change in some way I don't understand to give a surface cooling with low-level clouds. How does that fit into your analysis?

Schlesinger

In the feedback analysis the sign of the response is the same as the sign of the forcing unless the feedback f is positive and larger than unity. Although we cannot completely eliminate this possibility, it appears to be physically implausible.

Ghan

Well suppose you apply the analysis to a GCM. What sort of feedback value would be appropriate in that case with the clouds changing?

Schlesinger

The analysis in the chapter for the GISS GCM shows that the cloud feedback is positive. However, this model and all other GCMs do not

include cloud optical dept
plete cloud feedback until
clouds and their radiative
cussed in reply to Tom Crow

Henderson-Sellers

You just said that cl
do you feel about the fract
any mileage, insight, phys
of argument?

Schlesinger

There may be. Howeve
ourselves using mesoscale
It's not going to happen o
to be around for 10 to 20
is to simulate people to w

y changes in the
GFDL showing the feedbacks
the impact on the sea
the ocean. However,
from general circulation
n analyzed in terms of
1. However, what we need
eedbacks directly from the
oblem.

id not mention, namely,

has been developed largely
he adjoint method. That
models to determine the
ught should be given to
backs in general circula-

ted between negative
CO_2 forcing is positive
to me that somehow the
tand to give a surface
fit into your analysis?

response is the same as
is positive and larger
minate this possibility,

GCM. What sort of
se with the clouds

GCM shows that the cloud
all other GCMs do not

include cloud optical depth feedback. So we cannot determine the complete cloud feedback until we incorporate a physically-based model of clouds and their radiative interactions in the GCMs as I previously discussed in reply to Tom Crowley's question.

Henderson-Sellers

You just said that cloud fractional cover was very difficult. How do you feel about the fractal theory of clouds? Do you think there is any mileage, insight, physical understanding to be gained from that sort of argument?

Schlesinger

There may be. However, I think we are going to have to educate ourselves using mesoscale models and observations of the real world. It's not going to happen overnight. I think this cloud problem is going to be around for 10 to 20 years. One of the reasons for having this ASI is to simulate people to work in these areas.